

For Reference

NOT TO BE TAKEN FROM THIS ROOM

For Reference

NOT TO BE TAKEN FROM THIS ROOM

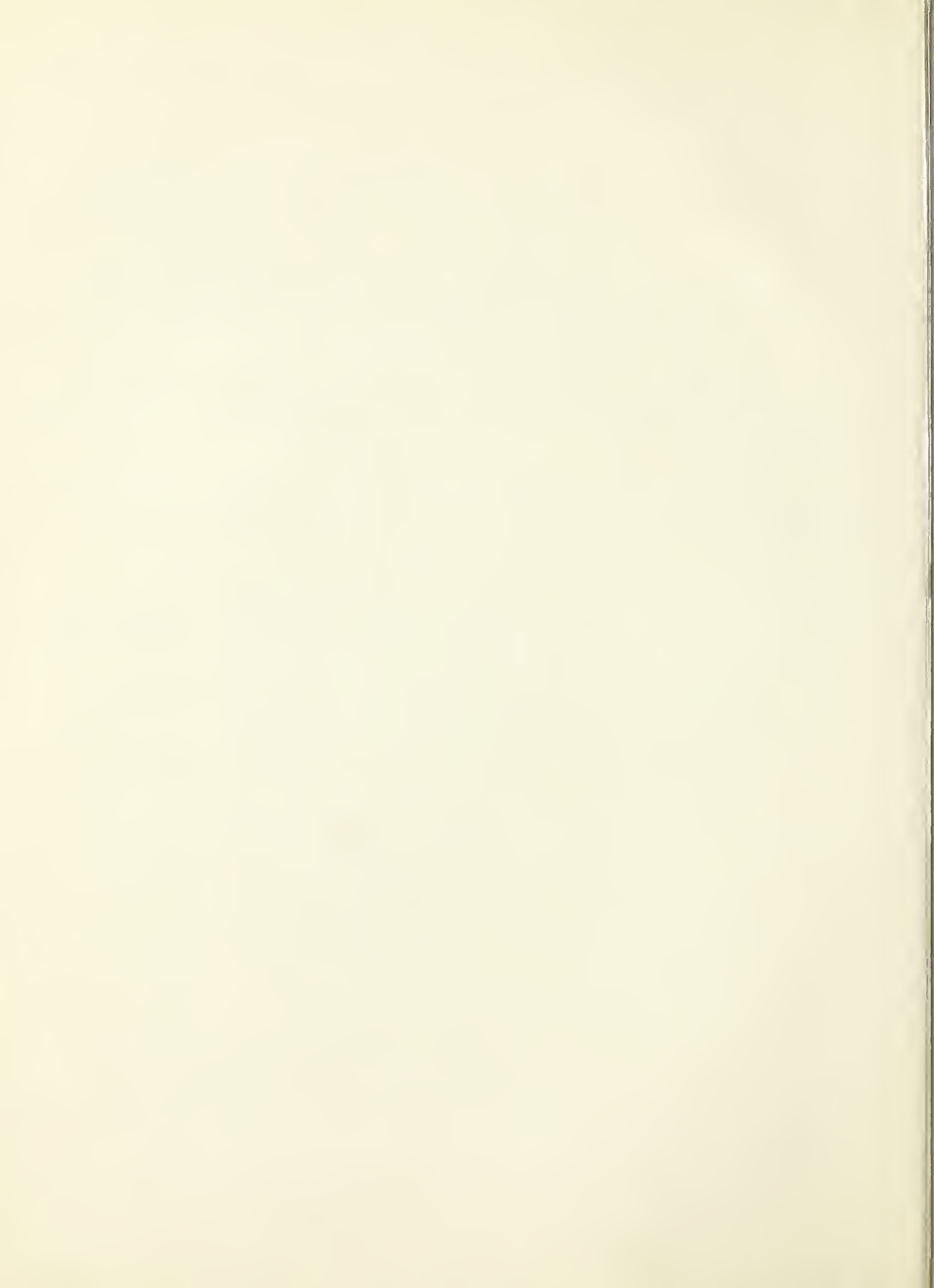
Ex LIBRIS
UNIVERSITATIS
ALBERTAENSIS





Digitized by the Internet Archive
in 2018 with funding from
University of Alberta Libraries

<https://archive.org/details/Newland1963>



68
THE UNIVERSITY OF ALBERTA

ON THE DIFFUSION OF RADIOGENIC ARGON FROM
POTASSIUM FELDSPARS

A THESIS

SUBMITTED TO THE FACULTY OF GRADUATE STUDIES IN PARTIAL
FULFILMENT OF THE REQUIREMENTS FOR THE DEGREE OF
MASTER OF SCIENCE

DEPARTMENT OF GEOLOGY

by

BERNARD TERENCE NEWLAND

Edmonton, Alberta

July, 1963

ABSTRACT

The diffusion coefficient of radiogenic argon in nine samples of feldspar was determined at a series of temperatures from 350 – 1230°C. The diffusion coefficients were calculated using two mathematical treatments, the first assuming volume diffusion from a sphere with zero concentration of argon at the surface and the other assuming that diffusion takes place from a boundary layer near the surface of the crystal.

In the Kinnekulle and Millcreek sanidines, which are of bentonitic origin, diffusion was found to occur from one position. The activation energy for loss from this position is approximately 42,000 cal./mole (Calculated assuming volume diffusion from a sphere). Diffusion coefficients found in three grain sizes of the Millcreek sanidine indicate that the physical grain size is the effective radius of diffusion.

In the Crowsnest sanidine, which was taken from a trachyte lava, and in the Yellowknife and Montevideo microclines, argon was found to diffuse from two positions. The activation energy of these positions is given, in the following table: (values in cal./mole; calculated assuming volume diffusion from a sphere).

	Crowsnest sanidine	Yellowknife microcline	Montevideo microcline
Position I	28,000	19,000	20,000
Position II	47,000	55,000	71,000

Comparison of the curves of the logarithm of the diffusion coefficient against reciprocal absolute temperature for different grain sizes of the Crowsnest sanidine, indicates that the effective radius of diffusion is approximately 30 microns.

...the ... of ...
...the ... of ...
...the ... of ...
...the ... of ...
...the ... of ...

...the ... of ...
...the ... of ...
...the ... of ...
...the ... of ...
...the ... of ...

...the ... of ...
...the ... of ...
...the ... of ...
...the ... of ...
...the ... of ...

...the ... of ...
...the ... of ...
...the ... of ...
...the ... of ...
...the ... of ...

It is suggested that the nature of the two positions is related to the fracture system present in the Crowsnest sanidine and to the twin planes in the microclines.

From values of the diffusion coefficient extrapolated to room temperature it is found that no diffusion would be expected from the Kinnekulle and Millcreek sanidines at temperatures below 200°C. over geological time. The Crowsnest sanidine was found to be at the threshold value for loss from position I at 150°C. (equivalent to an average depth of burial of approximately 5 kms.). It was found that if the two microclines were held at 150°C. for one billion years they would lose a considerable fraction of the argon present in position I by a process of diffusion. The mica-feldspar age discrepancy may be explained by diffusion from this position during geological time.

ACKNOWLEDGEMENTS

I wish to express my appreciation to Dr. H. Baadsgaard for his advice and assistance during the writing of this thesis.

My gratitude is extended to Dr. George Cumming, Department of Physics, for his assistance with the mass spectrometer, to Dr. R.S. Julius of the Computing Centre, for his advice on the mathematical relationships used to calculate the diffusion coefficients, and to Dr. W.S. MacKenzie, University of Manchester, for his helpful discussions on feldspar structure.

I wish to acknowledge the varied forms of assistance that have been given by members of the Department of Geology.

TABLE OF CONTENTS

	Page
ABSTRACT	i
ACKNOWLEDGEMENTS	iii
INTRODUCTION	1
<u>CHAPTER ONE</u>	
PREVIOUS WORK	2
<u>CHAPTER TWO</u>	
THE STRUCTURE AND STABILITY OF FELDSPARS.	16
<u>CHAPTER THREE</u>	
THE TECHNIQUE USED FOR THE DETERMINATION OF DIFFUSION COEFFICIENTS	
I. Introduction	27
II. Experimental technique	29
III. Mathematical treatment of the diffusion data	37
IV. Validity of this mathematical treatment	40
V. Calculation of the diffusion coefficients	42
VI. Method of presentation of the results.	47
VII. Accuracy of the measurements	48
<u>CHAPTER FOUR</u>	
EXPERIMENTAL RESULTS	
I. Kinnekulle sanidine	50
II. Millcreek sanidine	53
III. Crowsnest sanidine	58
IV. Yellowknife microcline	65
V. Montevideo microcline	69

CHAPTER FIVEON THE RELIABILITY OF THE CURVES OF THE
LOGARITHM OF THE DIFFUSION COEFFICIENT
AGAINST RECIPROCAL ABSOLUTE TEMPERATURE

I. Discussion and an alternative mathematical treatment	74
II. Comparison and appraisal of the curves obtained using the different mathematical treatments	78

CHAPTER SIX

DISCUSSION

I. Interpretation of the diffusion curves	88
II. Geological significance of the diffusion data	95
III. Conclusions	98

BIBLIOGRAPHY	99
------------------------	----

APPENDIX A

Values of $(Dt/a^2)^{1/2}$ against fraction of argon	104
--	-----

APPENDIX B

Experimental data	106
I. Kinnekulle sanidine	107
II. Millcreek sanidine	108
III. Crowsnest sanidine	111
IV. Yellowknife microcline	115
V. Montevideo microcline	117

APPENDIX C

Comparative chemical analyses of the samples	119
--	-----

LIST OF TABLES

		Page
Table 1	Si, Al disordering and charge balance in potassium feldspars	22

LIST OF FIGURES

Figure 1	The relationship between optic axial angle and chemical composition	17
Figure 2	The alkali feldspar phase diagram	21
Figure 3	A diagrammatic representation of the method	30
Figure 4	Design of the crucible furnace	32
Figure 5	A diagrammatic representation of the response curve of the mass spectrometer	43
Figure 6	A diagram indicating the methods used to calculate the fraction of argon released	44
Figure 7	Kinneville sanidine - curve of $\ln D$ vs. $1/T$ calculated using equations (3)-4 and (3)-5	52
Figure 8	Millcreek sanidine - curves of $\ln D$ vs. $1/T$ calculated using equations (3)-4 and (3)-5	56
Figure 9	Millcreek sanidine - curves of $\ln D/a^2$ vs. $1/T$ calculated using equations (3)-4 and (3)-5	57
Figure 10	Crowsnest sanidine - curves of $\ln D$ vs. $1/T$ calculated using equations (3)-4 and (3)-5	63
Figure 11	Crowsnest sanidine - curves of $\ln D/a^2$ vs. $1/T$ calculated using equations (3)-4 and (3)-5	64
Figure 12	Yellowknife microcline - curve of $\ln D/a^2$ vs. $1/T$ calculated using the equations (3)-4 and (3)-5	68
Figure 13	Montevideo microcline - curve of $\ln D/a^2$ vs. $1/T$ calculated using the equations (3)-4 and (3)-5	73
Figure 14	Kinneville sanidine - comparative curves calculated using both mathematical treatments	82

	Page
Figure 15 Millcreek sanidine – comparative curves calculated using both mathematical treatments	83
Figure 16 Millcreek sanidine – curves of the three grain sizes calculated using Wragge's mathematical treatment	84
Figure 17 Crowsnest sanidine – comparative curves calculated using both mathematical treatments	85
Figure 18 Crowsnest sanidine – curves of the three grain sizes calculated using Wragge's mathematical treatment	86
Figure 19 Yellowknife microcline and Montevideo microcline – comparative curves calculated using both mathematical treatments	87

INTRODUCTION

Feldspars, because of their wide geological distribution, were initially considered to be potentially one of the most useful minerals for isotopic dating by the potassium-argon method. Unfortunately, early measurements of the absolute age of feldspars demonstrated that variable losses of radiogenic argon occur during geological time and that the dates given by orthoclase and microcline are unreliable. (Wetherill et al., 1956, Wasserburg et al., 1956, Folinsbee et al., 1956, and others).

Greater interest in the loss of argon from feldspars was achieved when it was found that micas, cogenetic with microcline and orthoclase, frequently give ages that are concordant with other methods. The high retentivity of biotite and muscovite is, of course, enigmatic, as the basal (001) cleavage of micas would be expected to serve as a path for the loss of radiogenic argon. Further, subsequent age determinations indicate that biotite and sanidine from bentonites retain their argon quantitatively. (Baadsgaard et al., 1961).

In an attempt to ascertain the mechanism of argon loss from feldspars and other potassium minerals, the diffusion of argon at high temperatures has been studied and the activation energy of loss measured.

CHAPTER ONE

PREVIOUS WORK

In the past decade a significant number of papers have been published concerning the diffusion of argon from potassium minerals. Within these papers three theories are found that seek to explain those observed irregularities in diffusion that contradict the possibility of uniform loss of argon from the crystal lattice.

These theories are:

- a. That lattice changes occurring with rising temperature have a marked influence on the mechanism of argon loss.
- b. That argon atoms are held in more than one type of position within the crystal lattice. Each of these positions is unique and possesses a discrete energy of activation.
- c. That with rising temperature factors arise which influence the number of lattice vacancies. If it is assumed that argon diffuses through vacancy pairs in the lattice, then a close association would be expected between the number of vacancies and the rate of diffusion.

The experimental evidence by which these theories are sustained will be examined.

- a. Confirmation of the theory that lattice changes strongly influence rate of loss of argon is presented by many authors. Evernden et al. (1960) studied the diffusion of radiogenic argon from microcline, sanidine, leucite, glauconite and phlogopite. From their results they conclude that changes in the activation energy with rising temperature are a response to dynamic lattice changes, and are not a reflection of argon being lost from different lattice positions.

Their curve of $\log D$ vs. $1/T$ for microcline showed two inflections. [D = diffusion coefficient ($\text{cm.}^2/\text{sec.}$), T = absolute temperature.]. The first of these inflections occurred between 450°C. and 850°C. and was assumed to be a response to lattice disturbances caused by the mixing of perthitic layers in the microcline. Because the slopes of the diffusion curve below 450°C. and above 850°C. are virtually identical, it was concluded that the mechanism of diffusion from the perthitized and homogeneous feldspar was the same. The second inflection was observed above 1000°C. and was correlated with the disordering of the Si - Al atoms in the ordered microcline lattice. However in the published curves this inflection is not clearly seen.

The sanidine studied was homogeneous and monoclinic. The diffusion curve [$\log D$ vs. $1/T$] for this mineral was found to be a simple concave line throughout the temperature range $500 - 1050^\circ\text{C.}$ This must be taken as a reflection of the thermal stability of this sanidine lattice.

In leucite a decrease in the activation energy for the diffusion of argon was found in the temperature range $300^\circ - 600^\circ\text{C.}$ Evernden correlated this change to the second order transition from a pseudoisometric structure to a true isometric structure. Measurements of the electrical conductivity during this transition also show anomalous behavior, indicating an increased ionic mobility during the process of lattice transformation.

In both glauconite and phlogopite, a fall in the value of the diffusion coefficient was observed during the loss of hydroxyl ions from the lattice. Diffusion coefficients for phlogopite grains of equal thickness normal to the (001) plane, but of different dimensions in this plane, were obtained by invoking two theoretical diffusion models. One of these models satisfied the condition that diffusion takes place parallel to the basal (001)

cleavage, the other that it occurs normal to this cleavage. The diffusion model that satisfies the actual mechanism of argon loss, should give a similar solution for all grain sizes.

Evernden's results indicate that at temperatures below 600°C. diffusion occurs normal to the (001) cleavage, but that from 600 - 700°C. loss occurs parallel to this cleavage direction. This change of diffusion pattern is related to the separation of the (001) planes during the expulsion of water from the lattice. After all the (OH) radical is lost, diffusion again takes place in a direction perpendicular to the (001) cleavage with an activation energy of diffusion comparable to that found below 600°C.

b. The first suggestion that argon is held in more than one position came from Gerling and Morozova (1957, 1958). The experimental evidence for this concept is derived from plots of log (rate of argon loss) against time. Inflections or a progressive change in the slope of these curves were assumed to indicate loss of argon from more than one position. By obtaining a series of curves at successive temperatures, the number of such positions can be found.

Gerling and Morozova (1958) suggested that in a sample of microcline perthite, argon is retained in five positions. The first three positions contain 20 per cent of the total argon in the crystal and have activation energies of 15,000; 26,000 and 42,000 cal./mole respectively. The low value of the activation energy of these positions was correlated to an increase in the internal surface area of the lattice and a decrease in the effective grain size due to perthitization. The other two positions have very high activation energies (99,000 and 130,000 cal./mole) and it is suggested that diffusion from these positions is related to diffusion from the homogenized lattice.

Gerling and Morozova (1957) studied the diffusion of argon from biotite, muscovite, and phlogopite. In biotite they contend that argon is retained in three positions, the first of which contains only a few per cent of the total argon. Loss from this position occurs through lattice defects. The second position, which contains the greatest amount of the argon present, has an activation energy of argon loss of 57,000 cal./mole. Loss from the third position is associated with disruption of the crystal lattice.

Extremely strong criticisms of Gerling and Morozova's work have been published by Amirkhanov et al. (1960) and Brandt (1962). Amirkhanov's main points of criticism are:

- a. That the concept of different positions is difficult to reconcile with the modern theory of solids.
- b. That Gerling's mathematical treatment of his experimental data was incorrect and as a result his concept of positions is purely arbitrary.
- c. That the linearity of Gerling's curves is a result of the scale used for their presentation and the use of common instead of natural logarithm.

In a reply, Gerling, (1962), has partly justified himself, but it appears reasonable to agree with Amirkhanov that curves of the logarithm of the rate of argon lost against time cannot be used to provide conclusive evidence of argon in different lattice positions.

It is noticeable that in Gerling and Morozova's papers, insufficient concern has been given to the occurrence of lattice changes with rising temperature. Certainly in micas, the first 'position' can be most easily explained as due to loss of absorbed argon from grain boundaries. Further, the observation that the second position in

phlogopite contains 78 per cent of the total argon if the loss is observed at lower temperatures and only 34 per cent if measured at higher temperatures, can only indicate that the diffusion phenomena on which the second and third positions are founded are actually a reflection of loss of water from the mica lattice.

Amirkhanov et al. (1959) made diffusion studies on two pre-Cambrian feldspars. Unfortunately, petrological descriptions of the samples were not given. The diffusion behavior was explained by accepting the presence of argon in three positions, which are dependent on crystal structure. In the first feldspar the amount of argon in each position and the temperature at which argon loss occurs from these positions are:

Position I	$0.370 \text{ mm}^3 / \text{gm.}$ lost below 800°C.
II	$0.546 \text{ mm}^3 / \text{gm.}$ lost $800\text{--}1100^\circ\text{C.}$
III	$0.046 \text{ mm}^3 / \text{gm.}$ lost over 1100°C.

In the second feldspar the relevant data are:

Position I	$0.206 \text{ mm}^3 / \text{gm.}$ lost $500\text{--}650^\circ\text{C.}$
II	$0.659 \text{ mm}^3 / \text{gm.}$ lost $650\text{--}1050^\circ\text{C.}$
III	$0.067 \text{ mm}^3 / \text{gm.}$ lost over 1050°C.

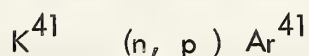
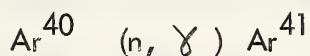
A further 'zero' phase was observed in the second feldspar, containing $0.060 \text{ mm}^3 / \text{gm.}$ Because the argon in this position is lost almost instantly below 400°C. it is suggested that this loss is due to desorption or to capillary diffusion possessing a small activation energy of argon loss.

In both feldspars the temperature at which argon begins to be lost from position II is 700°C. which is close to the temperature at which perthitic lamellae homogenize. Loss from position III begins at 1100°C. , which is close to the

temperature at which the order-disorder inversion is observed to occur at a reasonable rate. The lack of complete similarity in the diffusion characteristics of the two specimens was related to the influence of different alkali ion content on the lattice structure.

Diffusion coefficients at room temperature were found by extrapolation of the diffusion curves. Consideration of their values shows that volume diffusion is not an important process at low temperatures, but that desorption or capillary diffusion must account for the observed deficiencies of argon in these feldspars.

Hart (1960) conducted diffusion experiments on feldspar, muscovite, hornblende and pyroxene. The radioactive isotope of argon Ar^{41} , produced by bombarding the feldspar with fast neutrons, was used as a tracer in studying diffusion from an orthoclase - perthite. The possible reactions are:



The major advantages of the radioactive counting technique are the accuracy of the measurements, which can be made at room temperature, and the ease of counting procedures, which require no gas purification. Unfortunately, because of the possibility that neutron bombardment damages the crystal lattice, and the possibility that Ar^{41} is not present in the same structural positions as radiogenic argon, the data obtained using this technique is of uncertain geological significance.

The isothermal diffusion curve of activity vs. time for Ar^{41} found at 795°C. showed two segments, the first of which is assumed to represent diffusion from a stable structure. The second segment, which appears after heating for 50 minutes, indicates a higher diffusion coefficient and cannot therefore be explained by the assumption that

argon is present in a second position. The possibility that the second segment is a reflection of the homogenization of the perthitic lamellae, is not supported by X-ray study of heat treated samples. Although some structural change which cannot be "quenched-in" might have occurred, it is equally possible that the presence of two segments is related to lattice damage caused by the neutron irradiation of the sample. Hart concluded that there was no evidence that Ar^{41} is present in more than one activation site.

The diffusion of radiogenic argon from a similar sample of orthoclase - perthite was observed isothermally at 815°C. and 960°C. The results were plotted as values of $\frac{\pi^2 D t}{a^2}$ vs. t . (where t = time in minutes, a = radius of diffusion). From these studies it was concluded that argon is held in three lattice positions. The first of these positions was designated phase I, and was found to contain approximately 30 per cent of the total argon. The rate of loss from this position can be suitably explained either by the volume diffusion law, or as a solution to an equation that expresses the discharge of argon as a process of surface desorption. Phase II contains 50 per cent of the total argon and Phase III the remainder. If no structural changes occur between 815°C. and 960°C., then the activation energy of argon loss from phases I and II can be determined from the value of the diffusion coefficients at these temperatures. The activation energy of phase I is low, 15,000 cal./mole, indicating the ease of diffusion from this position. It was suggested that the mica - feldspar age discordancy could be explained if a quantity of argon equal in amount to that contained in phase I, were held in a further position of much lower activation energy.

By a comparison of the diffusion of Ar^{41} and Ar^{40} , evidence is obtained in support of the concept that argon is held in a number of structural positions within the feldspar lattice. Hart concluded that Ar^{41} shows simple diffusion because it is held

only in the position of the parent Ar^{40} atom. In contrast, he suggests that radiogenic argon has been redistributed by some later process to at least three lattice positions. However, it is very clear that lattice changes associated with homogenization of the perthitic lamellae could be the cause of the segmented diffusion curves.

c. Reynolds (1957) published diffusion data for a perthitic orthoclase - microcline and a cogenetic lepidolite. He found no evidence of a mica - feldspar age discrepancy. He suggests that if argon diffuses by migration through lattice vacancies in the perthite, then the rate of diffusion will depend on two factors. The first of these is the volume density of vacancies, and the second, the activation energy of the migration of rare gas atoms between these vacancies. A $\log D$ vs. $1/T$ plot would show three distinct regions, a low temperature region where diffusion takes place through lattice vacancies, the density of which is controlled by the number of bivalent atoms (impurities) in the lattice. Secondly, there is a transition region, then a third high temperature region, where a great increase in the number of lattice vacancies due to Schottky defects results in a decrease in the activation energy of argon loss.

A similar solution was proposed by Gentner et al. (1953, 1954) and Amirkhanov (1959) to explain the diffusion of argon in sylvite. If it is assumed that argon loss takes place through $\boxed{\text{K}^+} \boxed{\text{Cl}^-}$ vacancy pairs, then three factors that control the energy of activation can be found:

1. Component E_1 - which accounts for the probability of a jump of a Ar^{40} atom through a vacancy pair.
2. Component E_2 - which accounts for the activation energy required for the formation of vacancy pairs.
3. Component E_3 - which accounts for the mobility of the vacancy pairs.

Below 550°C. the density of $\boxed{\text{K}^+} \boxed{\text{Cl}^-}$ vacancy pairs was believed to be due to the bivalent impurity content of the lattice. With rising temperatures these vacancy pairs are dissociated, and Schottky defects are formed in large numbers, accounting for the observed drop in the energy of activation for argon loss from sylvite.

The final paper to be considered in detail is that of Baadsgaard et al. (1961). In this paper all the preceding theories are used to explain the observed diffusion anomalies. The diffusion of argon from two samples of sanidine and one of microcline was studied, the results being plotted on a curve of $\log D$ vs. $1/T$.

The Crowsnest sanidine was found as large zoned phenocrysts in a lava. On the basis of X-ray powder studies, it was contended that the zoning was not due to compositional variations, but to structural variations formed as a response to changes of temperature during crystallization. Three phases of diffusion were found. The first contains 6 per cent of the total argon and is lost from the crystal below 200°C. This phase was compared to the 'zero' phase of Amirkhanov et al. (1959) and evidence for its existence comes not from the diffusion data, but from the age deficiency of this sanidine when compared to cogenetic biotite. The presence of the other two phases is indicated by the change in the slope of the diffusion curve at 700 - 800°C. The theory advanced by Reynolds, (1957), was considered as a possible explanation of these segments, though it is clear that this explanation is not consistent with the uniform diffusion characteristics which have been observed in the Kinnekulle sanidine (this same paper), or in the Bishop sanidine (Evernden et al., 1960).

The proposal by Gerling and Morozova (1957, 1958) that argon is held in more than one lattice position was also considered. The activation energies of these positions could be dependent upon the proximity of the argon atoms to defects or

discontinuities in the regular lattice structure. The zoning observed in the Crowsnest sanidine could be a factor influencing the diffusion of argon. No lattice rearrangements could be observed by X-ray studies of samples heat treated to temperatures above 1000°C.

The Kinnekulle sanidine consists of fresh, generally untwinned grains and gives a concordant age with cogenetic biotite. The curve of $\log D$ vs. $1/T$ is a straight line, which is accepted as being indicative of simple diffusion from the lattice. This interpretation is supported by X-ray data, for no evidence is found of structural change in a sample heat treated to 900°C. for 24 hours. There is no indication of an increase in the volume density of vacancies, and consequently Reynolds' diffusion model does not provide a satisfactory solution to the experimental data.

The third sample studied was a microcline from Yellowknife. Age comparison with cogenetic muscovite indicates that there is a 36 per cent deficiency of argon. Polysynthetic twinning is prominent in the grains, and although no perthitic lamellae were observed optically, a slight shift in the (201) peak on heating suggests that some sub-microscopic exsolution might be present. The 2V was 83° perpendicular to the (010), indicating that the sample is close to maximum microcline. (MacKenzie and Smith, 1956).

The diffusion curve below 700°C. is approximately a straight line, suggesting that the diffusion of argon from the microcline is a simple process, possibly volume diffusion. Above 700°C. there is a decrease in the gradient of the slope, indicating a drop in the activation energy. This is possibly the result of structural change in the twinning or the cryptoperthitic texture.

The 36 per cent argon deficiency in the Yellowknife microcline is thought to be lost at temperatures below 200°C. and must therefore have a low energy of activation. Similar deficiencies have been observed in other feldspars, and in many

cases the deficiency is about 35 per cent regardless of the age of the feldspar. However in other cases no mica-feldspar age discordancies have been found.

A broad appraisal of previous work implies that argon which is lost at low temperatures from the feldspar lattice, belong to one particular type of position. The major contribution of this interpretation is that it suggests an explanation for the loss of argon from the feldspar lattice.

It is reasonable to assume that the initial position of the argon atoms within the crystal lattice is that of the parent K^{40} atom. Since argon is a member of the group VIII elements, the only form of chemical bonding possible with the surrounding atoms are van der Waals bonds, and these are too weak to explain the high degree of argon retention found in the mica and feldspar lattices. As a consequence it can be inferred that the argon atoms, being larger than the parent K^{40} atom, distort the lattice, and in turn are enclosed within the lattice framework.

This interpretation is supported by the determined values of the activation energy. Baadsgaard et al. (1961) found that the energy of activation for the diffusion of argon from the Kinnekulle sanidine was 52 K cal./mole. In each of two samples of feldspar Amirkhanov et al. (1961) found two positions, the activation energies of which are, for the feldspar (N 35): 33.6 and 98.0 K cal./mole respectively, and for feldspar (N 65): 36.5 and 39.0 K cal./mole. Gerling and Morozova (1957) give the bond energy for the Si - O bond as 98 K cal./mole, which is of the same order as the determined values for the diffusion of argon from micas and feldspars. It is therefore a reasonable conclusion that argon is held in the feldspar lattice by the bond strength of the (Si, Al-O) framework. Further evidence for such an interpretation is given by diffusion curves, which indicate a strong dependence between rate of argon diffusion and lattice changes (Evernden, 1961, Sardarov, 1961).

Diffusion experiments on orthoclase and microcline indicate that only a fraction of the argon in low temperature feldspars is easily lost, and that the major part is held more strongly than in sanidine or micas. (Gerling and Morozova, 1956). It can be concluded that the strongly held argon is retained in the lattice by the (Si, Al-O) bonds, and that the argon that is lost during geological time must be held in a much weaker position(s).

This concept immediately raises the following questions:

- a. How do argon atoms find their way from the original K^{40} position to the new position(s)?
- b. What is the nature of the new position(s)?
- c. How is the argon lost from these position(s)?

It is clear that these questions cannot be fully answered from the published experimental data. Physical evidence rejects the possibility that the recoil energy (30 ev.) associated with K - electron capture in the parent K^{40} atom be sufficient to force the daughter Ar^{40} atom through the lattice to a grain boundary, or any other position from which loss could easily occur. This conclusion is supported by the age concordancy shown by micas and sanidine with other dating techniques.

Sardarov (1957), on the basis of the age of 21 cogenetic pairs of microcline and mica, states that a broad correlation exists between the degree of age discordancy and the extent of perthitization. He also finds that the extent of age discordancy is not dependent on the age of the minerals and suggests that the replacement of potassium by sodium ions causes a distortion of the lattice, creating conditions favourable for the escape of argon atoms. This contradicts the tentative proposal of Reynolds (1957) that the argon is concentrated in the sodic phase of perthites.

Paul Pronko (unpublished M.Sc. thesis, University of Pittsburgh, 1962), found increased electrical conductivity in the direction of the cross-hatch twinning in microcline and along the planes of perthitization. As conductivity is related to potassium ion mobility it is highly probable that the ease of argon diffusion also increases in these directions.

Further evidence in support of the theory that perthitization and the degree of age discordancy are related, is provided by Kus'min (1960). He states that the loss of argon is proportional to the deformation of the feldspar. Fractures formed during deformation and during the process of perthitization, aid the escape of free argon and provide paths through which metasomatic changes, such as albitization may occur.

It appears reasonable to conclude that microclinization, perthitization and fracturing associated with these processes, produce channelways along which argon can escape from the feldspar lattice, and through which processes such as albitization and leaching can occur. In fairness, a paper by Murina and Sprintsson (1960) must be mentioned, that partly contradicts these speculations. On the basis of their investigations of argon loss from sanidine, orthoclase, and microcline, they assert that there is no direct connection between perthitization of feldspars and argon loss. Also Reynolds (1957) finds no argon deficiency in a 92 m.y. perthitic orthoclase - microcline.

More conclusive evidence for a position in feldspars from which argon is lost at low temperatures is provided by Gerling and Morozova (1957) and Amirkhanov (1957, 1958). They find that in micas, sylvite, and feldspars, a certain amount of loosely held argon is lost by desorption at low temperatures. Amirkhanov (1961) recognizes two zones, a 'steady' zone, which corresponds to argon in the undisturbed lattice and an 'unsteady' zone from which escape of argon is possible. Argon in the

'unsteady' zone may be removed by heating at 400°C. for 3 hours, and the potassium in this zone removed by exchange with thallium by heating the feldspar at 600°C. in a solution of TlNO_3 . Experimental evidence indicates that only a definite fraction (27-30 per cent) of the potassium is capable of being removed. This is in agreement with the concept that only that part of the argon in close proximity to plains of 'disturbance' can be lost at room temperature.

In this discussion of previous work, no rigid solution to the mechanism of argon diffusion has been achieved. While it would be incorrect to completely accept any of the suggested interpretations, I hope that this analysis of previous work does indicate those advances that have been made on the problems of the mica - feldspar age discordancy.

CHAPTER TWO

THE STRUCTURE AND THE STABILITY OF FELDSPARS

A brief consideration of the structure of feldspars and the stability fields of the various polymorphs is necessary in order to discuss the observed anomalies in argon diffusion. It should be realized that some of the concepts presented here are not agreed upon by all authorities in the field of feldspar research and that in the future they may be disproved or modified. In order to avoid excessive simplification, it will be assumed that the reader has a basic knowledge of feldspar structure, such as may be obtained in textbooks. (ie. Berry and Mason - Mineralogy).

The alkali feldspars occur in several polymorphic forms which have different, but interrelated optical and physical properties. The classification presented here is that which appears to have the widest acceptance (Figure 1).

a. Structure

Taylor (1933) determined the structure of sanidine. A summary of Taylor's work on sanidine is given by Bragg (1937). Structurally the feldspars are tectosilicates, each $(\text{Si}, \text{Al}-\text{O}_4)$ tetrahedra being joined at each of its corners to neighbouring tetrahedra. Every Si, Al atom is, therefore, surrounded tetrahedrally by four oxygen atoms and each oxygen atom is linked to two Si, Al atoms. Every group of four tetrahedra is linked to form rings, and these rings are stacked parallel to the a -axis. The rings are joined by sharing common oxygen cations to form chains. The chains are linked by sharing oxygen and alkali cations with other chains on all sides. This method of linking results in a three dimensional network of linked tetrahedra. All feldspars have this same basic structure which serves as an explanation of their closely related properties. The different feldspar polymorphs are

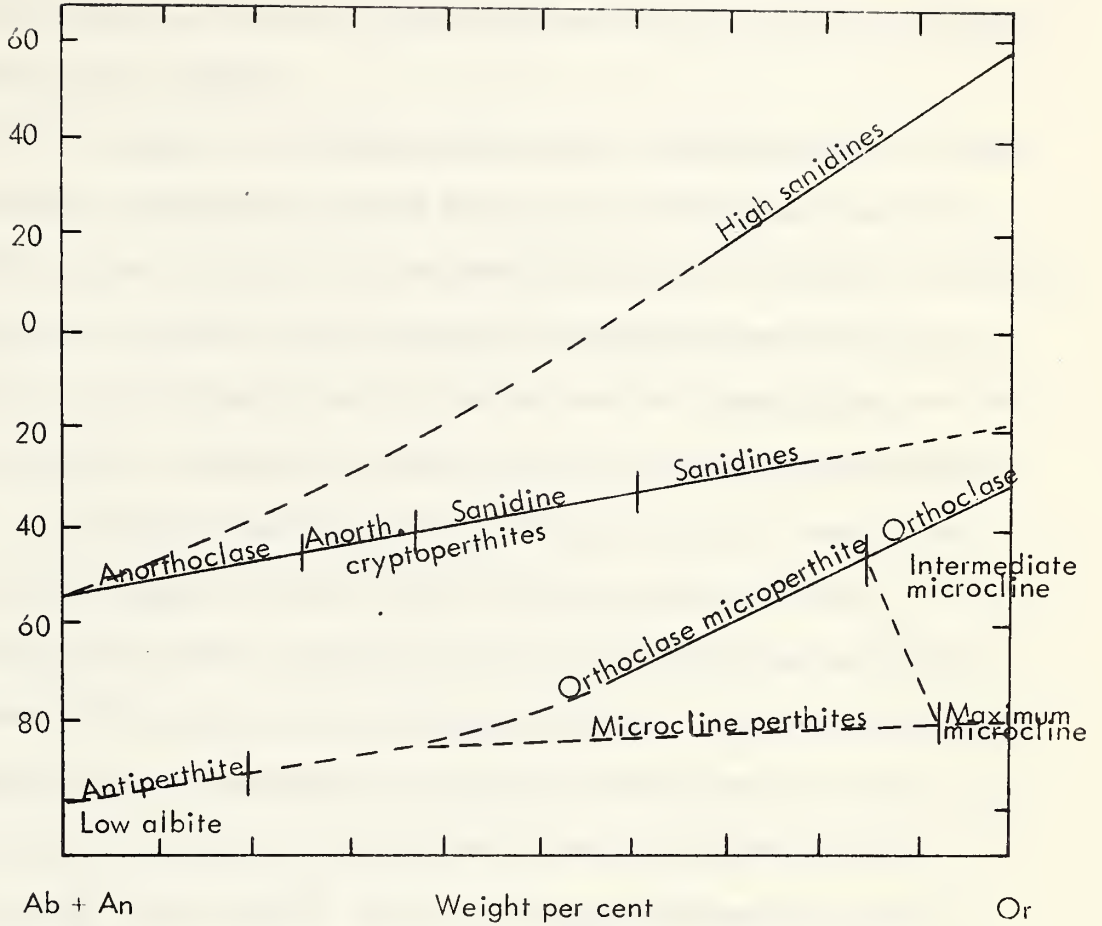


FIGURE 1. The relationship between the optic axial angle and chemical composition, after MacKenzie and Smith (1956) modified after Tuttle (1952). The parts of each series in which homogeneous specimens occur are separated from those in which the specimens are generally unmixed.

a reflection of variations in the structure due to order - disorder relationships between the Si, Al atoms and the influence of different proportions of K, Na, Ca, and Ba ions that link the structure together.

The first suggestion that feldspars showed order - disorder relations between the Si, Al atoms, resulted from a study of the symmetry relationships of sanidine by Taylor (1933) and Barth (1934). They concluded that sanidine is completely disordered with respect to Si, Al atoms, the Al being equally divided between the two sets of structurally equivalent atoms (Si_1 and Si_2) that are required to explain the monoclinic symmetry of sanidine. Conversely, maximum microcline is triclinic and completely ordered. It has four sets of atoms [$Si_1(o)$, $Si_1(m)$, $Si_2(o)$, $Si_2(m)$], three of which hold the twelve Si atoms, the fourth $Si_1(m)$, containing the four Al atoms.

The concept of order - disorder of the Si, Al atoms has been confirmed by determinations of the structure of some feldspar polymorphs. Jones and Taylor (1961) determined the structure of a pegmatitic orthoclase and found that the average value of the Si-O interionic distance in the first site Si_1 was 1.652 \AA and in the non-equivalent site Si_2 it was 1.633 \AA . Since the interionic distance for pure Si-O groups is 1.60 \AA and for pure Al-O groups is 1.77 \AA (Smith, 1954), the value of the Si-O distance for unheated orthoclase indicates partial ordering of the Si and Al atoms.

Cole, Sörum and Kennard (1949) studied the same feldspar that had been sanidinized by heating and found that the Si-O distance in both tetrahedral sites was 1.642 \AA , which indicates a completely disordered Si-Al distribution.

Bailey and Taylor (1955) determined the structure of a triclinic microcline. The values of the mean bond length of the four nonequivalent tetrahedral sites and their Al content indicates partial ordering.

b. Stability

The stability relations of the various feldspar polymorphs is an intricate problem due to the great complexity of the feldspar structure and because the synthesis of a low temperature ordered polymorph has never been achieved.

Dry heating experiments show that sanidinization of an ordered or partially ordered feldspar does not occur at an observable rate at temperatures below 1000°C. It must be realized that this temperature indicates nothing concerning the stability field of sanidine, since disordering at this temperature is probably a metastable transformation. Given a long period of geologic time it is conceivable that sanidinization will occur at a lower temperature.

Laves and Goldsmith (1954) found that the lowest temperature at which microcline recrystallized under hydrothermal conditions to form sanidine was 525°C. However it is clear from observation of natural feldspars that this temperature is again of uncertain significance. It is very possible that crystallization under hydrothermal conditions is metastable. The occurrence of adularia showing monoclinic symmetry (Chaisson, 1950) indicates that feldspars crystallizing rapidly at low temperature may do so in a metastable field.

The theory suggested by Hafner and Laves (1957) has clarified the relationships between the different feldspar polymorphs. They suggest that there are different ways of passing from the completely disordered sanidine structure to the fully ordered maximum microcline. The two extreme paths are:

- a. That three tetrahedra lose all their Al in one step to the fourth position $Si_1(m)$.
- b. Conversely, it is possible that two tetrahedra lose all their Al equally to the two other tetrahedra, $Si_1(o)$ and $Si_1(m)$ and then one of these tetrahedra loses all its Al to the fourth tetrahedra, $Si_1(m)$ to form maximum microcline.

This theory of multiple paths has been generally accepted. Its main advantage lies in that it helps to develop a concept of the stability relations between the feldspar polymorphs. During the first stage when the Al is lost to two sites, the feldspar remains monoclinic, and it is only during the second stage when loss to one position occurs, that the feldspar must become triclinic.

On this basis Smith and MacKenzie (1961) propose a stability field for orthoclase. If sanidine inverts to maximum microcline by a two stage process, the tendency for the first stage to occur must be higher than for the second, or a one stage process would be operative. It is possible that the stability field of orthoclase differs so little from that of microcline that it will persist almost indefinitely if other factors, such as stress, did not provide the additional activation energy to make the second stage of loss to the $Si_1(m)$ tetrahedra occur.

At present it seems generally agreed that the stable polymorph at low temperature is maximum microcline and that at high temperature is completely disordered sanidine. Figure 2 is a tentative phase diagram published by MacKenzie and Smith (1961). The great importance of this figure is that it illustrates the relationship between Si, Al order - disorder and Na, K order - disorder, and suggest an approximate temperature scale for feldspars with various degree of disorder.

Ferguson, Traill and Taylor (1958) have dissented from this opinion, and on the assumption that electrostatic charge balance controls stability, propose that orthoclase is the stable polymorph at low temperature and that microcline is metastable. Table 1 is taken from Jones and Taylor (1961) and indicates the degree of ordering of the polymorphs in which the structure has been determined, and their balance of charge.

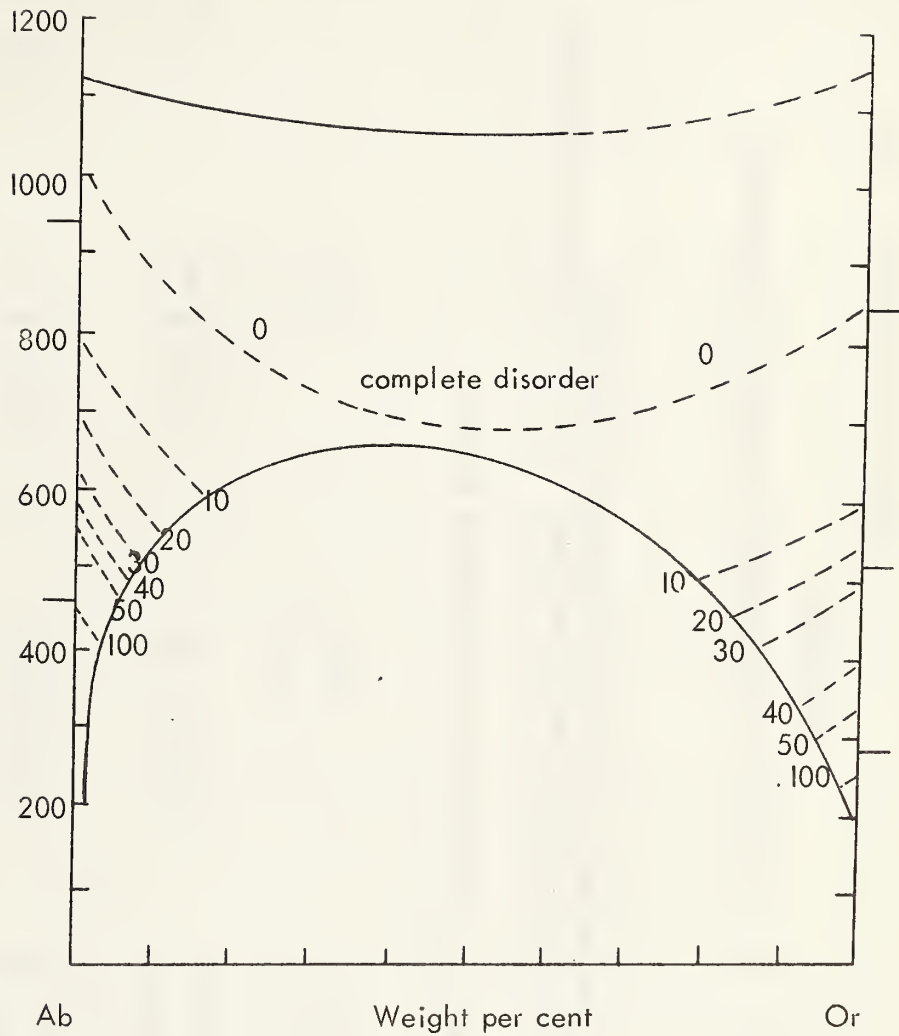


FIGURE 2. The alkali feldspar phase diagram after MacKenzie and Smith (1961). The numbers from 0 to 50 to 100 indicate the percentage of Si,Al ordering. The numbers on the ordinate indicate the temperature of stability of each degree of order.

Tetrahedron	Microcline	Sanidine	Orthoclase (Spencer C)	Orthoclase (ideal)
Si ₁ (o)	0.25 Al 8.11 }			
Si ₁ (m)	0.56 Al 7.87 }	0.25 Al 8.05	0.30 Al 8.03	0.36 Al 8.00
Si ₂ (o)	0.07 Al 8.00 }			
Si ₂ (m)	0.08 Al 8.08 }	0.25 Al 7.94	0.19 Al 7.98	0.14 Al 8.00
	<hr/>	<hr/>	<hr/>	<hr/>
	0.32	0.22	0.10	0.0
				<hr/>
				0.0

A. is the total deviation from balance for the four tetrahedral groups.

B. The nomenclature for microcline is that of Bailey and Taylor (1958). The figures for balance of charge for microcline, sanidine and ideal orthoclase are taken from Ferguson et al. (1958).

TABLE 1. Si, Al ORDERING AND CHARGE BALANCE IN POTASSIUM
FELDSPARS

(After Jones and Taylor, 1961)

It can be seen from Table I, that if charge balance determines the stability of the polymorphs, then orthoclase must be the most stable polymorph and sanidine is more stable than microcline. Ferguson et al. (1958) using charge balance as a measure of stability, also propose that the most stable sodium feldspar is highly-ordered albite.

Their theory of the origin of microcline follows directly from this concept. A highly-ordered Si, Al framework, characteristic of highly ordered low albite is formed at high temperatures due to the influence of a high sodium content. It is suggested that with cooling, a temperature is reached at which the Al-O, Si-O bonds are too strong to be broken by thermal vibration, but at which Na and K ions are still mobile. At a still lower temperature, the sodium is replaced by potassium and a highly-ordered potassium feldspar is formed. It will be noticed that this feldspar will have an electrostatic charge unbalance.

Much theoretical and observational evidence contradicts the theory that charge balance controls stability. Firstly, this theory assumes that the bonding in feldspars is exclusively ionic. Further, during the determination of electrostatic charge balance, Ferguson presupposes that ionic forces act over long distances. Both of these assumptions are of uncertain validity. The belief that the Al-O, Si-O bonds are immobile at low temperatures was suggested by Ferguson because on heating sanidinization does not occur at an appreciable rate below 1000°C. But this heating is a non-equilibrium process. Observation of natural feldspars suggests that ordering processes may occur at relatively low temperatures.

It is also found that microcline-perthite is the most characteristic feldspar of the oldest rocks and of pegmatites, which suggests that microcline is more stable at low temperatures than either orthoclase or sanidine. The effect of heating microcline

or orthoclase is to produce sanidine, which indicates that sanidine is stable at high temperatures. MacKenzie and Smith (1959) conclude that while the influence of electrostatic charge balance is important in controlling which tetrahedra the Al enters, other factors such as entropy and the internal energy of the lattice are of greater importance in determining the stability of each polymorph.

Order - disorder of Na, K as expressed by perthitic texture, is probably one of the most commonly realized features of feldspars. The origin of perthites is indicated by the work of Bowen and Tuttle (1950) on the system $\text{NaAlSi}_3\text{O}_8$ - KAlSi_3O_8 - H_2O . At high temperatures complete solid solution exists between sodium and potassium feldspars, but with falling temperature the mutual solubility declines and under conditions of slow cooling a feldspar of composition of approximately Or_{50} - Or_{95} will unmix to form domains within the crystal, some of which are sodium rich, the others potassium rich. These domains are expressed as lamellae parallel to the 100. Heating of perthites at 700°C. for 24 hours or at 950°C. for 1 hour will homogenize the feldspar, but on slow cooling the lamellae will reappear in those positions they held prior to homogenization. This may be interpreted as showing that the (Si, Al-O) framework in the sodium rich and the potassium rich domains has a different degree of order. If this interpretation is correct, then ordering must be able to occur at a low temperature. It must be stressed that there is a strong interdependence of Al, Si order - disorder and Na, K order - disorder. Development of order must also be strongly affected by substitution of Ca and Ba atoms in the alkali feldspar lattice, as these will result in the addition of extra Al atoms in the structure.

It has been shown by Laves (1950) that the cross-hatch twinning in microcline indicates that the feldspar crystallized with monoclinic symmetry, the twinning being a result of an inversion from monoclinic to triclinic symmetry. If the theory of ordering

by paths, as suggested by Hafner and Laves (1957) is correct, it is reasonable to correlate the twinning in microcline with the inversion from partially ordered orthoclase to ordered microcline.

Since it appears possible that the stability of orthoclase differs so little from that of microcline that it will persist almost indefinitely, unless an effect such as stress provides the necessary activation energy for conversion to microcline, the inversion may occur at a considerable time after crystallization. During this inversion argon could be lost from the lattice. Further, it has been found that orthoclase may have up to 15 per cent Na in the lattice, while maximum microcline does not contain more than 7-8 per cent Na in the K - feldspar lattice. This indicates that alkali mobility could occur at a fairly low temperature.

In conclusion, the influence of structure on diffusion at high temperatures will be considered. It is possible that increased ease of diffusion will occur along planes of perthitic lamellae, twin planes, and planes of structural or compositional zoning. This is sustained by the observance of increased electrical conductivity in this direction by Pronko (1962).

In diffusion experiments at progressively higher temperatures, the effect of homogenization of the perthitic lamellae would be expected to be observed. A more significant change in the rate of diffusion should be observed during disordering of Si, Al atoms, for this transformation requires the breaking of the Si-O, Al-O bonds. Since dry heating experiments indicate that disordering does not occur below 1000°C. in the time available for the experiments, it might be presumed that disordering will have no effect on the rate of diffusion below this temperature. However it is possible that this temperature is one of metastability and the influence of disordering might be observed at a lower temperature.

It is also very possible that reversible displacive transformations occur in feldspars during heating to high temperatures. These transformations, which could have a marked effect on the rate of diffusion, could only be detected by X-ray studies on a hot stage.

CHAPTER THREE

THE TECHNIQUE USED FOR THE DETERMINATION OF DIFFUSION COEFFICIENTS

1. Introduction

This thesis presents the determination of the diffusion coefficient for radiogenic argon in nine samples of feldspar at a series of temperatures from 350 - 1230°C. In two feldspars, experiments with three different grain sizes were made in order to ascertain whether the physical grain size is the effective radius of diffusion. In addition detailed X-ray and petrographic analyses of the samples were made in order to obtain a greater knowledge of the influence of the feldspar lattice on the mechanism of diffusion.

The diffusion coefficient of argon in feldspars may be found from a solution of Fick's law, for those boundary conditions that define volume diffusion from a sphere.

This solution is (Crank, 1956):

$$f = 1 - \frac{6}{\pi^2} \sum_{n=1}^{\infty} \frac{1}{n^2} e^{-\frac{n^2 \pi^2 D t}{a^2}} \quad (3) - 1$$

Where f = fraction of argon released in time t .

t = time of diffusion in seconds.

D = diffusion coefficient.

a = radius of the sphere.

A description of the mathematical treatment will be given later in this chapter. It is seen that this equation expresses the fraction of argon released in a given time t , as a function of the diffusion coefficient.

The first experimental technique used to determine the fraction of argon released involved heating the potassium mineral to a known temperature for a given period of time, and collecting the argon released in activated charcoal cold traps. The amount of argon released is determined using a McCloud gauge or by the isotope dilution technique. Knowing the total volume of argon present in the original mineral, the fraction of argon released during any time interval can easily be calculated.

Because this method of determining the fraction of argon released is extremely time consuming, it was natural that an attempt would be made to develop a more rapid technique. Gerling and Morozova (1958) determined the rate of argon release from a microcline-perthite by passing the argon lost from a mineral during heating directly into a mass spectrometer. Since the response of the mass spectrometer is proportional to the amount of argon entering the tube, they were able to determine the rate of loss of argon from the crystal with time.

A similar method was used in this thesis. The argon released from the feldspar crystal during heating, was passed directly into the tube of a mass spectrometer. As the response of the mass spectrometer is proportional to the amount of argon entering the tube, the area under the curve of response against time must be proportional to the volume of argon released. If all the argon is lost from the crystal, the total area under the curve can be measured and the fraction of argon released at any time after the beginning of the experiment may be calculated.

II. Experimental Technique

General considerations

A weighed sample of feldspar was placed in a silica crucible, which was then joined to the sample inlet of a 60°, 6 inch Nier-type mass spectrometer for gases. After the sample system had been outgassed to 10^{-7} - 10^{-8} mm. Hg., the valve to the sample pumping system was closed and the valve to the mass spectrometer opened. The furnace surrounding the silica crucible was then raised to a temperature at which a measureable rate of argon diffusion from the feldspar occurred. The argon released was cleaned by passage through a cold finger cooled in liquid nitrogen, and through a titanium sponge getter heated at 750°C. The argon was passed directly into the mass spectrometer and the positive ion current measured using a vibrating reed electrometer. The voltage, after amplification, was recorded on one pen of a two pen recorder. The other pen recorded the output of the calibrated Pt - Pt 13% Rh. thermocouple used to determine the temperature of the furnace. A diagrammatic representation of the method is given in Figure 3.

Description of the equipment

Crucible. - The silica crucible was approximately 15 cms. in length, had an external diameter of 9 mm. and an internal diameter of 7 mm. This diameter crucible was selected because a 1 gram sample would fill it to a length of 2 cms. This sample length permits a compact furnace design. In addition the spacial arrangement of the sample within the furnace ensures a uniform temperature over the whole length of the sample and allows accurate measurement of the temperature.

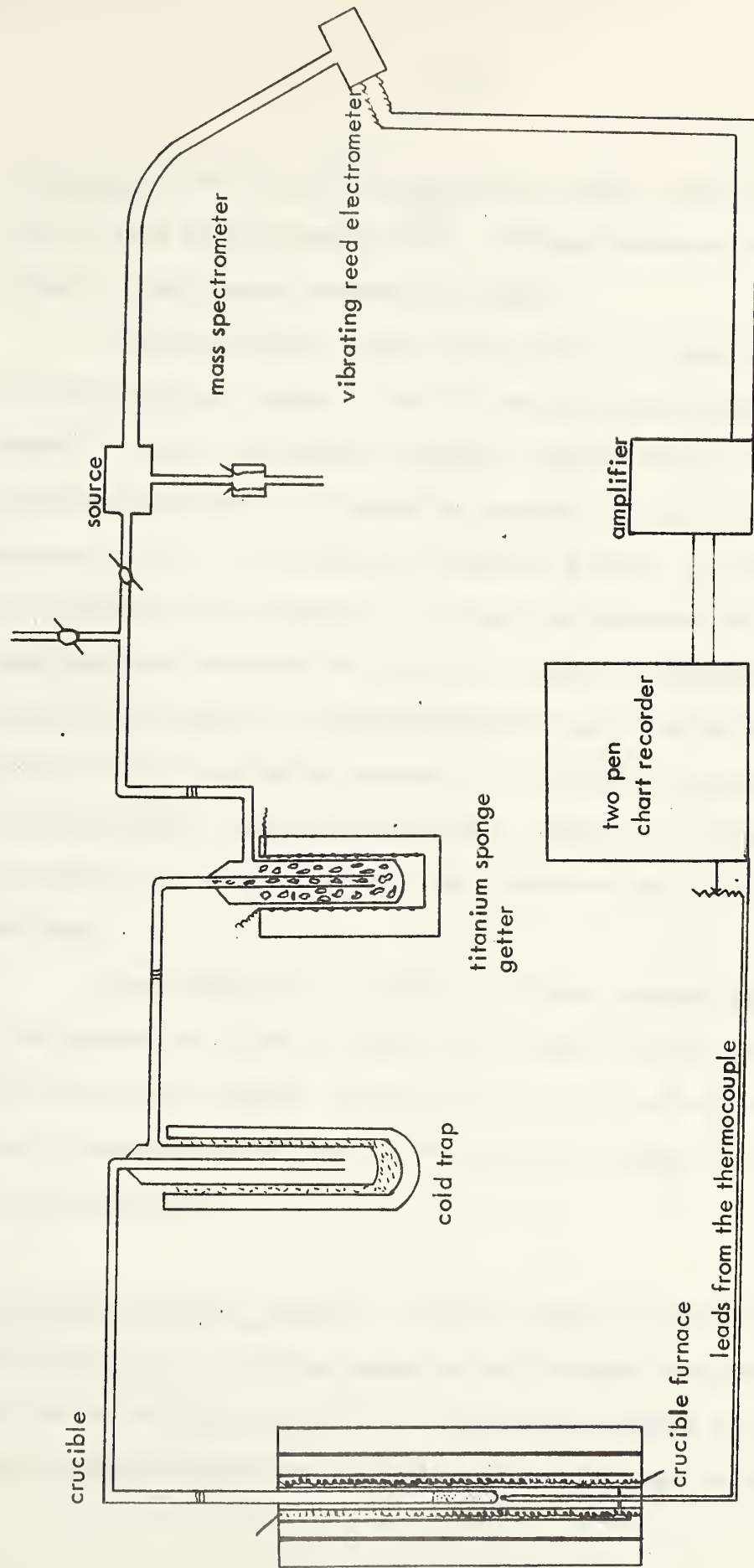


FIGURE 3. A diagrammatic representation of the method.

The furnace. - The silica crucible was held in a vertical position and heated by a furnace capable of being used to 1250°C. The major features of the furnace design is shown in a longitudinal cross-section in Figure 4.

The heating elements used in the crucible furnace were made of Kanthal A-1 wire of 0.25 mm. diameter. The wire was wound around a glass form 3 mm. in diameter, in order to make coiled elements of a suitable diameter to place inside the quartz form which was used to support the elements. The quartz form had an internal diameter of 2.3 cms. and an external diameter of 2.8 cms. Six notches were cut in both ends and six coiled elements were placed lengthwise along the inside of the form. The elements were retained at the ends by the notches, and imbedded in alundum. The placing of the elements in a longitudinal position assures that the heat production is uniform along the length of the furnace and so minimizes the possibility of a temperature gradient over the sample position. The furnace was insulated by asbestos and alundum. An outer layer of Sauereisen cement was used to give a hard coat to the furnace.

As each element had a resistance of 20 ohms, a furnace could be made with a final resistance of 30 ohms by joining three elements in series and then joining two sets of three coils in parallel. When running at 90 volts such a furnace would have an output of approximately 300 watts and the temperature inside, with this design, was approximately 1250°C.

Purification of the argon released. - The silica crucible was connected by a quartz-graded glass-pyrex seal to a cold finger cooled by liquid nitrogen during the experiments. The length of the cold finger was 15 cms. and the external diameter was 2.5 cms. Another quartz-graded glass-pyrex seal was used to join the cold finger to the titanium sponge

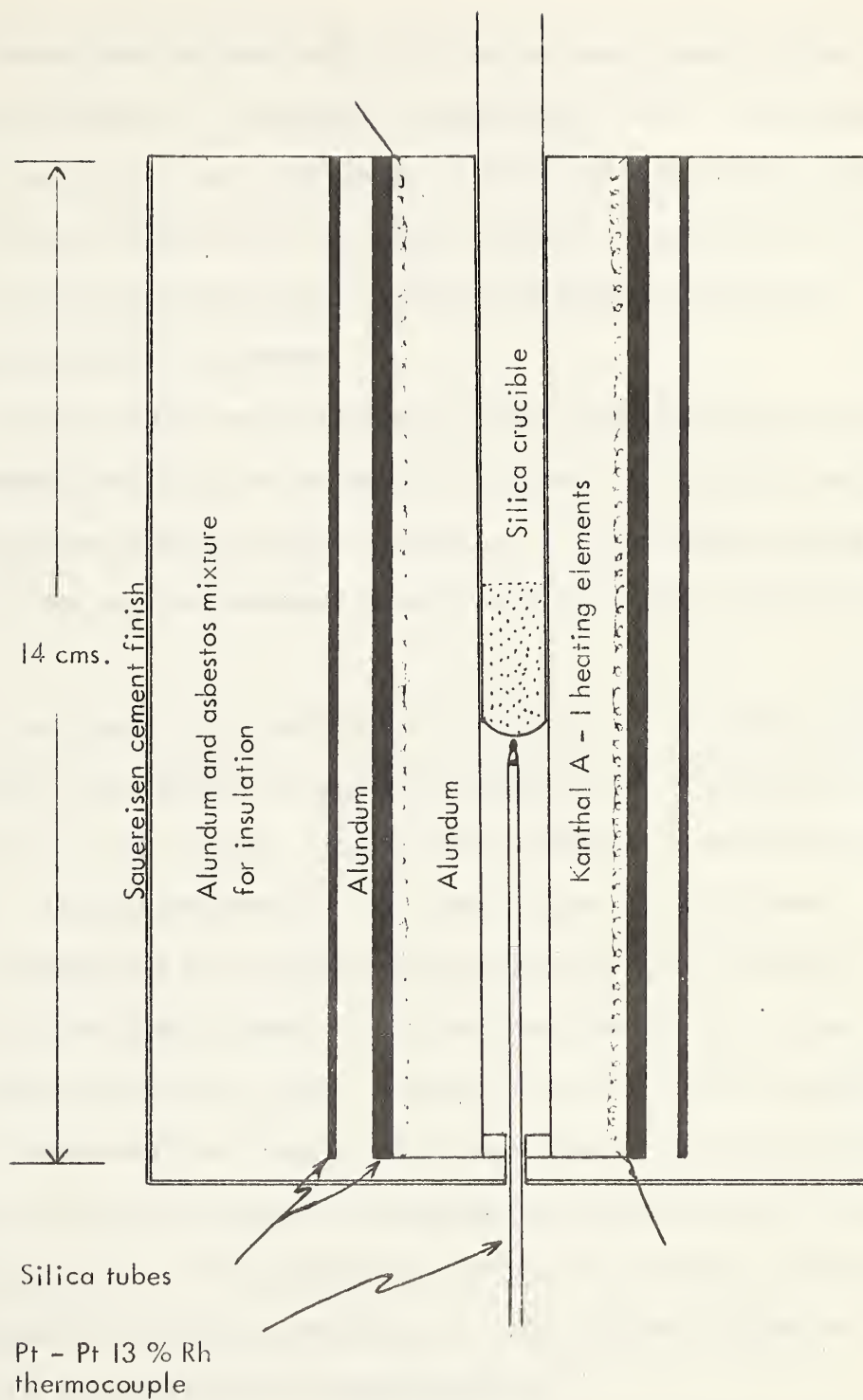


FIGURE 4. Crucible furnace design. (natural scale)

getter. The getter tube was made out of silica and was approximately 10 cms. long and 1.5 cms. in diameter. It was heated at approximately 750° C. during experiments. The getter heater was of a very simple design, a spiral screw was made in a silica tube 2.5 cms. in external diameter and 8 cms. long. Kanthal A-1 tape (0.8 mm. wide) was wound in these grooves and the furnace insulated with asbestos and alundum. The voltage was controlled by a powerstat.

The titanium getter was connected by a quartz-graded glass-pyrex seal to the leads of a mass spectrometer, and the argon was passed directly into the tube of the spectrometer. Because the tube was pumped during the experiment, it is reasonable to assume that the response of the mass spectrometer is proportional to the amount of argon entering the tube.

The mass spectrometer used was a Nier 60° type, with a six-inch tube. The positive ion flux is measured by a vibrating reed electrometer, amplified and recorded on one pen of a two pen recorder. Since the rate of diffusion increases greatly with temperature, a series of calibrated shunts are used to keep the pen on scale.

The temperature of the crucible was determined by a Pt - Pt 13% Rh thermocouple placed through a small hole in the lower surface of the crucible furnace in such a position that the tip is almost touching the base of the silica crucible. The output of the thermocouple was recorded by the second pen of the chart recorder and in this manner a continuous record of the temperature was made alongside the output of the mass spectrometer. The advantage of recording the temperature in this manner lies in the simplicity of operation and because it is the only way in which the temperature can be easily held at any determined level.

Since the pen recorder gives a maximum scale reading with an input of 10 millivolts, and the output of the thermocouple at 1200°C. is over 13 millivolts,

it is necessary to lower the input voltage to the recorder by means of a potentiometer. As a consequence, the chart recorder must be calibrated for a certain setting of the potentiometer by means of a standard thermocouple.

For calibration, the chart thermocouple was placed beside a standard thermocouple in a furnace. [The standard thermocouple was Pt - Pt 13% Rh standardized at the National Research Council of Canada, Ottawa, to $\pm 1^{\circ}\text{C}$. It was borrowed for the duration of the experiments from the Department of Mining and Metallurgy, University of Alberta.] The furnace was raised to approximately 1150°C . and the potentiometer on the chart thermocouple was adjusted so that the recorder pen gave the maximum scale reading at this temperature. The furnace was then allowed to cool to approximately 200°C . and with rising temperature the chart reading was calibrated against a series of temperatures determined by the standard thermocouple. The cold junction of both thermocouples was at room temperature, so that a room temperature correction must always be made to determine the true temperature.

The calibration results were plotted on a series of curves relating chart reading to temperature at that particular setting of the potentiometer on the chart thermocouple. Accordingly, the potentiometer on the chart thermocouple was readjusted to the standard curves immediately prior to each run, by comparison of the recorder reading with a series of temperatures determined with the standard thermocouple. Those temperatures above 1150°C . were determined by readjusting the potentiometer. Because the amount of readjustment can be read on the chart, the corrected chart reading is easily determined and the temperature found.

Method of experimentation

The weight of sample that must be taken using this technique depends on the age of the specimen. For Cretaceous feldspars a 1 gm. sample is necessary, but in pre-Cambrian samples 0.2 gm. would be adequate. However it is advisable to use 1 gm. of sample in all cases because heating at 1230°C. may not remove all the argon, and the larger sample is necessary to determine the remaining amount of argon in the lattice by the normal K - Ar dating technique.

A weighed sample of a known grain size was placed in a silica crucible and the crucible placed inside the furnace in such a position that the sample was in the middle of the furnace. The crucible was then connected to the sample inlet of the mass spectrometer and the sample train opened to the sample train pumps. After pumping for 2 - 3 minutes, all the glass leads were tested for leaks. The crucible furnace was then switched on and the sample outgassed at approximately 200°C. The tube of the mass spectrometer was baked to assist outgassing of the mass spectrometer.

After pumping for 12 hours, the sample system is at a high vacuum ($<10^{-6}$ mm. Hg.) and the titanium getter furnace was switched on and the getter outgassed at approximately 1000°C. At this stage all the glass leads were torched as often as possible to desorb attached gases.

After pumping for 36 hours the pressure in the sample train was approximately 10^{-8} mm. Hg. and the sample was ready to run. The following steps were taken.

- a. The valve leading to the sample train was closed and the valve to the mass spectrometer was opened.
- b. The temperature of the titanium sponge getter was lowered to 700 - 750°C. Its cooling usually helps to lower the pressure in the mass spectrometer still further.
- c. The mass spectrometer was switched on and allowed to stabilize for 1/2 hour.

- d. The chart thermocouple was adjusted to the experimentally determined curves of chart reading against temperature by comparison with the temperature found from the standard thermocouple. The chart thermocouple was then put through a hole in the base of the crucible furnace so that the tip was almost touching the silica crucible.
- e. The cold trap was immersed in a Dewar of liquid nitrogen.
- f. The chart was then switched on, the speed of running being 1/2 inch per minute.
- g. The $44 = \text{CO}_2$ peak was found knowing its rough position on the dial that controls the current in the electromagnet of the mass spectrometer. The 44 peak is the largest peak in the neighbourhood of this dial position.
- h. The peaks are then scanned down to the $28 = \text{N}_2$ peak. Similar measurements of the peak height are made throughout the experiment to determine the rate of change of background, if any.
- i. The background height of the Ar^{40} peak at the start of the run is measured and its influence subtracted from the amount of argon released during the experiment.
- j. During the experiment the position of the baseline was determined at frequent intervals, so that the true peak height may be found. This is most particularly important when the baseline varies with time.
- k. Room temperature was recorded frequently during the experiments, as it is necessary for correction in the temperature measurements.

To begin the experiment, the position of the $40 = \text{Ar}$ peak was found and held. The temperature of the crucible was raised until a significant response in the 40 peak was observed on the X 10 scale of the mass spectrometer. The temperature of the furnace was stabilized at this temperature as rapidly as possible by means of a powerstat and the rate of argon loss at this temperature observed. When the rate of argon loss fell to a low level, or when diffusion had been observed for about an hour, the temperature of the furnace was raised in successive increments and diffusion observed at each new temperature until 1230°C was reached. This was the maximum temperature at which the furnace could operate. At 1230°C . the sanidines studied had lost all their argon, but the two microclines still retained some argon. The remaining amount of argon in the microclines was determined by the usual K - Ar dating method for determining the amount of argon in a mineral.

III. Mathematical treatment of the diffusion data.

The mathematical theory of diffusion in isotropic substances is based on the hypothesis that the rate of transfer of the diffusing substance through a plane normal to the direction of diffusion is proportional to the concentration gradient in the direction of diffusion. This may be expressed by the function (Barrer, 1951):

$$J = -D \frac{\partial c}{\partial x} \quad (3) - 2$$

where J = diffusion flux.
 c = concentration.
 x = direction in which diffusion occurs.
 D = diffusion coefficient.

This relationship is known as Fick's first law. The negative sign signifies that diffusion occurs in a direction opposite to that of increasing concentration.

Fick's second law, which is directly obtainable from the first law, states that,

$$\frac{\partial c}{\partial t} = D \frac{\partial^2 c}{\partial x^2} \quad (3) - 3$$

where t = time.

Solutions of Fick's law for various diffusion models can be made satisfying the following boundary conditions: that the initial phase is homogeneous and that the concentration of argon at the surface is at all times the same (in this case essentially zero). Since feldspars are tectosilicates, the most reasonable diffusion model to employ is that involving isotropic volume diffusion from a sphere.

Crank (1956) publishes the following solution:

$$f = 1 - \frac{6}{\pi^2} \sum_{n=1}^{\infty} \frac{1}{n^2} e^{-\frac{n^2 \pi^2 D t}{a^2}} \quad (3) - 1$$

where f = fraction of argon released in time t .
 a = radius of the sphere.
 D = diffusion coefficient.
 t = time during which diffusion occurs.

It is clear that a solution of D for values of f from this equation is extremely difficult. Fortunately this series converges rapidly and one term is a reasonable approximation for $f > 0.85$.

For values of $f < 0.85$ the following approximation is used.

$$f = \frac{6}{\pi^{1/2}} \left(\frac{D t}{a^2} \right)^{1/2} - \frac{3 D t}{a^2} \quad (3) - 4$$

Before using the approximations it is necessary to ascertain their validity. The following treatment is adopted from Reichenberg (1953).

If one term of the equation (3) - 1 is used then:

$$\frac{\pi^2 D t}{a^2} = -\ln \frac{\pi^2}{6} - \ln (1 - f) \quad (3) - 5$$

When $f = 1$ this approximation gives the true value of $D t / a^2$. For all other values of f the values of $D t / a^2$ are too low. For lower values of f the equation (3) - 1 may be transformed giving:

$$f = \frac{6}{\pi^{3/2}} \left(\frac{\pi^2 D t}{a^2} \right)^{1/2} - \frac{3 D t}{a^2} + \frac{6}{\pi^{3/2}} \int_0^{\frac{\pi^2 D t}{a^2}} \sum_{n=1}^{\infty} \left(\frac{D t}{a^2} \right)^{-1} e^{-\frac{\pi^2 n^2 a^2}{D t}} \quad (3) - 6$$

If only the first two terms are considered we have the equation:

$$f = \frac{6}{\pi^2} \left(\frac{D_t}{a^2} \right)^{1/2} - \frac{3 D_t}{a^2} \quad (3) - 4$$

This relationship is used for $f < 0.85$. When $f = 0$ the last term of equation (3) - 6 is zero and the approximation (3) - 4 is valid. For any other values of f the equation (3) - 4 gives a too high value of D_t/a^2 .

Consequently an appraisal of these approximations at $f = 0.85$ will give the maximum error that results in their use.

At $f = 0.85$ the value of D_t/a^2 found from using only one term of the equation (3) - 1 is 1.418×10^{-1} .

At $f = 0.85$ the value of D_t/a^2 found from the approximation (3) - 4 is 1.4225×10^{-1} .

The difference between these values is 0.0045×10^{-1} and the mean error in using these approximations is 0.00225×10^{-1} . Such an error is not significant in view of other sources of error and the approximations used are valid.

From a knowledge of the diffusion coefficient at two temperatures the activation energy of argon diffusion between these temperatures can be determined from the relationship:

$$D_t = D_o e^{-\frac{Q}{RT}} \quad (3) - 7$$

where D_t = the diffusion coefficient at a certain temperature.
 D_o = a constant.
 R = gas constant.
 T = absolute temperature (degrees absolute)
 Q = activation energy (cal./mole)

By taking logarithms the equation (3) - 7 may be presented in the following form:

$$\ln D_t = \ln D_0 - \frac{Q}{RT} \quad (3) - 8$$

A plot of $\ln D_t$ against $1/T$ will give a straight line if the activation energy does not change. Factors which cause variations in Q will cause inflections in this curve.

Fortunately, inflections in the experimental curves are common. Their value lies in that they indicate changes in the activation energy of argon diffusion with rising temperature, and it is from such changes that a greater insight into the mechanism of argon diffusion may be obtained.

In order to facilitate the treatment of the diffusion data, values of $(Dt/a^2)^{1/2}$ were obtained at a series of values of fraction of argon released, from $f = 1 \times 10^{-3}$ to $f = 0.85$ using the approximation (3) - 4. A series of curves were then drawn relating values of f against $(Dt/a^2)^{1/2}$, the scale being chosen so that no significant errors were introduced by using these curves. These values are tabulated in appendix A,

For values of $f > 0.85$ values of D were determined individually using one term of equation (3) - 1. The approximation is:

$$f = 1 - \frac{6}{\pi^2} e^{-\frac{\pi^2 Dt}{a^2}} \quad (3) - 9$$

IV. Validity of this mathematical treatment

It is now of importance to discuss the question of the validity of applying the previous mathematical treatment to these diffusion experiments.

The clearest divergence from mathematical rigidity lies in that the previous equations are developed for isotropic diffusion from a sphere, while it is clear that diffusion from a feldspar lattice most certainly will not meet this requirement completely. If diffusion occurs with equal ease along the three crystal axes, then it is probable that the above relationship is the most reasonable one available. However Pronko (1962) found increased ease of ionic conductivity along the direction of cross-hatch twinning in microcline and along the planes of perthitization, which suggests that there would be an increased ease of argon diffusion in these directions. The importance of this effect is difficult to appraise, but it is reasonable to suggest that provided the departure from isotropic diffusion is not large, this effect is not of great consequence. In all events, it is difficult to suggest a more reasonable relationship that can be used to construct a model for diffusion in feldspars.

It is more important to realize that this technique, when used to determine the diffusion coefficient at more than one temperature relies on finding the fraction of argon released from an inhomogeneous crystal. Mechanistically this can be easily pictured. At the first temperature interval, argon is lost from a homogeneous crystal, but at the next and succeeding temperature intervals diffusion occurs from a lattice which is initially inhomogeneous. Since Fick's law assumes diffusion from an initially homogeneous lattice, the calculated values of the diffusion coefficient at succeeding temperatures will be too low. It is to be expected that in certain cases this effect will not be too serious. The rate of argon diffusion is extremely sensitive to temperature, so that if the diffusion coefficient increases significantly between two temperature intervals, the effect of inhomogeneity will be masked. Further, as the time interval during which argon loss at one temperature is observed becomes greater, the effect of original inhomogeneity becomes less. However, in those cases in which

the diffusion coefficient does not increase significantly with temperature, this departure from Fick's law becomes quite serious.

In order to appraise the magnitude of this inexactness, the diffusion coefficients were determined using three basically different assumptions. These assumptions are described in the following section on the calculation of the diffusion coefficient.

V. Calculation of the diffusion coefficients

Because the argon which diffuses from the feldspar was passed directly into the mass spectrometer, it is reasonable to conclude that the peak height is directly proportional to the amount of argon being released from the crystal lattice. Consequently the area under the curve of response against time is proportional to the amount of argon being released. It is clear that from measurements of the area under the response curve it is possible to determine the fraction of argon released during any time interval.

Figure 5 is a diagrammatic representation of a typical chart of response against time.

The technique of determining the fraction of argon released will be described referring to Figure 6. At the beginning of the experiment at time t_0 , the mass spectrometer was held on the Ar^{40} peak and this peak height background is corrected for in subsequent determinations of the area under the curve. In Figure 6, $t_1, t_2, t_3, t_4, t_5, t_6$, refer to the times after the start of the run. The values A. B. C. D. E. F. refer to the area under the curve corrected for the Ar^{40} background between the times $t_0 - t_1, t_1 - t_2, t_2 - t_3, t_3 - t_4, t_4 - t_5, t_5 - t_6$ respectively. T is the total area under the curve.

Because the mathematical treatment used in this paper is not a rigid solution of Fick's law, the diffusion coefficient at each temperature was determined using three

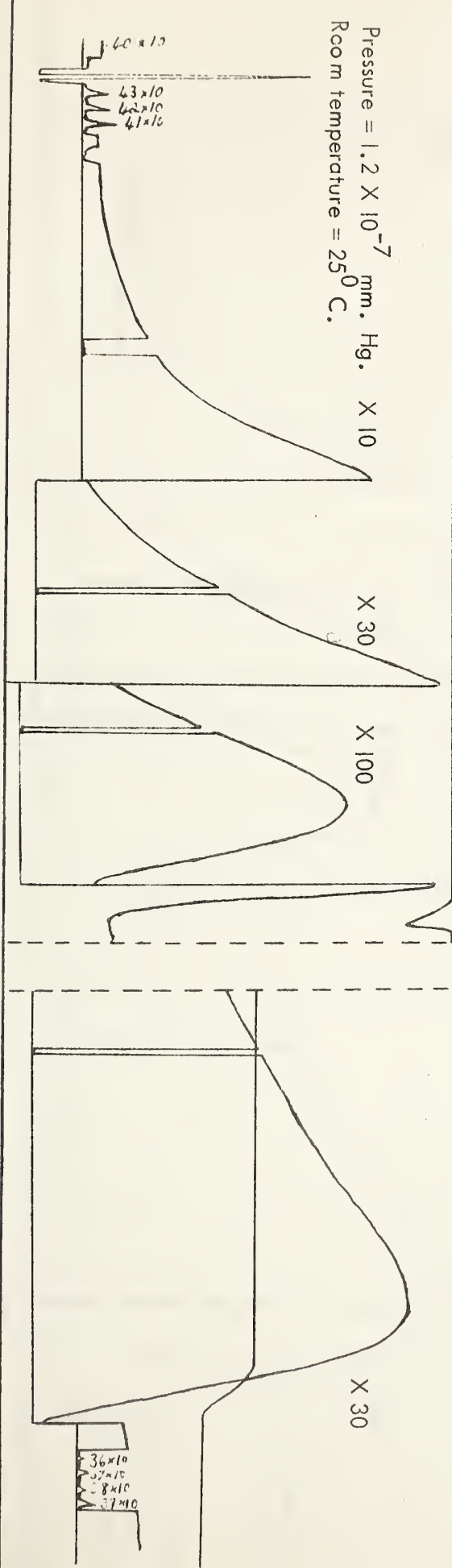
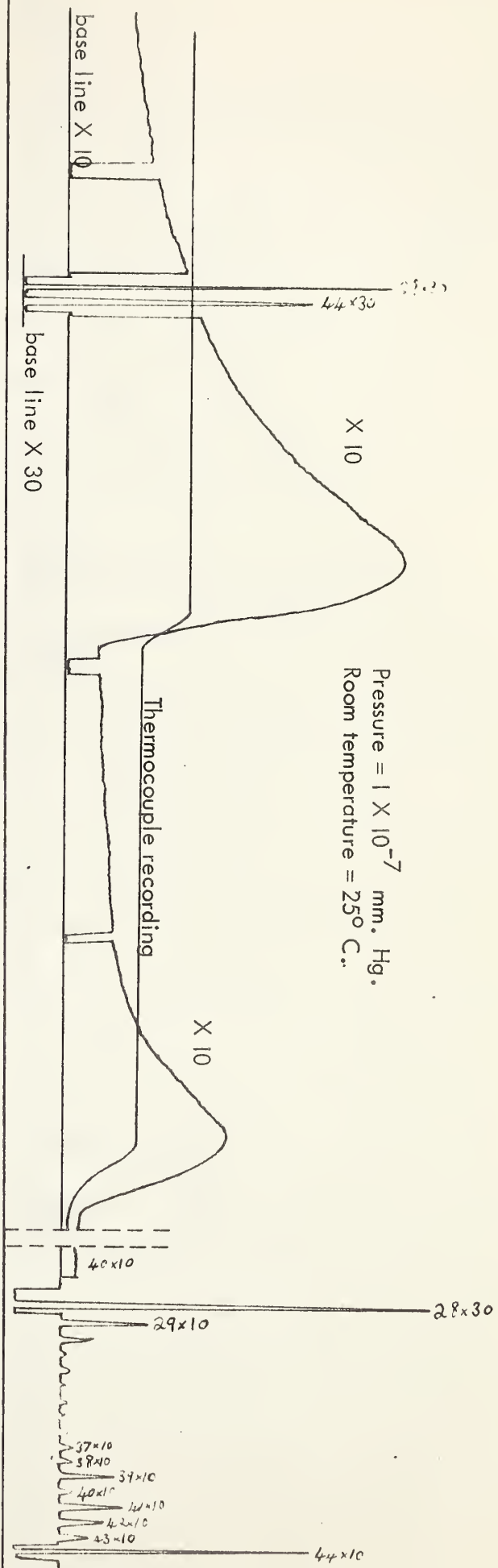


FIGURE 5. A diagrammatic representation of the response curve of the mass spectrometer.

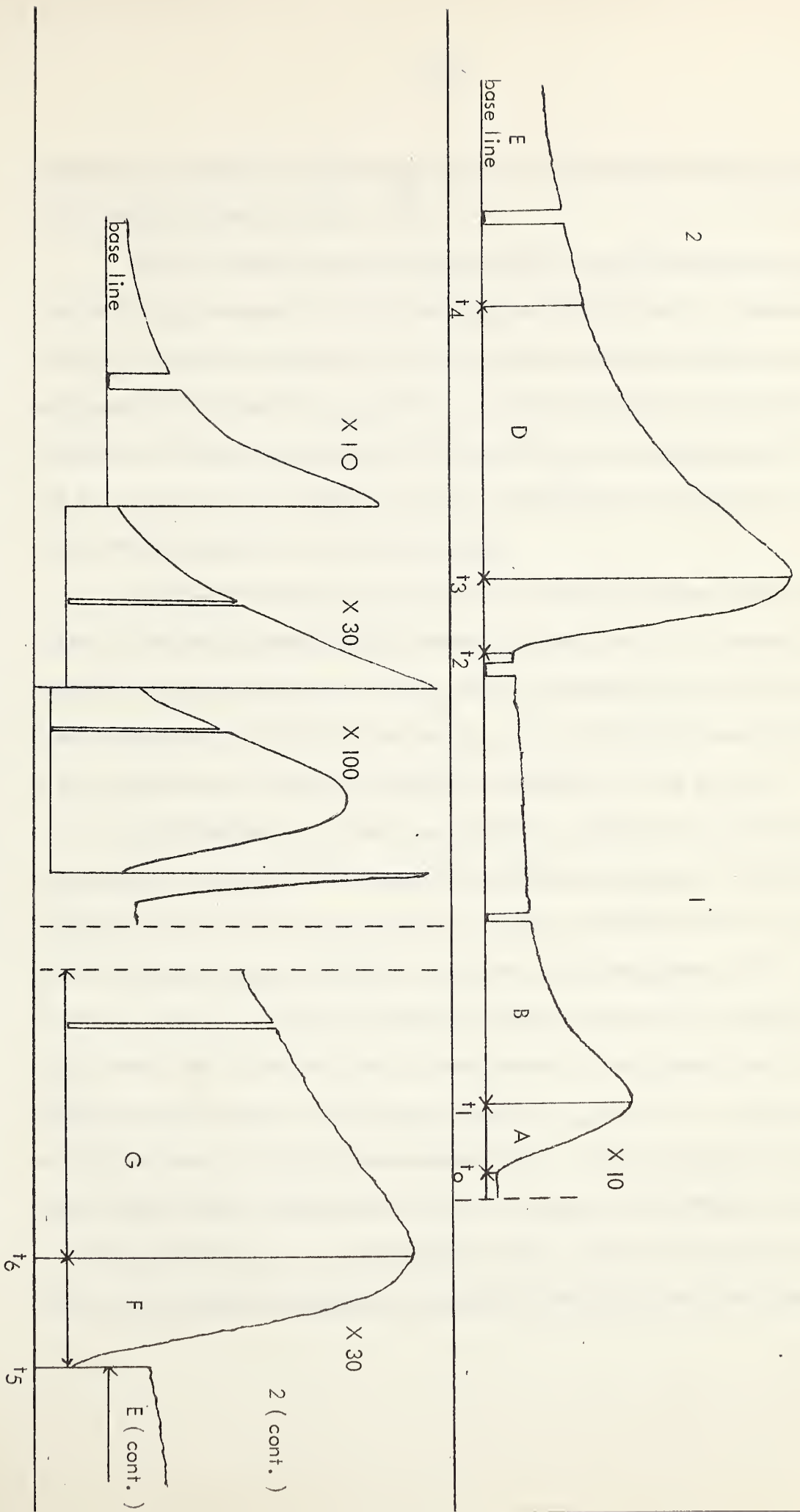


FIGURE 6. A diagram indicating the method used to calculate the fraction of argon released.

independent assumptions in order to make a more valid appraisal of the significance of the diffusion curves of $\ln D$ vs. $1/K$.

The first method of determining the diffusion coefficients made use of the fraction of argon released from the moment of gradient stabilization. Referring to Figure 6; in the first temperature interval 1, the time of gradient stabilization is t_1 and the amount of argon in the crystal at this time is proportional to the area $T - A$. The amount of argon lost during the time interval $(t_2 - t_1)$ is proportional to the area B , and the fraction of argon released is $B/T - A$. Knowing the value of f and t , a value of the diffusion coefficient can be determined.

In the second temperature interval 2, the amount of argon present in the lattice at the time of gradient stabilization t_3 is proportional to $T - (A+B+C)$. The amount of argon lost between the times t_3 and t_4 is proportional to the area D and the fraction lost is $D/T - (A+B+C)$ in the time $(t_4 - t_3)$. Similarly between the times t_3 and t_5 , the fraction of argon lost is $(D+E)/T - (A+B+C)$ in a time $(t_5 - t_3)$.

The determination of two or more diffusion coefficients in each temperature interval gives information on the nature of the diffusion processes. Considering the temperature interval 2 at time t_3 ; when the gradient is established the lattice has already lost some argon and diffusion occurs from an inhomogeneous lattice. Since the argon lost in the temperature interval 1 creates a concentration gradient, the outer layers of the crystal must have a lower concentration of argon than the original feldspar and the volumes lost between the times $t_3 - t_4$ and $t_3 - t_5$, must be less than would occur from an originally homogeneous crystal. This would cause the determined values of the diffusion coefficient to be low. However, if the diffusion coefficient increases significantly at a new temperature interval, then with increasing time the effect of the original inhomogeneity must decline, and the value of the determined

diffusion coefficient will increase to approach the true value. The difference in the values of the diffusion coefficient at various times after the gradient was established, must be a function of the original gradient in the concentration of argon at the time t_3 and a measure of the increase in the diffusion coefficient.

In the case where the diffusion coefficient decreases with time during any temperature interval, then important conclusions may be made concerning the mechanism of diffusion from the crystal lattice. If argon diffuses from more than one lattice position, that argon occupying the position with the highest diffusion coefficient is lost first and when most of the argon is lost from this position, the loss from positions with a lower diffusion coefficient can be observed. This will result in a decrease of the diffusion coefficient with time. It is significant that such lowerings of the value of D have been observed in this study.

Though a decrease in the diffusion coefficient with time can indicate that argon is held in more than one position, it is also possible that a progressive lattice change could cause this effect. Further, at lower experimental temperatures the influence of loss from inclusions and surface desorption, which do not follow Fick's law, must be considered.

In the second method of determining the diffusion coefficients, the area under the curve was taken from the time when the response started to rise. Considering Figure 6, it is clear that the time when the temperature is established at t_0 is the only case when diffusion is considered from a homogeneous lattice. In interval 1 the fraction of argon released is $A+B/T$, and from this a value of Dt/a^2 may be found. The divergence arises in the use of time, which can be considered in two ways.

Firstly, the time interval $t_2 - t_0$ was used to calculate the diffusion coefficient. This gives the minimum value of the diffusion coefficient that can be calculated using any

reasonable assumption. This value D_{\min} must be the lowest because at t_0 the temperature is not properly established.

Secondly the time interval $t_2 - t_1$ is used as the time of diffusion. This gives the maximum value of the diffusion coefficient that can be determined using any reasonable assumption. The reason that it is the maximum value is that it conceives that diffusion starts at t_1 while yet including that part of the argon that has diffused between the times t_1 and t_0 . At the first temperature interval this treatment is not important because any unbalance in the homogeneity in the crystal is insignificant. However, at temperature interval 2 and beyond, this method of mathematical treatment should allow a much better appraisal of the results to be made.

The difference between the two values D_{\min} and D_{\max} determined at each temperature interval clearly depends on the length of time of heating before the new gradient is established at the higher temperature and on the extent of the inhomogeneity.

VI. Method of presentation of the results

In the presentation of the results, graphs are given of values of $\ln D/a^2$ vs. $1/T$ and $\ln D$ vs. $1/T$. Comparison of values of D/a^2 and D for different grain sizes for the same sample allows the effective radius for argon diffusion to be ascertained.

For each graph two curves were drawn. Values of the diffusion coefficient determined on the basis of the first method described, define the lower curve. This is the lower because the crystal has a high degree of inhomogeneity when the fraction of argon released is determined by this method. The second and upper curve was drawn through the two values of the diffusion coefficient determined by the second method, (D_{\min} and D_{\max}), because these two values are usually quite close.

The degree of similarity of the two curves found by these methods will give confidence that the inflections in the regular diffusion curve are real. The distance

between the two curves must be a reflection of the capacity of the increased activation of Ar atoms at higher temperatures to mask the effect of the original inhomogeneity in the crystal. When the two curves are in close proximity we can be reasonably confident that the shape of the curve is correct, but when they diverge, an explanation for this divergence must be found. It seems clear that the two curves diverge when the diffusion coefficient no longer increases with temperature. In such cases the influence of the original inhomogeneity of the argon concentration in the crystal is enhanced and the diffusion coefficient determined by method 1 will be too low. The 'maximum' value determined by method 2 will possibly be close to the real value.

In conclusion it is clear that though uncertainty may be present in the accurate value of the diffusion coefficients in certain instances, in all cases the inflections found are real and reflect a change in the activation energy of argon diffusion.

VII. Accuracy of the measurement

a. Accuracy in the determination of fraction of argon released.

The error arising from the incorrect determination of area was calculated and found to be insignificant. The accuracy with which an area can be determined depends on,

- a. The stability of the pen recorder.
- b. The magnitude of the peak height.
- c. The stability of the base line.

If the accuracy of the area was 8 per cent then the variation in the value of $\ln_e D$ was of the order of ± 0.1 . If the area was determined to within 4 per cent the

variation in the value of $\ln_e D$ was of the order of ± 0.05 . These variations are very slight in the overall picture and have no effect on the shape of the curves.

b. Accuracy in the determination of temperature

In most cases the temperature was determined with an accuracy of $\pm 3^\circ\text{C}$. This error would cause a variation in the reciprocal absolute temperature of 0.005 at 500°C . and 0.001 at 1150°C .

At temperatures above 1150°C . the average error in the temperature is approximately 6°C . This gives a variation in the reciprocal absolute temperature of 0.0027 at 1200°C .

These variations are insignificant and are not measureable on the scale of the graphs.

CHAPTER FOUR

EXPERIMENTAL RESULTS

I. Kinnekulle Sanidine

Geological occurrence. The sample was obtained from the bentonitic beds that outcrop at Kinnekulle, Sweden. A description of these beds has been given by Byström (1954). The bentonite consists of illite and montmorillonite, together with a silt-sized fraction containing sanidine, biotite, plagioclase, quartz and zircon. Fossiliferous limestones and shales occurring above and below the bentonite horizon, allow the beds to be correlated with the Caradoc stage of the Ordovician. Dating of the biotite and sanidine by the K-Ar method (Byström-Asklund et al., 1961) yields the dates of 447 m.y. for the biotite and 440 m.y. for the sanidine. Byström finds no evidence of deep burial or subsequent metamorphism of the bentonite.

Description of the sanidine. Optical examination of the sanidine shows it to be very clear. Byström found that the sanidine showed no signs of weathering, but in the grains used in this experiment some surface irregularities were observed that are possibly due to interstratal solution. Chemical analysis of the sanidine gives (Byström, 1954):

K_2O = 12.5% (75 wt. % Or)

Na_2O = 2.9% (25 wt. % Ab)

2V = 15 – 18 degrees

Curve of the logarithm of the diffusion coefficient against reciprocal absolute temperature for the Kinnekulle sanidine, calculated using equations (3) - 4 and (3) - 5

Because the partical size used was 170 - 230 mesh the experimental curve is comparable with that given in Baadsgaard et al. (1961). The curves are given in Figure 2.

The lower curve is determined when the fraction of argon lost and the time of loss are taken from the time of apparent stabilization of argon loss from the crystal. The upper curve is drawn through diffusion coefficients found using the fraction of argon lost during the whole temperature interval, taking into account the period of temperature stabilization. It is seen that both curves are very similar in shape and slope. Such similarity was found in all the prepared graphs, and in order to avoid unnecessary complications of the results due to a multiplicity of curves, only the lower curve will be presented in the following descriptions. It is clear that the neglect of the period when temperature is being established does not cause any significant change in the shape of the curve.

The diffusion curve for the Kinnekulle sanidine is a straight line, which is in agreement with the results obtained by Baadsgaard et al. (1961). It is clear that diffusion of argon from the lattice is occurring in a simple manner, a result which would be expected from the sanidine lattice. The steepening of the curve above 1020°C. is most probably due to increased ease of argon loss as the melting point of the lattice is approached.

Determination of the activation energy of argon diffusion for the straight line part of the curve gives a value of 42,500 cal./mole. The diffusion coefficients at low temperature may be calculated if it is assumed that no lattice changes occur at lower temperatures and that the activation energy found at high temperatures still explains diffusion at lower temperatures.

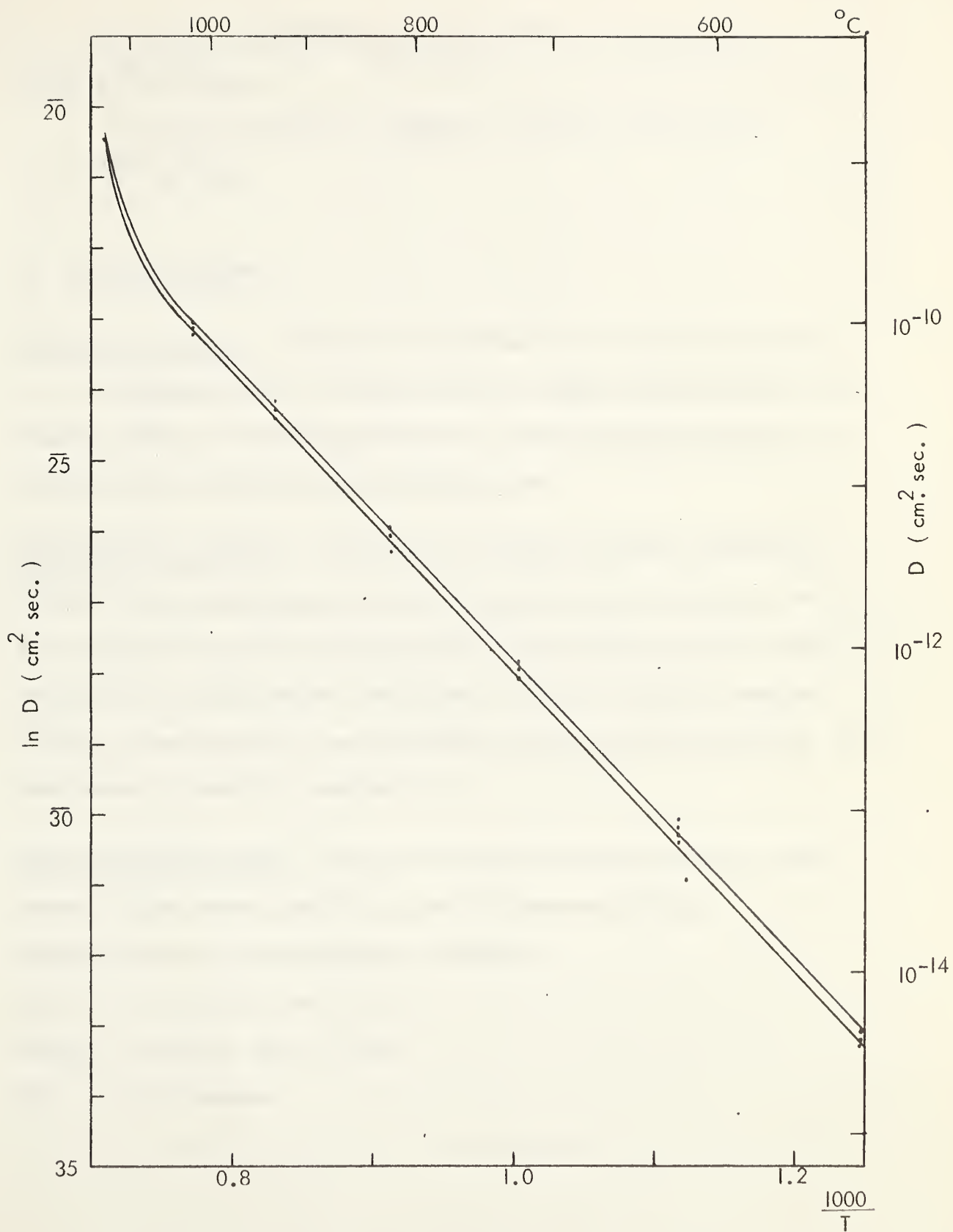


FIGURE 7. KINNEKULLE SANIDINE

(calculated using equations (3) - 4
and (3) - 5)

The value of the diffusion coefficient at 27°C. was found to be $1.9 \times 10^{-34} \text{ cm.}^2/\text{sec.}$

The value of the diffusion coefficient at 150°C. was found to be $1.5 \times 10^{-25} \text{ cm.}^2/\text{sec.}$

II. Millcreek Sanidine

Geological occurrence. - The sample was obtained from a bentonite collected by Dr. R.E. Folinsbee and Dr. K. Crook at Millcreek, approximately 20 miles S.E. of Coleman, Alberta. The Millcreek bentonite is Upper Cretaceous in age (95 m.y.) and has not been affected by any metamorphic event.

Preparation of the sample. - The bentonite was washed in order to obtain the grit fraction, and the sanidine separated from the grit by the usual techniques with the Franz isodynamic separator and heavy liquids. The sanidine was recycled through the separation procedure several times in order to obtain a high-purity separate. The final contaminant grains were hand picked under the binocular microscope. The final separate is essentially completely pure.

Description of the sanidine. - The grains under the microscope are clear, but the surface is faintly etched, possibly as a result of interstratal solution.

Chemical analysis of the sanidine gives (Newland):

K_2O = 11.24% (62.6 wt. % Or)

Na_2O = 3.26% (27.59 wt. % Ab)

2V = 0 - 5 degrees

Curve of the logarithm of the diffusion coefficient against reciprocal absolute temperature for the Millcreek sanidine, calculated using equations (3) - 4 and (3) - 5

Diffusion curves were obtained for three grain sizes. These sizes are, 80-120 mesh, 120-170 mesh, and 170-230 mesh. In the two succeeding graphs, the curves for all three grain sizes are plotted. Figure 8 presents values of $\ln D$ as the ordinate, and Figure 9 values of $\ln D/a^2$ on the ordinate, both with reciprocal absolute temperature plotted on the abscissae.

Inspection of these curves, shows that from 500 - 900°C. the value of the diffusion coefficient at any temperature is essentially the same for all grain sizes. This implies that the physical grain size is the true radius of diffusion and suggests that the boundary conditions on which the mathematical treatment is based are reasonable.

From 950 - 1050°C. all three curves show an inflection which is most marked in the smallest grain size. Above 950°C. the $\ln D$ curves for the three grain sizes separate, while the $\ln D/a^2$ curves approach each other. The separation of the $\ln D$ curves must indicate that the physical grain size is no longer the diffusion radius, while the closeness of the $\ln D/a^2$ curves must be taken to indicate that the effective radius of diffusion is very small.

Three possible explanations present themselves for the shape of the diffusion curves. Firstly, it may be suggested that the inflection between 950 and 1050°C. is a result of depletion of argon in the lattice. Because the smallest grain size would be depleted most rapidly, the inflection for this grain size would be most marked. In this case, the increase in the slope above 1050°C. may be assumed to be a result of the (Si,Al-O) bonds becoming weaker as the melting point is approached, with the

consequent rapid release of argon. However, it is not possible to substantiate this suggestion as the shape of the loss curve from the mass spectrometer indicates that diffusion is occurring from a melting lattice only at 1230°C.

The second possible explanation is that argon is present in two positions. The curve below 900°C. reflects diffusion from the first position and the inflection at 950°C. is a result of depletion of argon in this position. Diffusion above 1050°C. is from the second position of higher activation energy.

The third possibility is that the inflection is the result of a lattice change. However, X-ray examination of the heated sample shows no structural change, except a decrease in the peak height of the heated sample due to melting. This does not reject the possibility of a reversible lattice change.

In order to calculate the activation energy of argon loss from the Millcreek sanidine, it is assumed that the argon is present in two positions. A curve was prepared for cumulative fraction of argon lost against temperature. Inspection of this curve showed that each position contained 50 per cent of the total argon present in the sanidine, and the values of the diffusion coefficient were recalculated on this assumption. From these values the activation energy may be calculated.

Determined values of the activation energy are:

For position I (loss below 850°C.)

<u>Mesh size.</u>	<u>Activation energy</u>
80 - 120	39,000 cal./mole
120 - 170	41,400 cal./mole
170 - 230	42,300 cal./mole

For position II (loss above 1050°C.)

<u>Mesh size.</u>	<u>Activation energy</u>
80 - 120	54,000 cal./mole
120 - 170	60,200 cal./mole
170 - 230	51,700 cal./mole

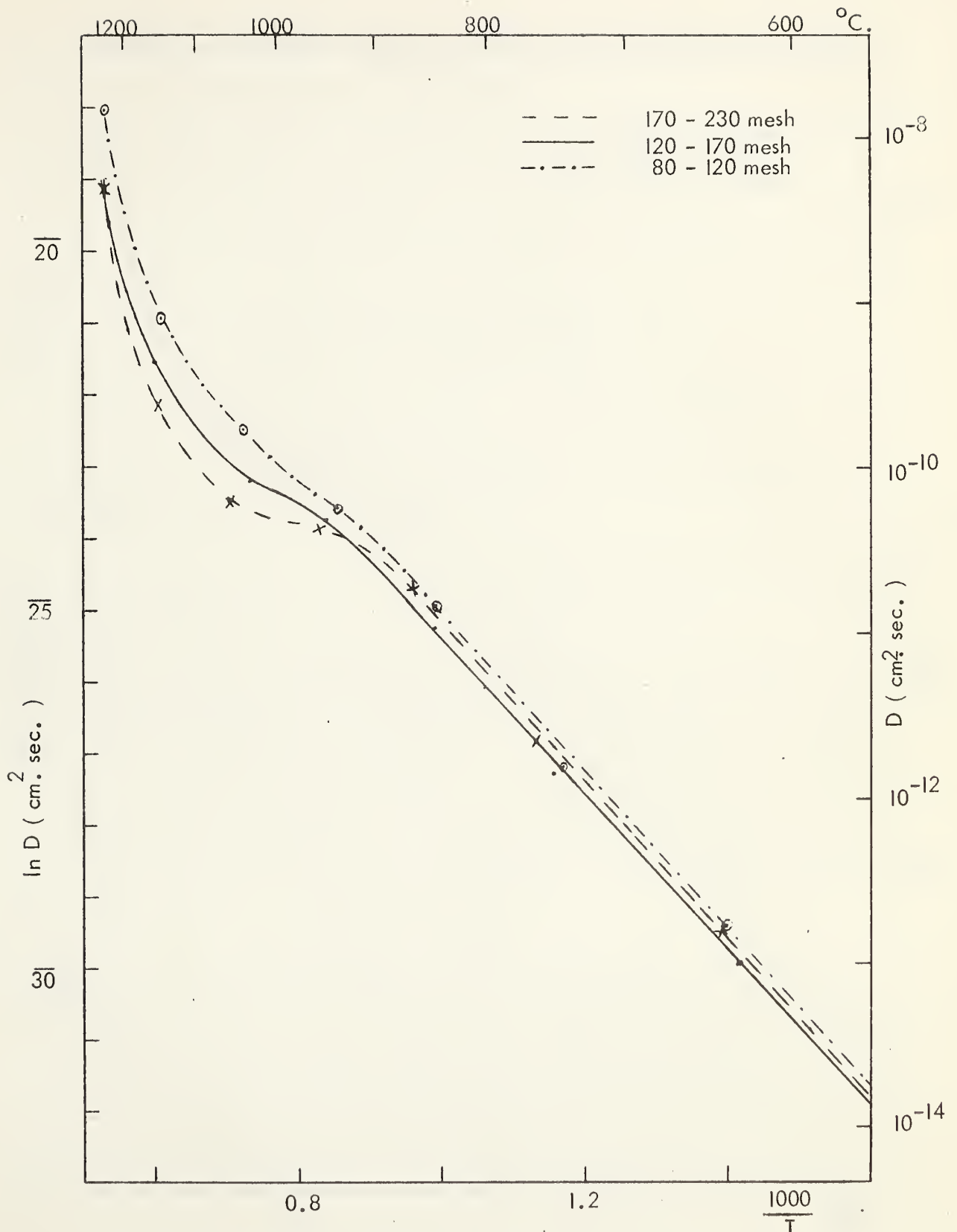


FIGURE 8. MILLCREEK SANIDINE. (calculated using equations (3)-4 and (3)-5)

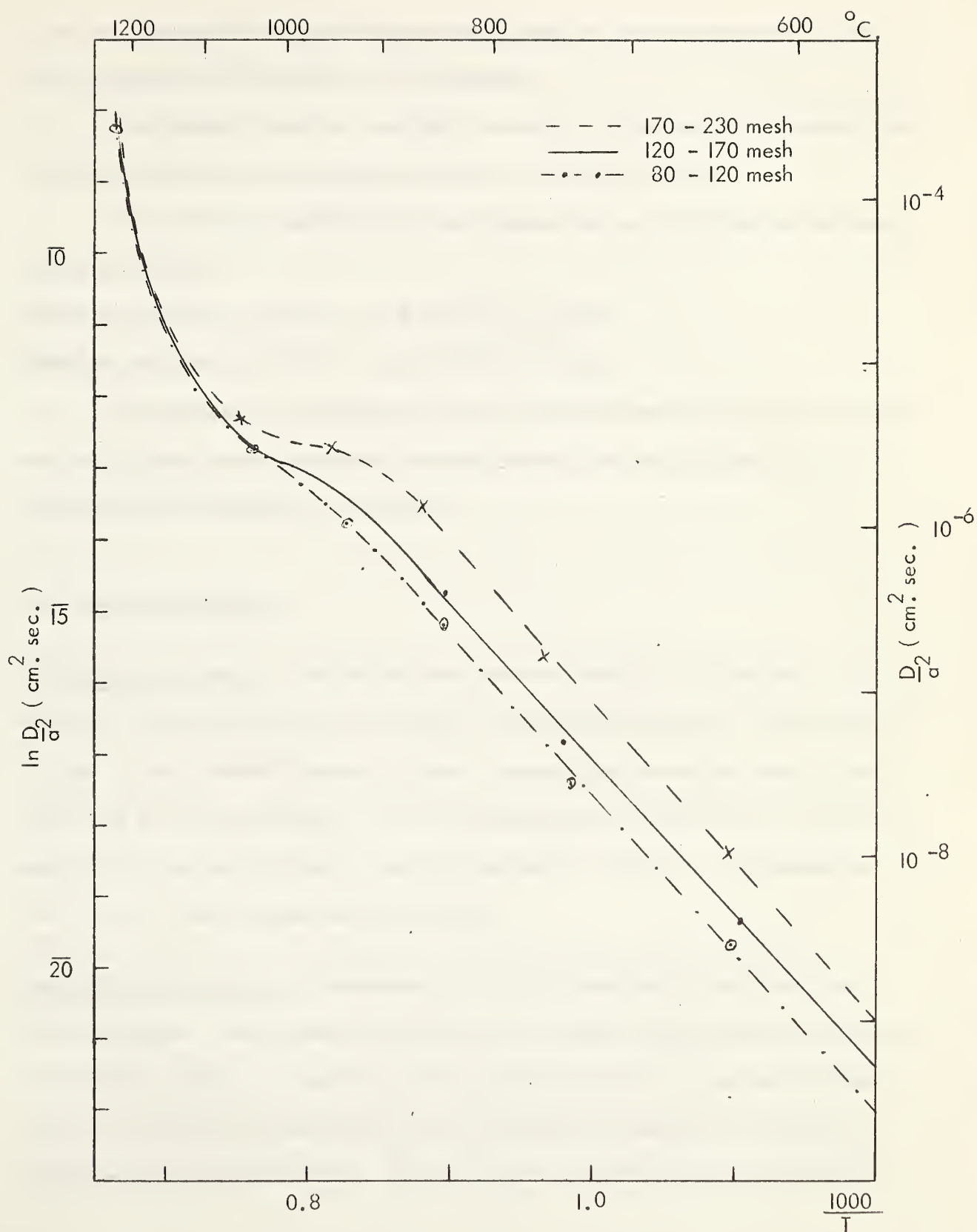


FIGURE 9. MILLCREEK SANIDINE (calculated using equations (3) - 4 and (3) - 5)

It must be stressed that the values for the second position are very approximate, and that the presence of this position is only tentative.

The values for position I are fairly constant. If one position is assumed, then the value of the activation energy was found to be 43,900 cal./mole.

If the diffusion coefficients at room temperature are calculated the following values are obtained.

Diffusion coefficient at 27°C. = 2.4×10^{-34} cm.²/sec.

Diffusion coefficient at 150°C. = 2.6×10^{-25} cm.²/sec.

These values are comparable with those obtained from the Kinnekulle sanidine and also indicate that leakage from this sanidine would not be significant until a temperature of at least 200°C. is reached.

III. Crowsnest Sanidine

Geological occurrence. - The samples were obtained from Dr. H. Baadsgaard. The sanidine occurs as phenocrysts in a trachytic lava flow that outcrops in a fresh road cutting, 1/2 mile west of Coleman, Alberta. Large single phenocrysts were crushed and sieved to various grain sizes. As this sanidine gives an age of 94 m.y. while the age of biotite and sanidine from a correlated bentonite is 100 m.y., it is suggested that there is a possible argon loss of 6 per cent.

Description of the sample. - Baadsgaard et al. (1961) describe this sanidine in the following manner. The Crowsnest sanidine occurs as large, strongly zoned phenocrysts. As no multiple peaks were observed on X-ray powder patterns, it is assumed that each crystal is chemically homogeneous and that the zoning is a response to variations in the temperature of crystallization. Crystals vary in composition between individuals

in the range $Or_{76.8} - Or_{84.5}$. Zoning covers a wide range in 2V. Variations in the 2V occur from $19.9^\circ \perp (010)$ to $24.4^\circ // (010)$. Crystals are occasionally twinned on the Baveno law. No metamorphic alteration was found, but some iron oxides have been exsolved from the phenocrysts.

Optical examination of a slide of the lava flow, shows that some of the large fractures are filled with quartz or calcite. Other numerous small fractures are present and in some crystals cleavage fractures are very marked. It is assumed that this marked fracture system is a result of the phenocrysts being distorted during the eruption and flow of the lava.

The zoning is quite marked in the hand specimen, but in thin section it is more difficult to observe. Close inspection under crossed nicols at the point of extinction shows very weak zoning in some crystals. Baadsgaard et al. (1961) state that there is no variation in potassium content between the zones and that the zoning may be a response to variations in the temperature of crystallization. However, the X-ray method of finding the Or content of sanidine is accurate only to ~ 1 per cent Or, so it is possible that there are small variations in the alkali content between the zones. Another possibility is that there are differences in trace element concentration between the zones.

Curves of the logarithm of the diffusion coefficient against reciprocal absolute temperature for the Crowsnest sanidine, calculated using equations (3) - 4 and (3) - 5

Diffusion from the sanidine was observed for three grain sizes. These grain sizes are, 60 - 80 mesh, 170 - 200 mesh and 270 - 325 mesh. Slides of the grains show no evidence of zoning within the crystals but the grains are fractured and show extensive inclusions.

The experimentally derived curves are presented in the following graphs. Figure 10 shows $\ln D$ as the ordinate, and Figure 11 shows $\ln D/a^2$ as the ordinate. Both curves have reciprocal absolute temperature on the abscissae. These curves are extremely anomalous and the most difficult to interpret of all the curves found.

The curve for the 60-80 mesh size is anomalous when compared with the other two curves. This is possibly due to diffusion occurring from interfering subunits (related to fractures) in the coarser sample. The curves of $\ln D$ are separated for all grain sizes, which indicates that the grain size is not the radius of diffusion. Comparison of the two curves for the finer grain sizes suggests that the radius for diffusion is possibly 200 - 270 mesh (37-26 microns).

The most marked feature of these curves is the inflection which occurs at 1000°C. for the two finer grain sizes and at 900°C. for the 60 - 80 mesh size. It may be assumed that this inflection is a result of diffusion from two positions. Until the temperature of 800 - 850°C. is reached, diffusion occurs from the first position, but at this temperature depletion of this position occurs and it is not until 1000°C. that diffusion from the second position commences.

The nature of the two positions is uncertain. X-ray examination of the heated and unheated samples does not confirm the possibility that the positions are related to phase changes. Optically and with inspection by X-ray diffraction, there is no indication of lattice change. This is confirmed by a sample (270 - 325 mesh) heated for 5 days at 990°C. This sample showed no evidence of structural change on X-ray examination. There is, of course, the possibility that a reversible change is occurring.

It is not felt that the curves above 1050°C. reflect loss of argon from a melting lattice. Evidence for this comes from the $\ln D/a^2$ curves from 1000 - 1150°C.

which show their own individuality, which does not indicate that the lattice structure is breaking down.

It is tentatively concluded that argon is present in two positions in the Crowsnest sanidine.

The activation energy for the three grain sizes was calculated assuming two positions. The proportion of argon in each position was determined from curves of cumulative fraction of argon lost against temperature. The percentage of argon in position I for each grain size was found to be:

<u>Mesh size</u>	<u>Percentage in position I</u>
60 - 80	32
170 - 200	48
270 - 325	52

The variation shown by the coarsest grain size is disquieting, being too large to be explained by variations in the rate of heating.

Diffusion coefficients were recalculated for each of the positions, using the assumption that loss from the two positions does not mutually interfere except in the inflection zones of the curves.

The activation energy for argon diffusing from position I (below 850°C.) was found to be:

<u>Mesh size</u>	<u>Activation energy</u>
60 - 80	24,900 cal./mole
170 - 200	27,000 cal./mole
270 - 325	29,900 cal./mole

These values are rather erratic. The cause of these variations may be due to a distortion of the lattice structure, related to fracturing, that interferes with volume diffusion.

The activation energy for loss from position II (above 1050°C.) is uncertain, but the most reasonable figure is 47,000 cal./mole. It may be assumed that this

diffusion position is related to loss from a stable lattice as in the Kinnekulle sanidine, and that diffusion from position I must come from a different lattice site, a site possibly related to the fracture system.

Using the activation energy and the diffusion coefficient calculated for position I in the 270 - 325 mesh size, the following values of the diffusion coefficients at low temperature were determined.

$$D_{27^{\circ}\text{C.}} = 3.7 \times 10^{-27} \text{ cm.}^2/\text{sec.}$$

$$D_{150^{\circ}\text{C.}} = 1.6 \times 10^{-20} \text{ cm.}^2/\text{sec.}$$

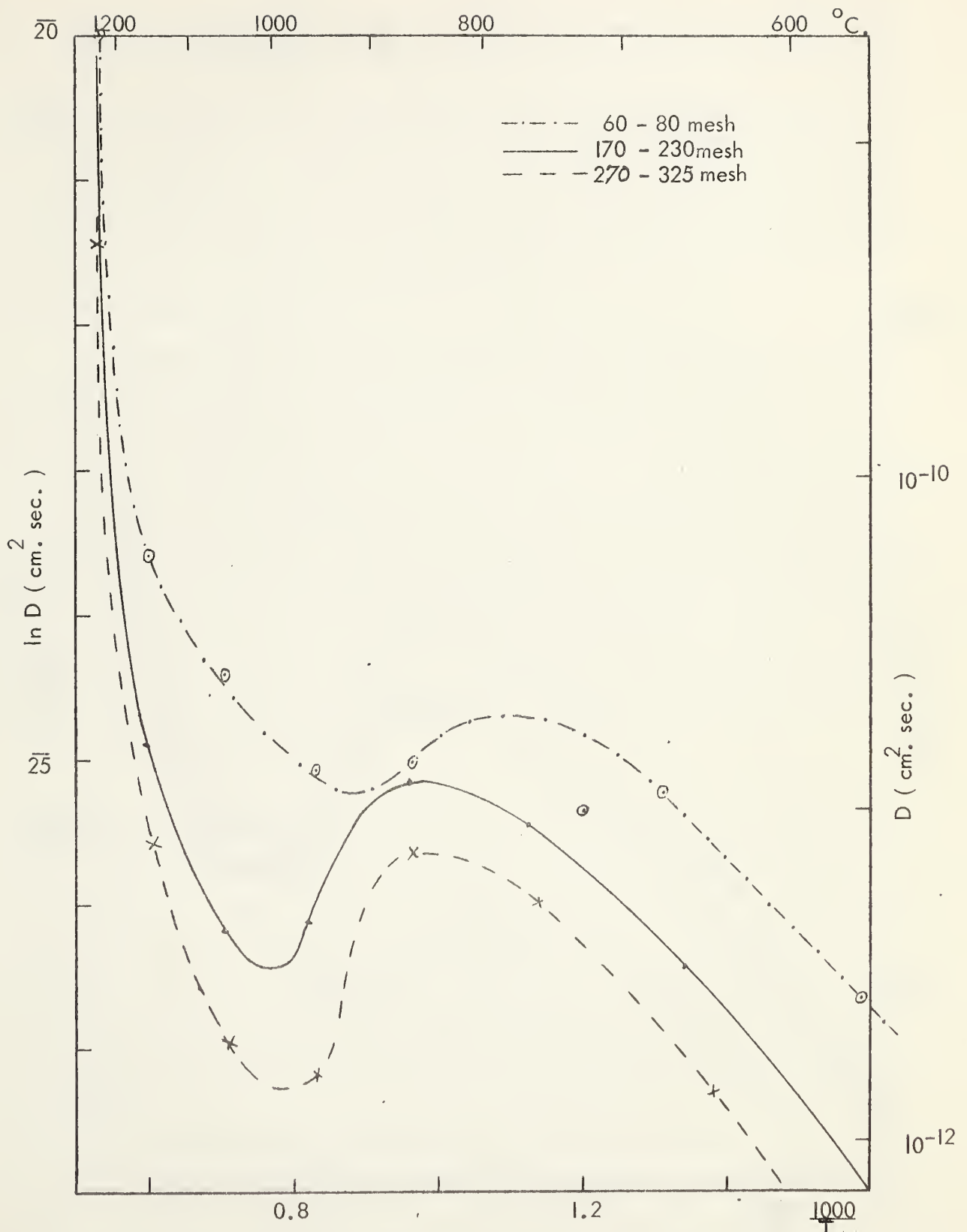


FIGURE 10. CROWSNEST SANIDINE. (calculated using equations (3) - 4 and (3) - 5)

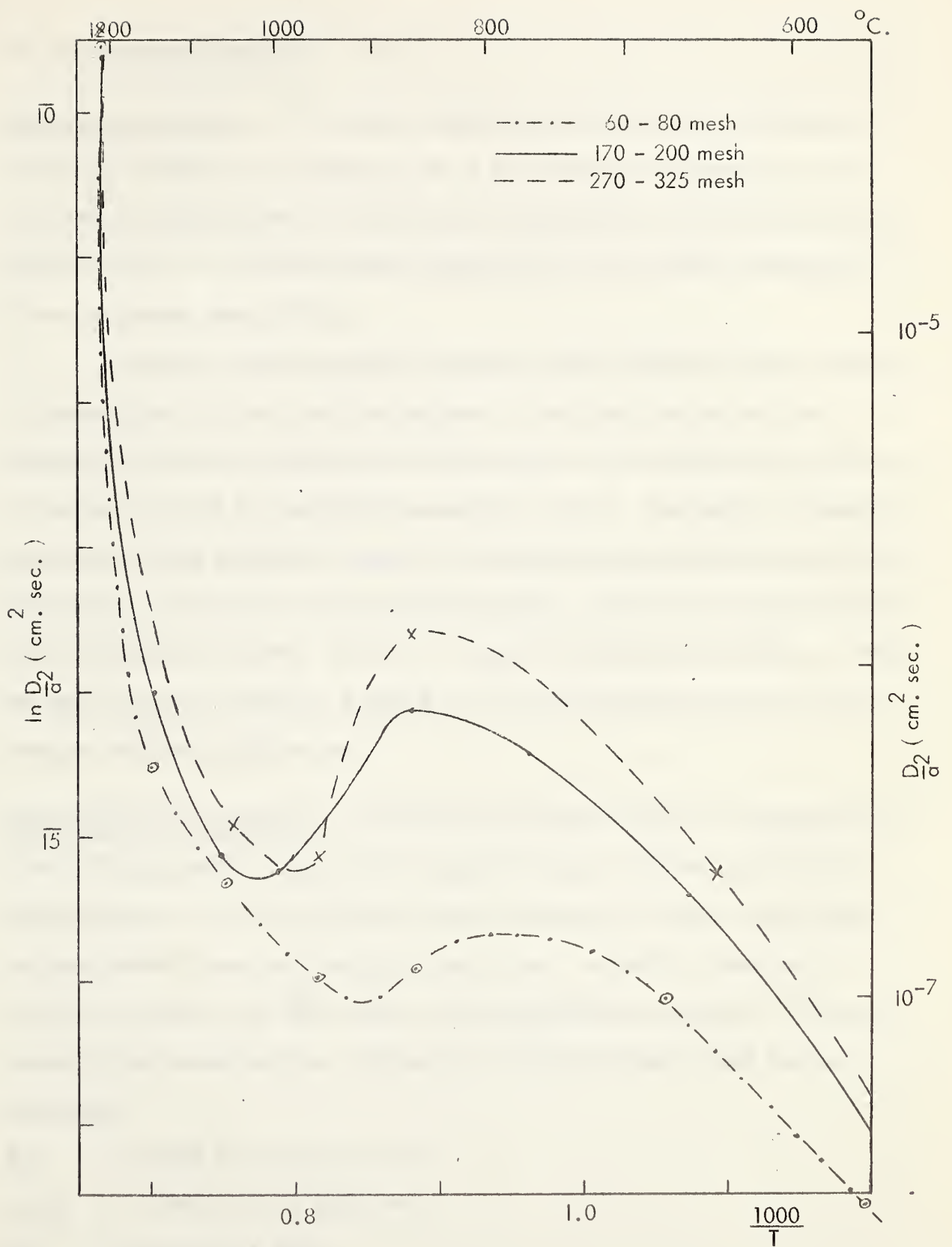


FIGURE 11. CROWSNEST SANIDINE (calculated using equations (3) - 4 and (3) - 5)

IV Yellowknife Microcline

Geological occurrence. - The sample, obtained from the Department of Geology, University of Alberta, was collected by Dr. R.E. Folinsbee. The microcline occurs in a muscovite-biotite granite in the Walmsley Lake map area, Yellowknife Geologic Province, N.W.T. This area has been mapped by Dr. R.E. Folinsbee (Geological Survey of Canada, Map 1013 A).

The oldest rocks outcropping in the area are the Yellowknife series, a group of metamorphosed volcanic rocks and sediments. The oldest intrusive rocks are believed to be three small bodies of hornblende diorite and hornblende-quartz diorite. In the greater part of the area biotite granodiorite outcrops. The absence of pegmatite associated with the granodiorite suggests that this rock has consolidated at great depth. The sample was taken from a muscovite-biotite granite, which is the youngest igneous rock outcropping in the area. As the K - Ar age of the microcline is 2000 m.y., while the age of cogenetic muscovite is 2600 m.y. it is calculated that the microcline has an argon deficiency of 36 per cent.

Description of the microcline. - The following description is given by Baadsgaard et al. (1961). The microcline occurs as white anhedral crystals in granite, poikilitically enclosing quartz. In thin section the mineral is colourless, but under crossed nicols the characteristic cross-hatch twinning is very clear. No perthitic lamellae are evident, but a shift in the $\bar{2}01$ peak on heating suggests some exsolution. Chemical analysis of the microcline gives: (Stelmach; University of Alberta, Rock Analysis Laboratory)

K_2O = 15.28% (Or = 90.25 wt. %)

Na_2O = 1.09% (Ab = 9.22 wt. %)

2V = 83 degrees \perp (010)

A slide of the microcline shows marked cross-hatch twinning. The grains are clear, but contain some small inclusions that show a tendency to be aligned along the twin planes.

Curve of the logarithm of the diffusion coefficient against reciprocal absolute temperature for the Yellowknife microcline, calculated using equation (3) - 4 and (3) - 5

A curve was prepared for the 60 - 80 mesh size, in the temperature range 301-1226°C. Figure 12. In order to determine if a low temperature 'zero phase' is present, as suggested by Amirkhanov (1959), the sample was outgassed at a low temperature (57°C.) for 36 hours. On heating at 301°C., 424°C., 526°C. and 650°C., a small amount of rapidly lost argon was found, but at each temperature release of this argon falls off rapidly with time. Inspection of the mass spectrometer curve of peak height against time, shows an extremely large initial peak which rapidly declines, so that after 500 seconds a flatter diffusion curve is observed. This suggests that only a certain amount of argon may be released at each temperature and that loss occurs very rapidly as each new temperature is established.

The effect of this argon loss on the values of the diffusion coefficient may be seen at the four lowest temperature intervals, which indicate that the diffusion coefficient is decreasing with time. The possibility that this rapidly lost argon is air argon that has been held due to the low temperature of outgassing, is not supported by inspection of the background peak heights. The most probable solution is that this argon is released from inclusions that occur within the lattice. If the rapidly lost argon is estimated for each of the four lowest temperatures and its influence subtracted from the argon which diffuses from the lattice, then new diffusion coefficients may be calculated. This recalculated curve, which I feel to be more reliable, produces a straight line below 850°C.

At 850°C. there is a marked inflection in the curve, which is definitely real. At this temperature 35 per cent of the total argon has been released. Above 1050°C.

the curve shows a marked increase in the diffusion coefficient, but at 1230°C. still only 64 per cent of the total argon has been released from the lattice.

The most natural explanation for the inflection in the curve at 850°C. lies in structural changes, changes either in the twinning or in the ordering of the Si-Al atoms. Optical examination of the heated and unheated samples shows the continued presence of cross-hatch twinning and there is no suggestion of melting of the grains. X-ray examination shows no significant changes in the position of the diffraction peaks in the heated sample. Unless a reversible structural change is occurring, it seems necessary to conclude that no lattice changes are taking place and that argon is diffusing from at least two positions.

As in the Crowsnest sanidine, the amount of argon in each position was determined by preparing a curve of cumulative fraction of argon lost against temperature. It was found that position I contains 35 per cent of the total argon present. If it is assumed that diffusion of argon from the two positions interferes only in the inflection zone, it is possible to recalculate the diffusion coefficients for each position. From these values the activation energy of argon loss from each position may be calculated.

The activation energy for loss from position I is $19,000 \pm 2,000$ cal./mole. The error was calculated from the possible variations in the curves that may be drawn through the values of $\ln D$ (D for position I).

The activation energy for position II is more uncertain. Values ranging from 55,000 cal./mole to 70,000 cal./mole were calculated. The most probable value which lies close to 55,000 cal./mole is certainly sufficiently high that no loss will occur from position II during geological time.

The calculated value of the diffusion coefficient at 27°C. is 1.8×10^{-21} cm.²/sec. (for position I)

The calculated value of the diffusion coefficient at 150°C. is 1.5×10^{-17} cm.²/sec. (for position I)



V Montevideo Microcline

Geological occurrence. - The sample was obtained from Dr. H. Baadsgaard. The microcline was taken from the Montevideo granite gneiss, which outcrops in the Minnesota River Valley. A geological description of the area is given by Lund (1956). The oldest rocks are a basic complex of gabbro and diorite gneisses, quartz diorite gneisses and garnetiferous quartz diorite gneisses. This group of basic gneisses is intruded by a series of granite of late pre-Huronian or Huronian age (2400 m.y. - 1700 m.y.). Since these late granites intrude along the foliation of the basic gneisses it is assumed that the gneissic texture was formed prior to the intrusion of the granite.

The Montevideo granite gneiss is one of these later granite intrusions. Conspicuous granulation and shearing at many places within the gneiss indicate that the gneissic structure is largely secondary. In Keweenawan times (~ 1000 m.y.) a series of basic dykes and two small masses of granite were intruded.

The K-Ar age of the microcline (KA 54) which was obtained from the Granite Falls Quarry, is 1.64 b.y. and the age of cogenetic biotite is 1.75 b.y. This indicates an argon discrepancy of 11 per cent in the feldspar. These dates suggest a rather simple picture, but a Pb-U age on the zircon from the Montevideo granite gneiss gives an age of 3.2 b.y. Further, the K-Ar age of the Montevideo granite gneiss (KA 27) at an unspecified locality gives a feldspar age of 1.36 b.y. while cogenetic biotite gives an age of 1.85 b.y. This indicates an argon deficiency of the feldspar with respect to the biotite of 36 per cent. The most reasonable explanation of these age relationships is that these rocks have been subjected to a later period of metamorphism. The difference in the ages of the two feldspars is most probably due to a difference in the degree of metamorphism between the two samples.

Description of the microcline. - The sample is pink in colour, due to exsolved iron oxides. On heating in a vacuum the grains become white due either to the reduction of the iron to the ferrous state or to absorption of iron in the lattice. Optical examination shows the grains to be cloudy and to contain many inclusions. In the thinner margins of the crystal cross-hatch twinning is clearly observable, but in the thicker grains the twinning is more difficult to observe. Cleavage is marked.

Optical examination suggests a perthitic nature, possibly of exsolution origin. The thickness of the grains make this difficult to observe. X-ray diffraction study of the powdered sample shows the presence of double peaks in the unheated sample which is indicative of perthitic structure. A shift in the $(\bar{2}01)$ peak on heating substantiates this conception. X-ray examination of the heated sample shows the disappearance of the double peaks, but no changes are observed that suggest disordering of the lattice. Chemical analysis of the feldspar (University of Minnesota, Rock Analysis Laboratory).

$K_2O = 12.89\%$ (76.18 wt. % Or)

$2V = 80-90^\circ \perp (010)$

Curve of the logarithm of the diffusion coefficient against reciprocal absolute temperature for the Montevideo microcline, calculated using equations (3) - 4 and (3) - 5.

Diffusion was observed from the 35-60 mesh size, in the temperature range 254-1243°C. As in the Yellowknife microcline, the sample was outgassed at a low temperature (40°C.) in order to determine if a 'zero phase' is present, as suggested by Amirkhanov (1959). It was found that at all temperatures below 850°C., those diffusion coefficients determined at a short time after the commencement of the temperature rise were higher than those found after argon had been diffusing for

about an hour. This effect is more noticeable at the lower temperatures and indicates that there is a certain amount (2 per cent) of easily lost argon present.

The nature of this loss is very much the same as in the Yellowknife microcline, the peak height at each temperature on the mass spectrometer chart shows a large initial response which rapidly dies out, giving way to a normal diffusion curve of considerably lower slope. The greatest effect of this easily lost argon is shown not at the lowest temperature, as would be expected if the argon was desorbed from the crystal boundaries, but at 418°C., the next higher temperature. It is felt that only a certain amount of argon will be lost in this manner at each temperature and it is therefore presumed that this type of argon does not diffuse from a different 'lattice position', but is lost from the inclusions that are seen to be present in large numbers in the crystal. Observation of the background at each of the temperatures does not indicate any large amount of air argon contamination, although the pressure at 546°C. and 651°C. shows a noticeable increase, possibly due to loss of water.

By extrapolation of the curves of peak height against time obtained from the mass spectrometer, the effect of the rapidly lost argon was subtracted and values of the diffusion coefficient were recalculated. These values define a steeper curve of $\ln D$ against reciprocal absolute temperature. However, it must be mentioned that correction for this rapidly lost argon, which represents 2 per cent of the total amount present, is extremely difficult because it represents a large percentage of the argon being released at these low temperatures. The probable error in these low temperature points is therefore quite large.

Inspection of the diffusion curve shows a marked inflection at 750°C., which is probably due to homogenization of the perthitic lamellae. Above 950°C. the curve becomes much steeper. The possibility of structural change as a cause of

this steeper curve is accepted, but optical examination of the heated sample shows the continued presence of cross-hatch twinning, and X-ray examination of the heated and unheated samples shows no structural change other than the homogenization of the perthitic lamellae. It is therefore suggested that the steeper curve is indicative of argon diffusing from a second position.

From a curve of cumulative fraction of argon lost against temperature it was found that position I contains 12 per cent of the total argon in the lattice. If it is assumed that diffusion from the two positions interfere only in the inflection zone, the diffusion coefficients for position I may be found and the activation energy for the positions calculated.

The value of the diffusion coefficient for position I was found to be 20,000 \pm 2,000 cal./mole. There is rather a large uncertainty in this value, due to the correction that has to be made for the rapidly lost argon at the four lowest temperatures.

The activation energy for position II is tentatively suggested as 71,000 cal./mole, a value which is in keeping with the observed high retentivity for the argon in position II.

If it is assumed that the activation energy for position I is 20,000 cal./mole and the diffusion coefficient at 418°C. is 2.54×10^{-12} cm.²/sec., then the diffusion coefficients at 27°C. and 150°C. for position I are:

$$D_{27^{\circ}\text{C.}} = 1 \times 10^{-20} \text{ cm.}^2/\text{sec.}$$

$$D_{150^{\circ}\text{C.}} = 7 \times 10^{-16} \text{ cm.}^2/\text{sec.}$$

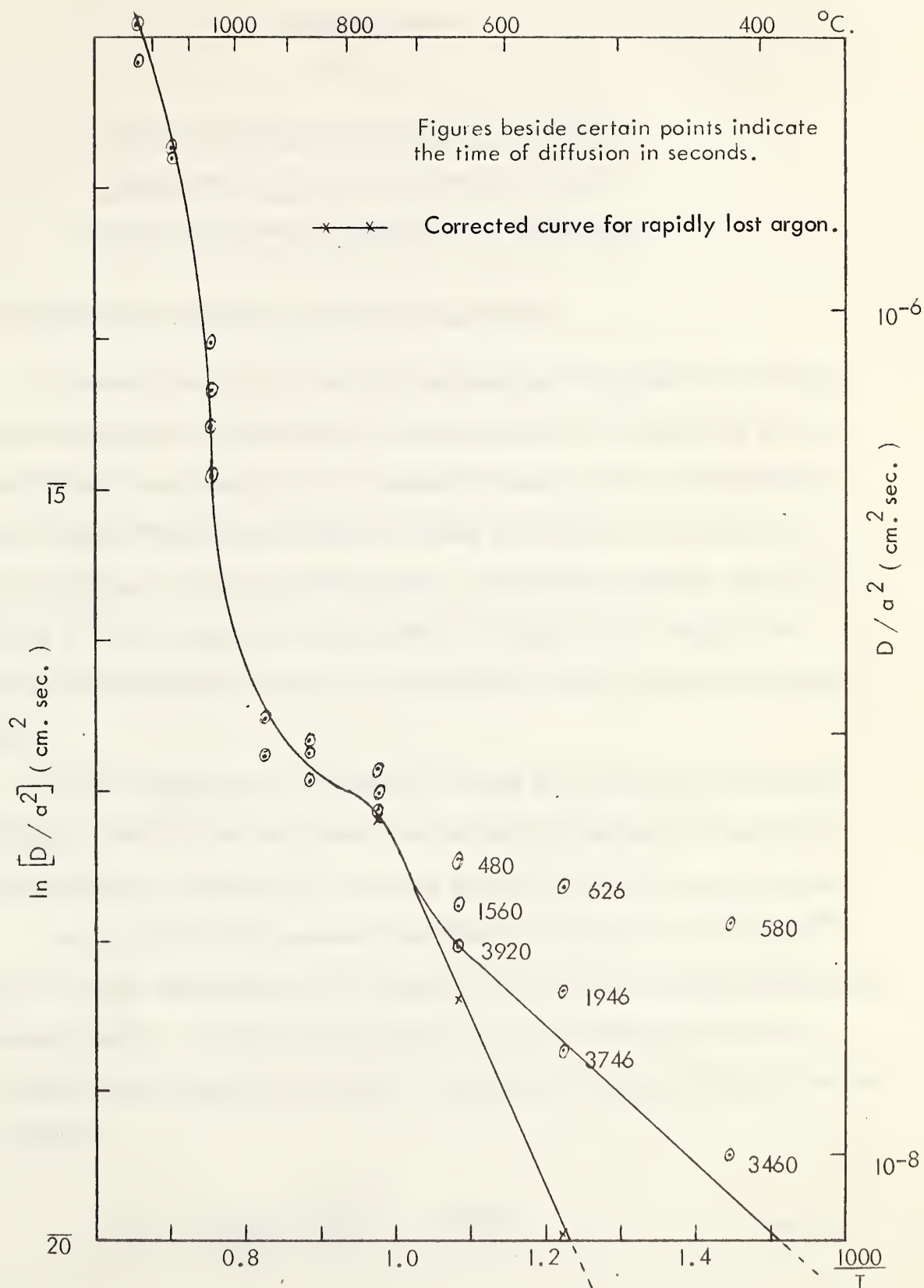


FIGURE 13. MONTEVIDEO MICROCLINE (calculated using equations (3) - 4 and (3) - 5)

CHAPTER FIVE

ON THE RELIABILITY OF THE CURVES OF THE LOGARITHM OF THE DIFFUSION COEFFICIENT AGAINST RECIPROCAL ABSOLUTE TEMPERATURE

1. Discussion and an alternative mathematical treatment

In chapter three the mathematical treatment used to calculate the diffusion coefficients was given. In those pages it was mentioned that the equations used to explain diffusion from feldspars were developed for those boundary conditions that describe volume diffusion from a sphere of uniform initial concentration and with zero concentration at the surface of the crystal. Since the same sample was used at a series of rising temperatures, the condition of uniform initial concentration held at the first temperature interval, but was violated at all succeeding temperature intervals.

Similar misgivings were expressed by Fechtig et al. (1961), who measured the diffusion coefficient for the release of the radioactive isotopes Ar³⁷ and Ar³⁹ in samples of sanidine, synthetic sylvite, augite, phonolith and in a Bohemian tektite.

Fechtig et al. (1961) measured the diffusion of radioactive Ar³⁷ and Ar³⁹ (formed by neutron bombardment of the samples) at successively increasing temperatures on the same sample. As Fechtig's losses did not usually exceed 10 per cent of the total amount of argon present in the crystal, he used the first term of the approximation: Crank (1956)

$$f = \frac{6}{\pi^{\frac{1}{2}}} \left(\frac{Dt}{a^2} \right)^{\frac{1}{2}} - \frac{3Dt}{a^2} \quad (3) - 4$$

On the samples of the moldavite (Bohemian tektite) and sanidine, the diffusion of Ar^{37} was measured at successively rising temperatures. After the activity had been measured at the highest temperature, the sample was cooled and the run repeated. In this manner three runs were made on each sample. In all cases it was found that the curve of $\log D/a^2$ vs. $1/T$ was a straight line, but it was found that the values of the diffusion coefficient at any one temperature decreased from the first run to the third. This result would be expected because of the violation of the boundary condition on which the mathematical treatment is based. If irradiation produces a uniform initial concentration of radioactive argon in the crystal, then only at the first temperature interval of the first run is there a uniform concentration of argon throughout the crystal. At all succeeding temperature intervals, argon is diffusing from an inhomogeneous lattice. When the second run is started on the same sample, the lattice has lost argon from the outer layers of the crystal, which will reduce the amount diffusing at any temperature interval as compared to that diffusing during the first run, and the calculated diffusion coefficient will be low. At the start of the third run this effect will be even more marked, so that the calculated value of the diffusion coefficient will be even lower.

It is noticeable that the values of the diffusion coefficient in sanidine calculated for the three runs using equation (3) - 4, differ more at low temperatures than at high temperatures. This implies that the increased activity of the argon atoms at high temperatures has the effect of concealing the initial inhomogeneity of argon in the lattice, and that the determined diffusion coefficients are essentially correct.

Since the boundary condition by which the equation (3) - 1 is developed (uniform concentration of argon at the beginning of measurement) is broken in these

experiments, Fechtig recalculated his diffusion data making use of a mathematical relationship that explains the measured loss as coming from a boundary gradient at the surface of the crystal. This mathematical treatment was developed by Wragge (1962) by solving Fick's law by the method of approximations, applying the boundary layer theory which has been experimentally tested by von Karman (1921) and Pohlhausen (1921).

His solution uses δ_k as a measure of the thickness of the gradient layer near the surface which has formed after the k^{th} measurement on the crystal. The diffusion coefficient may then be obtained from the following formulae: (Fechtig et al., 1961)

$$\delta_k = \frac{a (C_o - C)_k}{C_o} + \delta_{k-1} \quad (5) - 1$$

$$D_k = \frac{a}{6} \frac{(C_o - C)_k}{C_o} \left(\frac{\delta_{k-1}}{t_k - t_{k-1}} \right) \quad (5) - 2$$

If $\frac{(C_o - C)_k}{C_o} = f_k$, then (5) - 2 may be rewritten:

$$\frac{D_k}{a^2} = \frac{\delta_{k-1} \cdot f_k}{6 (t_k - t_{k-1})} \quad (5) - 3$$

Where: a = radius of the grains

$(C_o - C_k)$ = argon loss for the k^{th} measurement

C_o = total argon content

$t_k - t_{k-1}$ = time of measurement of the k^{th} measurement

In order to estimate the reliability of the diffusion curves and to justify the conclusions that will be made, the diffusion data were calculated using three different mathematical assumptions. These assumptions are:

- a. That at each successive temperatures, the fraction of argon released of that present at the start of the temperature interval is a reliable function which may be used to determine the diffusion coefficients. Curves derived using this assumption were presented in the preceeding chapter, and were calculated using the mathematical relationships developed in chapter three, using equations (3) - 4 and (3) - 5.
- b. The second assumption is that if the crystal is heated at successive temperature intervals T_1 , T_2 , T_3 , etc., then at the T_n^{th} interval, the argon that has been released at all preceeding temperature intervals together with that released at the T_n interval, during time (t_n) would have come off in the same period of time (t_n) if the sample had been directly heated to T_n . From this assumption the cumulative fraction curves were calculated.

This assumption is not valid for very short time intervals of heating, but as the time of heating exceeds 3 hours it must approach a reasonable approximation. Evidence for this is obtained from the Crowsnest sanidine: A sample of the 60 - 80 mesh sanidine was heated directly to 1040°C . for 4000 seconds (including 800 seconds heating time) during which time 30 per cent of the total argon present was released. A similar sample was heated at eight successive temperatures for approximately 1 hour at each temperature, and was then heated at 1052°C . for 3200 seconds. This sample had lost 40 per cent of the total argon at the end of the successive temperature intervals.

- c. The third assumption assumes that diffusion takes place from a boundary layer as suggested by Gentner et al. (1961). The mathematical treatment was developed by Wrage (1962) and has been used to calculate values of D_k/a^2 .

Comparative results of the three methods are presented in Figures 14-19.

II Comparison and appraisal of the curves obtained using the different mathematical treatments

The diffusion data were calculated using three assumptions. The mathematical treatment presented in chapter three was used to calculate the diffusion coefficients using the individual fraction of argon lost at each temperature, and secondly using the cumulative fraction of argon lost at the end of each temperature interval. The data were also recalculated using the mathematical treatment presented in Wragge (1962) and Fechtig et al. (1961).

Consideration of the curves for the Kinnekulle sanidine (Figure 14), which is the simplest case, shows that the slope of the curves are remarkably similar. The major point of divergence in behavior is observed at the highest temperatures, when the curve calculated using Wragge's mathematical treatment shows a marked decrease in the gradient, while the curves from the other techniques show an increase in the gradient. It is felt that since the mass spectrometer curve shows very rapid loss at 1135°C., the uptrending curve is more real. The conclusion presented in the previous chapter that the Kinnekulle curves indicate volume diffusion from a stable lattice is sustained.

The value of the activation energy derived from the 'Wragge' curve is 45,700 cal./mole (Baadsgaard) and that found using the individual fraction curve is 42,500 cal./mole.

The comparative curves for the Millcreek sanidine (170-230 mesh) are given in Figure 15. The curves at low temperatures are parallel, but at 950°C. they show a marked break in the slope. As in the Kinnekulle sanidine, the 'Wragge's' curves show a decrease in the slope, while the curves calculated using individual and cumulative fractions rise strongly.



In Figure 16, the curves are presented which were calculated for the three grain sizes of the Millcreek sanidine using Wragge's mathematical treatment. Comparison of these curves with the curves in Figure 9, which were calculated using equations (3)-4 and (3)-5, shows that below 950°C. both treatments result in very similar curves. At 950°C. both curves show a decrease in the slope, but at 1050°C. the curves in Figure 9 show a marked rise, while the 'Wragge' curves continue their decrease in slope. It is felt that because the Millcreek sanidine shows extensive melting at the highest temperature of diffusion, then the up-trend, in curves of individual fractions are the most reasonable, and that Wragge's mathematical treatment possibly fails when argon losses exceed 50 per cent of the total amount originally present.

In the case of diffusion from one position, the curve obtained using the assumption that diffusion occurs from a boundary gradient, would be a straight line at low temperatures, declining at higher temperatures due to depletion of argon in the crystal. If the curve from Wragge's treatment shows an upward inflection at high temperatures it must be due to diffusion from a second position, or to a lattice change allowing diffusion to occur more readily.

The possibility of there being two positions in the Millcreek sanidine from which argon may diffuse, appears to be discounted. The inflections in Figures 9 and 10 are most probably due to depletion of the lattice, and the renewed upward curves must indicate rapid loss of argon as the crystal melts.

The activation energy calculated for the Millcreek sanidine from the 'Wragge' curves is 45,700 cal./mole (Baadsgaard) which compares with 43,900 cal./mole using the individual fraction curve when positions are discounted.

The Crowsnest sanidine shows a more interesting series of curves. Figure 17 presents the results of the three assumptions, calculated for the 270-325 mesh size.

It is noticeable that the individual fraction and the Wragge's curve are comparable in form, but that Wragge's curve shows a smaller inflection. The cumulative fraction curve appears to conceal the inflection that has been observed in the other treatments. Since inspection of the mass spectrometer diffusion curves shows these inflections to be most definitely real, the cumulative curves have been largely neglected in the following pages.

In Figure 18 it is seen that all the 'Wragge' curves for the Crowsnest sanidine show an inflection, which in the two finer grain sizes assumes the form of a minimum. Above 1050°C. all the curves show a marked increase in slope. If the Kinnekulle sanidine and Millcreek sanidine curves (Figures 14, 15, 16) are used as a measure of the shape of the 'Wragge' curve when diffusion occurs from one position, then a better understanding may be achieved of diffusion from the Crowsnest sanidine. The upward inflection of the diffusion curve above 1000°C. for the Crowsnest sanidine may be due to (a.) a phase change (b.) argon diffusing from a second position, or (c.) a change in the mechanism of diffusion. No explanation is given for the anomalous points which are found at 750°-800°C. in all three grain sizes.

The activation energy calculated for the Crowsnest sanidine from the 'Wragge' curves is 26,000 cal./mole for position I and 91,500 cal./mole for position II (Baadsgaard). Using the individual curves, a value of 28,500 cal./mole was found for position I and 47,000 cal./mole for position II. While values for position I are comparable, the values for position II are very different. It is felt that since argon is lost very easily at the highest temperatures (at a comparable rate with the Kinnekulle and Millcreek sanidines) then the lower value of 47,000 cal./mole is the more correct.

Curves derived for each of the microclines using Wragge's mathematical treatment and using the individual fractions of argon lost, are similar (Figure 19). The activation energy calculated for the Yellowknife microcline from the 'Wragge'

curve is 23,000 cal./mole for position I (the curve below the inflection) and 57,000 cal./mole for position II (Baadsgaard). Comparable values for the individual fraction curve are 19,000 cal./mole and 55,000 cal./mole.

For the Montevideo microcline the activation energy calculated from the 'Wrage' curve for position I was 20,200 cal./mole, and 52,600 cal./mole for position II (Newland). Values for the individual fraction curve are 19,000 cal./mole for position I and 71,000 cal./mole for position II. As heating the Montevideo microcline at 1240°C. failed to remove all of the argon present, the activation energy at high temperatures must be very large. Consequently, it is felt that the more probable value of the activation energy for position II is $71,000 \pm 6,000$ cal./mole.

By virtue of the comparison between the curves calculated using the theory of diffusion from a boundary layer, and those derived using relationships describing volume diffusion from a sphere, it is clear that either of these mathematical treatments is acceptable. However, by comparison of the diffusion curves calculated using both assumptions, more valid deductions concerning the nature of diffusion may be made.

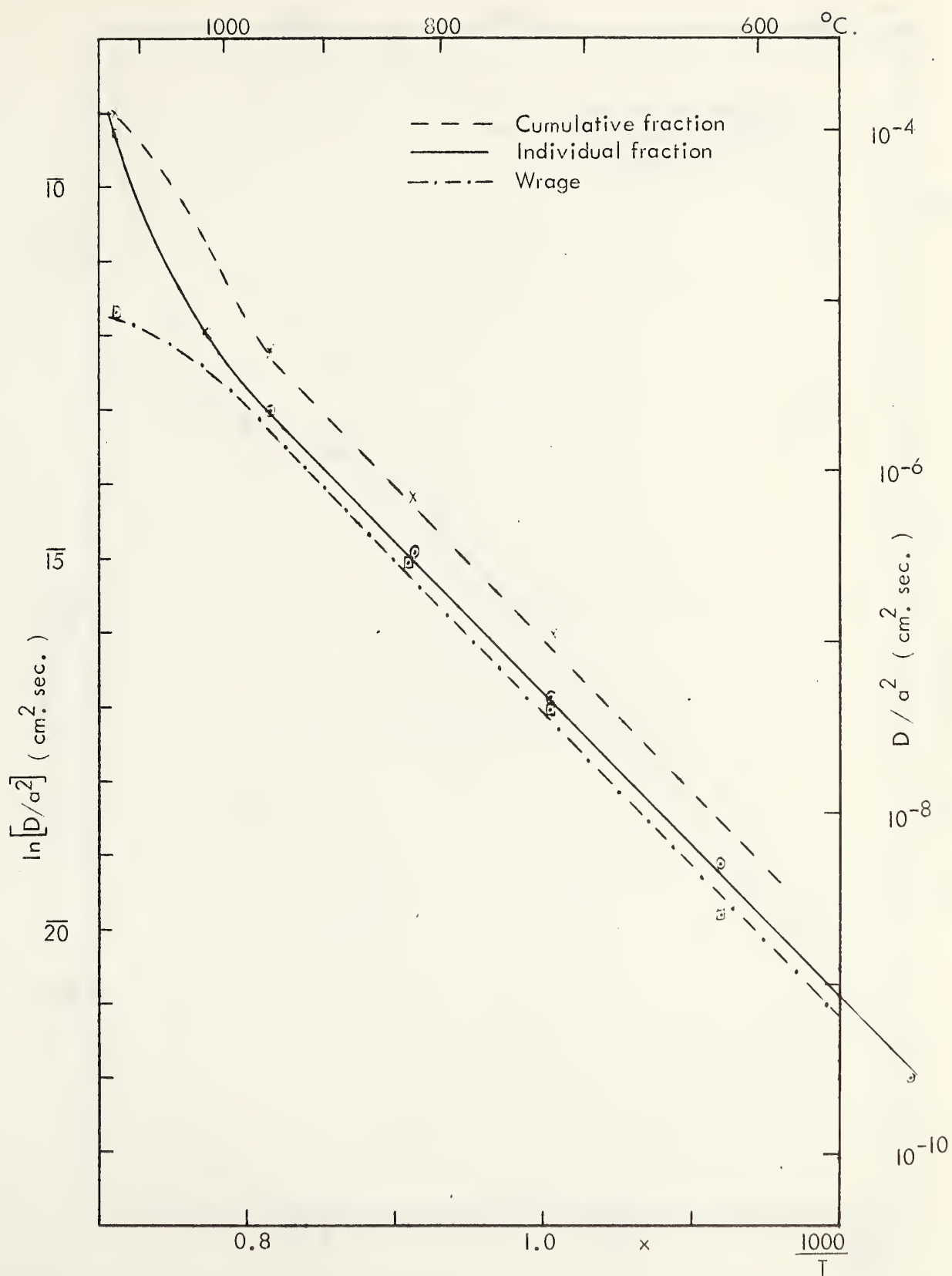


FIGURE 14. KINNEKULLE SANIDINE (Comparative curves)

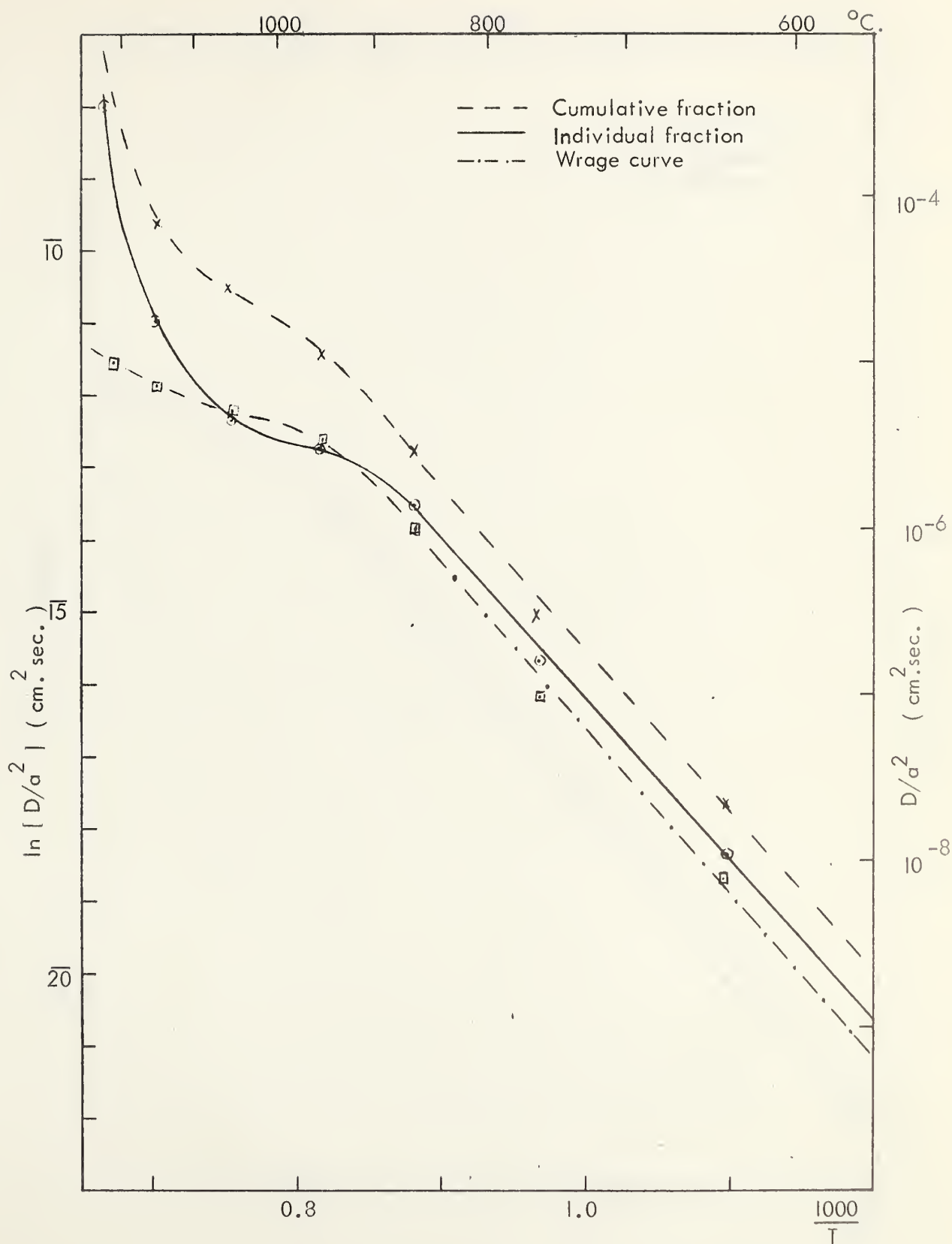


FIGURE 15. MILLCREEK SANIDINE 170 - 230 mesh. (Comparative curves)

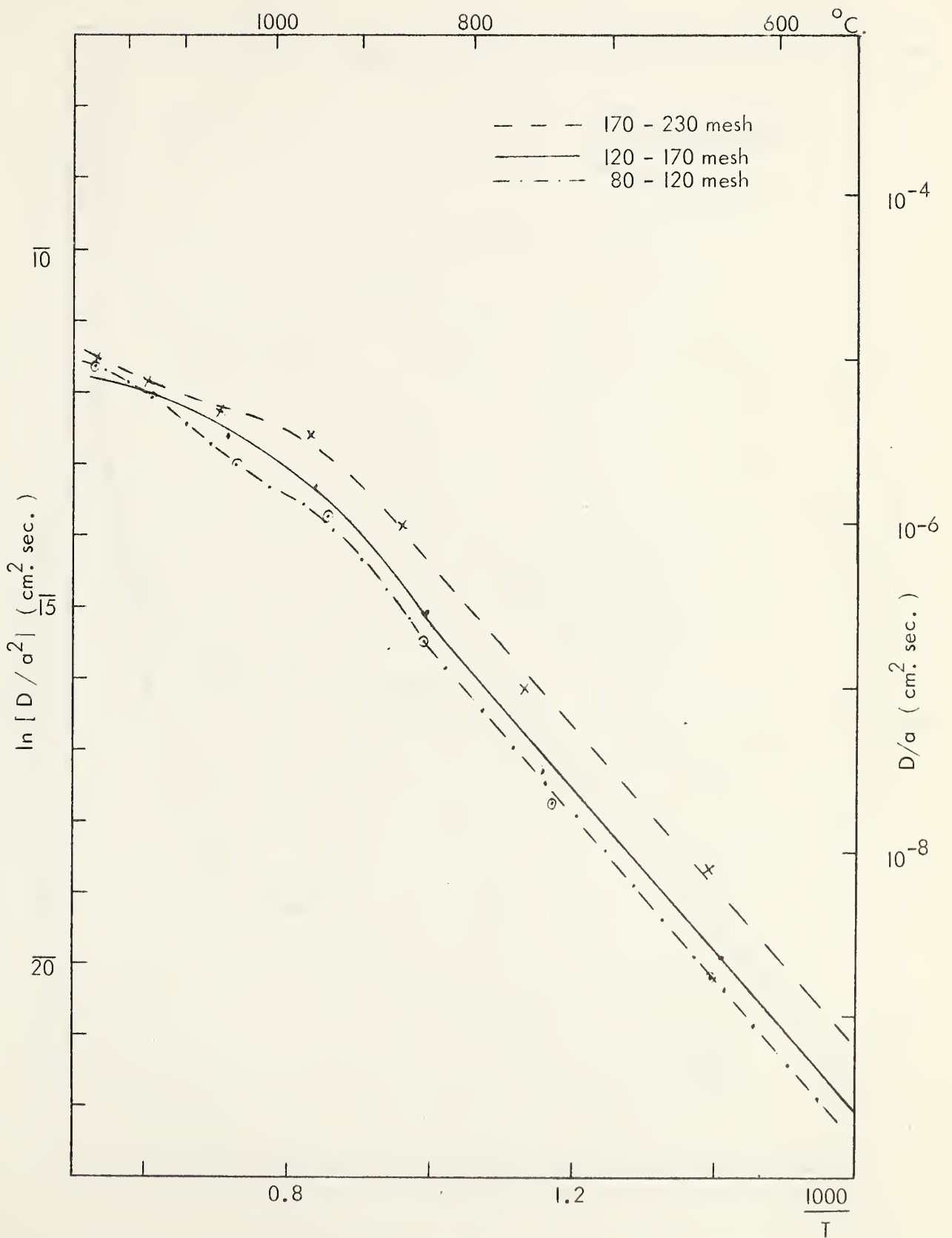


FIGURE 16. MILLCREEK SANIDINE (Wrage treatment)

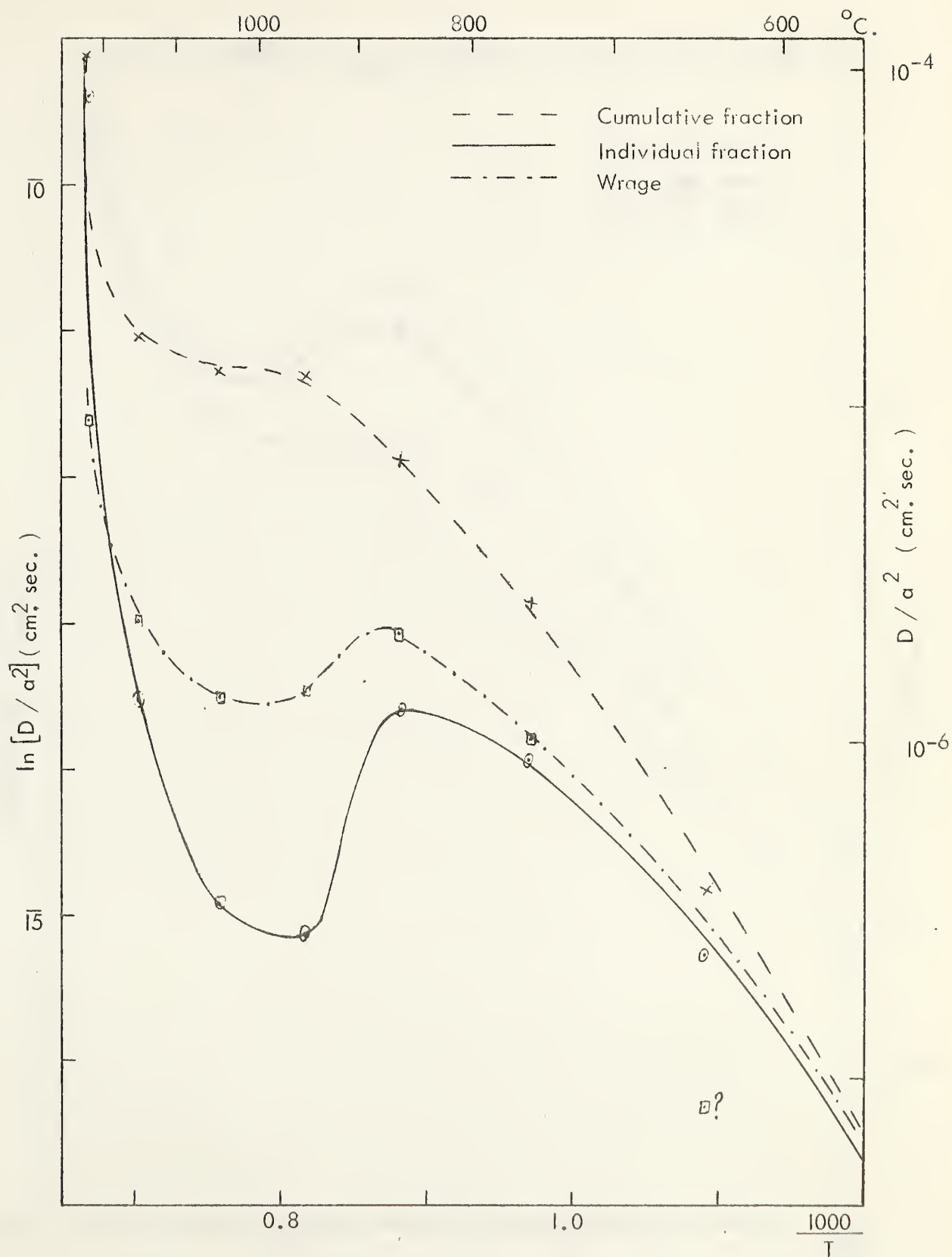


FIGURE 17. CROWSNEST SANIDINE 270 - 325 mesh (Comparative curves)

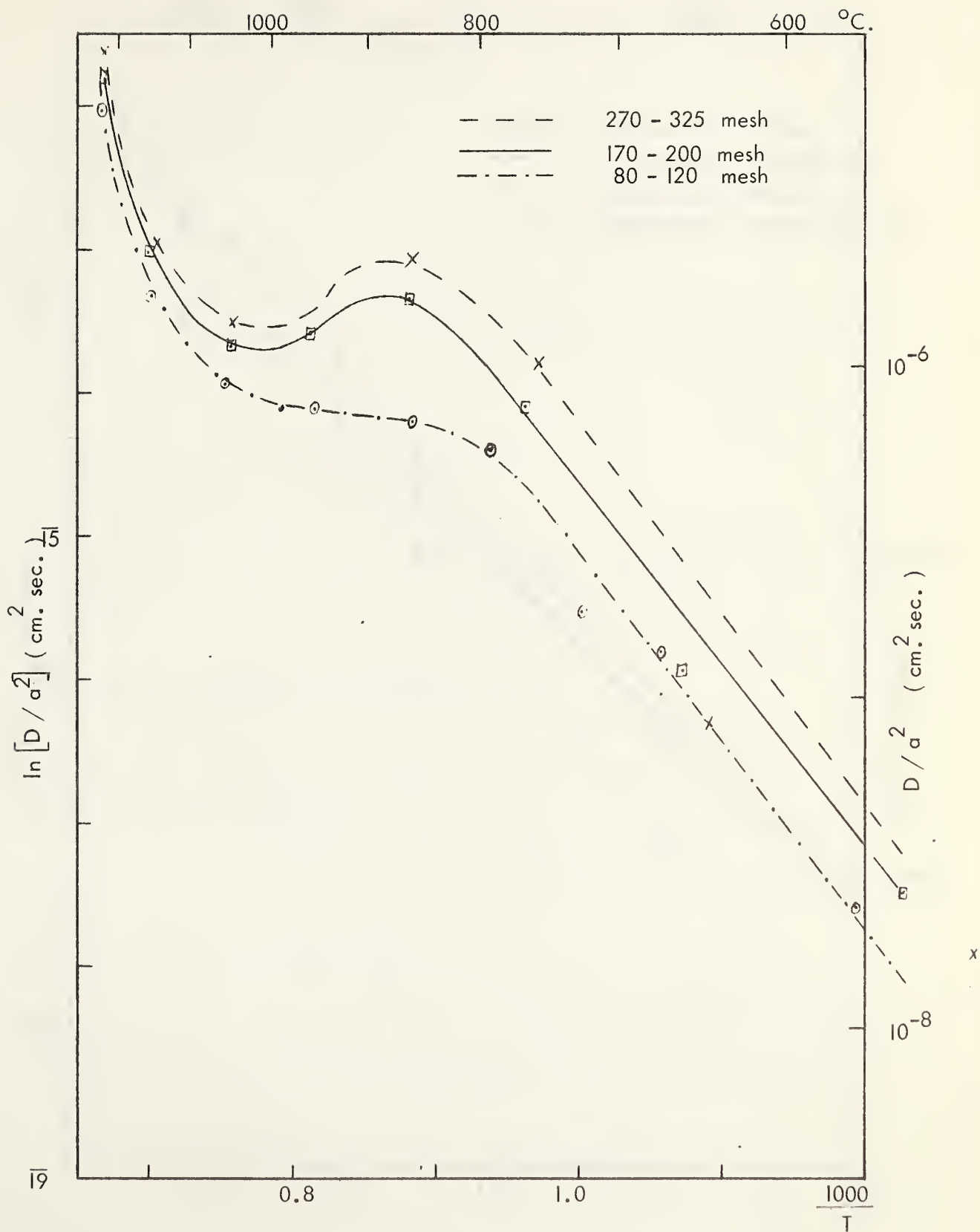


FIGURE 18. CROWSNEST SANIDINE (Wragge curves)

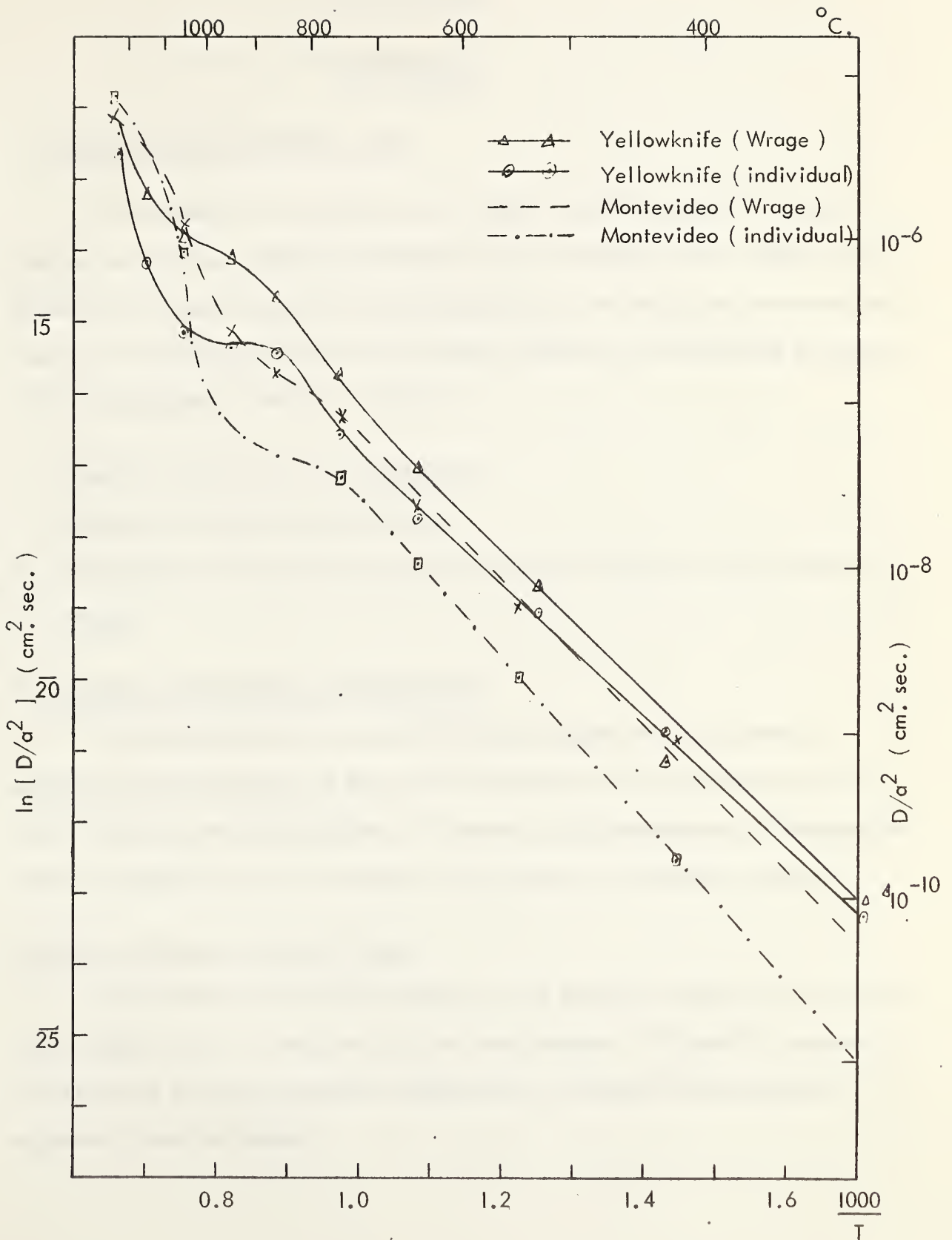


FIGURE 19. YELLOWKNIFE AND MONTEVIDEO MICROCLINES.
(Comparison of ' Wrage ' and Individual fraction curves)

CHAPTER SIX

DISCUSSION

I Interpretation of the diffusion curves

The curves of the logarithm of the diffusion coefficient against reciprocal absolute temperature, indicate that diffusion from the feldspars is not a simple process. Three factors suggest themselves as being responsible for the inflections that have been observed in the diffusion curves of the Crowsnest sanidine, the Yellowknife microcline and the Montevideo microcline. These are:

1. Changes in the structure with temperature.
2. Change in the mechanism of diffusion.
3. That argon is held in two lattice positions, each of which has a unique activation energy.

1. Changes in the structure with temperature

Consideration of the structure of feldspars suggests that the following phenomena may be the cause of the observed inflections in the experimental curves; (a) an increase in the disorder of the Si,Al atoms at high temperatures, (b) homogenization of the perthitic layers, (c) changes in the twinning, and (d) phase changes.

(a) Order - disorder of the Si,Al atoms.

The diffusion curves for the Kinnekulle and Millcreek sanidines indicate that loss of argon occurs in a simple manner from these feldspars. This result is expected, for as sanidine is the high temperature polymorph, no structural change would be expected to occur on heating.

However, the diffusion curves obtained for the Crowsnest sanidine were found to show inflections at 1000°C. for the two finer mesh sizes and at 900°C. for the 60-80 mesh size. It has been shown (p. 79) that the curve of steeper gradient observed above 1050°C. cannot be due to melting of the lattice, but must have another explanation. Since the Crowsnest sanidine is extremely disordered, it appears very unlikely that the inflection in this sanidine is due to disordering of the lattice during the experiments.

It is in the microclines that the order - disorder relationship would be expected to be most clearly seen. As the diffusion curves show an increase in gradient at approximately 1050°C., for the Yellowknife microcline and at 950°C. for the Montevideo microcline, the belief that the inflections in the curves are a result of disordering of the (Si,Al-O) framework in the ordered microcline lattice would be reasonable. However, as X-ray inspection of the heated samples shows no significant changes in the position of the peaks that can be related to disordering, it must be concluded that disordering of the Si,Al atoms is not the cause of the inflections.

(b) Mixing of the perthitic layers

The Montevideo microcline is the only sample which is distinctly perthitic. X-ray diffraction studies of the heated and unheated samples shows that heating has homogenized the perthitic lamellae. Since homogenization takes place in 24 hours at 700°C., and in 1 hour at 950°C. (Bowen and Tuttle, 1950), it must be considered as a possible cause of the inflection found in the curve of the Montevideo microcline. However, as the Crowsnest sanidine and the Yellowknife microcline are not perthitic (though there may be small variations in the alkali content within the crystals), it is felt that there is no evidence that homogenization of perthitic lamellae is a major cause of the observed inflections.

(c) Changes in the twinning

Changes in the twinning must be considered as a very possible cause of the inflections that occur in the diffusion curves of both microclines. In the Crowsnest sanidine, the marked zoning and abundant fractures might have a similar influence in facilitating diffusion.

It is reasonable to suggest that diffusion in microcline at low temperatures is assisted by the twin lamellae. At higher temperatures diffusion will occur at a higher activation energy through the unstrained lattice. However, the inflections are not related to removal of twins as optical examination shows the continued presence of twins in the heated sample, and X-ray examination of the heated sanidine showed no structural change.

Because reversible changes in the twinning and in the lattice structure must be considered as a reasonable possibility, optical and X-ray inspection with rising temperature is necessary to form a valid conclusion.

(d) Phase change

A possible cause of the observed inflections are phase changes. The most easily realized phase change that occurs in feldspars is disordering of the Si, Al atoms, but optical and X-ray inspection shows that disordering does not occur in the heating time of these experiments.

Possibly the position may be clarified by comparison of the 'Wrage' curves. In the Kinnekulle sanidine, simple diffusion from one position results in a straight line at low temperatures, which decreases in gradient at high temperatures due to depletion of argon. It is difficult to realize how a phase change, by increasing the activation energy, is able to make the 'Wrage' curves show the increase in the gradient observed in the Crowsnest sanidine and in the microclines.

As in the literature on feldspar structure there is no mention of reversible phase changes and because Sahama (1962) working on nepheline (a feldspathoid) found no evidence of immediately reversible phase change in an optical study at progressively higher temperatures, it is felt that phase changes cannot be a cause of the inflections.

2. Change in the mechanism of diffusion

Three basic mechanisms have been proposed to explain diffusion in solids. (Grey, 1956).

- a. Atoms may interchange positions directly. If this is the case, neighbouring atoms have to separate when the interchange takes place to make room for the interchanging atoms. Since this will strongly distort the lattice during the process, it is doubtful that this mechanism is very prevalent.
- b. Atoms may leave their normal lattice positions and migrate through interstitial sites. An atom doing so may eventually fall into a vacant site left by a diffusing atom. In this mechanism, one type of atom moves with respect to another type which remains stationary.
- c. The presence of vacant lattice sites will promote another diffusion mechanism. Atoms may diffuse by jumping into these vacant sites. In this case the vacancies may be considered as diffusing. These Schottky defects will be present at any finite temperature.

In the case where Frenkel defects predominate (an ion leaving a normal lattice site to take up an interstitial position), all types of mechanism are possible. When Schottky defects predominate (defects caused by ions leaving the normal lattice site to take up a position on the surface of the solid), the third mechanism will be the most important.

Reynolds (1957) suggested that if argon diffuses by migration through lattice vacancies, then the rate of diffusion will depend on two factors. The first of these is the volume density of vacancies, and the second, the activation energy required for the migration of rare gas atoms between the vacancies. It is supposed that at low temperatures the impurity content controls the number of vacancies, but at high temperature there is a marked increase in the number of vacancies due to Schottky defects, resulting in a decrease in the activation energy. As in all these experiments the activation energy of position II is higher than that of position I this theory is discounted. It is also difficult to reconcile a theory which requires a marked change in the density of vacancies, with the simple curves obtained for the Kinnekulle and Crowsnest sanidines. However, it must be realized that lattice diffusion occurs through vacancies, so that a change in the number of vacancies would affect the rate of diffusion.

3. That argon is held in two lattice positions, each of which has a unique activation energy

The presence of argon in more than one lattice position is a concept which has continued to appear in papers concerning diffusion of argon from feldspars. In this series of experiments, evidence was obtained for the presence of two positions in both the Crowsnest sanidine and in the two microclines.

If two positions are assumed, the inflection in the diffusion curves may be easily explained. The segment of the curve at temperatures below the inflection is due to loss from the first position and the inflection is due to depletion of this position. When the temperature is sufficiently high that diffusion may occur from the second position of higher activation energy, the curve begins to curve upward again. In the microclines a third position might be present, containing that argon which is retained at high temperatures.

Evidence in support of the concept of positions may be taken from Amirkhanov (1961), who distinguished two zones in feldspar, a 'steady' zone which corresponds to an undisturbed lattice and an 'unsteady' zone from which the argon is lost by heating at 400°C. for three hours. The potassium in this zone may be removed by heating at 600°C. in a solution of TiNO_3 . Hart (1962) found that feldspar ages in the first 1000 feet of the thermal aureole of a Tertiary intrusive in a pre-Cambrian schist were higher than biotite. Also the microcline in the first 100 feet has been changed to orthoclase and the perthitic structure homogenized. Since the feldspars even under these conditions retained some pre-metamorphic argon, Hart suggested that a certain part of the argon is very strongly held. This interpretation is confirmed by the experimental work for this thesis, for it was found that microcline showed high retentivity for part of its argon even at 1230°C.

The main difficulty in the concept of positions lies in determining the nature of the two positions. It is impossible to conceive that the positions are internal lattice positions because they would be also expected in the Kinnekulle and Millcreek sanidines. It must be realized that the concept that explains the presence of positions in the Crowsnest sanidine must also explain their absence in the two bentonitic sanidines.

I feel that it is reasonable to conclude that changes in the mechanism of diffusion and phase changes are not the cause of the anomalies in the diffusion curve. It appears a valid conclusion that argon is present in two positions, the nature of which must be related to the proximity of the argon atoms to structural defects. In the Crowsnest sanidine these defects are strain planes formed during the flowing of the lava, and in the microclines the structural defects may be equated to the proximity of argon atoms to the twin lamellae.

It is obvious that the simplest method of testing the concept of positions would be to heat the sample at a temperature at which diffusion may only occur from position I (850°C. for the 270-325 mesh Crowsnest sanidine) in order to remove all the argon from this position. A normal diffusion curve would then be prepared. If argon occurs in discrete positions, then no diffusion from position I would be found after heat treatment. If the inflections are related to lattice changes either in twinning, order-disorder or phase changes, diffusion would still be observed at low temperatures.

II Geological significance of the diffusion data

1. It is clear that consideration must be given to the limiting value of D/a^2 below which no loss of argon would be expected during geological time. Amirkhanov et al. (1961) gave the following equation relating diffusion losses that will occur in geological time with values of $D/\lambda a^2$

$$Ar^{40} = \frac{\lambda_e}{\lambda} K_o^{40} \frac{6}{\pi^2} \sum_{n=1}^{\infty} \frac{1}{n^2} \left(\frac{e^{-\frac{n^2 \pi^2 D t}{a^2}} - e^{-\lambda t}}{1 - \left(\frac{n\pi}{a}\right)^2 \frac{D}{\lambda}} \right) \quad (6) - 1$$

where: λ_e = decay constant of K^{40} to Ar^{40}
 λ = decay constant of K^{40}
 D = diffusion coefficient
 a = radius of diffusion
 t = time

The equation (6) - 1 contains two terms, one explaining the formation of argon by the decay of K^{40} , the other loss of argon by spherical diffusion. From curves of Ar^{40}/K_o^{40} against time for different values of $D/\lambda a^2$, it may be seen that diffusion losses are not significant as long as $D/\lambda a^2$ is less than 10^{-4} .

By use of this relationship it has been shown that no significant loss of argon can occur from the Kinnekulle and Millcreek sanidines at temperatures below 200°C. (see p.56).

For position I in the Crowsnest sanidine, it was found that $D/\lambda a^2 \sim 10^{-4}$ at 150°C. (equivalent to an average depth of burial of ~ 5 km.). This is a threshold value for loss of argon by diffusion in geological time.

For the Yellowknife and Montevideo microclines, the effective radius of diffusion is assumed to be 30 microns. In both cases at 150°C. the value of $D/\lambda a^2 \sim 10^{-1}$. This value is sufficiently high to cause loss of argon during geological time. If the feldspar was held at 150°C. for 2 billion years then a 25 per cent loss of argon would have occurred from position I.

It is evident that diffusion of argon contained in position I during geological time is a sufficient cause for the argon deficiency found in microcline. The extent of the argon deficiency depends on the value of the activation energy for position I, on the thermal history of the feldspar and on the age of the feldspar.

It is also concluded that sanidine obtained from lava flows could show a deficiency of argon due to increased ease of argon diffusion along fractures. The present work indicates that loss by diffusion will become important only if the sanidine is held for a considerable period of time above 200°C. (equivalent to an average depth of burial of approximately 7 kms.).

2. Inspection of the data for the two finer grain sizes of the Crowsnest sanidine suggests that each position contains 50 per cent of the total argon. If, in both of the microclines, it is assumed that 50 per cent of the total argon produced in the crystal and 50 per cent of the total potassium, are held in position II and that during geological time no loss of argon occurs from position II, then corrected ages for the microclines may be calculated.

The recalculated age for the Yellowknife microcline was made assuming that 65 per cent of the argon presently in the crystal is held in position II. The age found was 2.34 b.y. The determined ages for the feldspar was 2.0 b.y. and the age for cogenetic biotite 2.6 b.y.

The recalculated age for the Montevideo microcline was made assuming that 86 per cent of the argon presently in the crystal is held in position II. The recalculated age was 2.29 b.y. The determined age for the feldspar was 1.64 b.y. and that for cogenetic biotite 1.75 b.y.

It is evident that these dates are of very little significance. This probably indicates that the original assumptions (that 50 per cent of the argon and potassium are held in position II) are invalid.

3. If argon is held in two positions, an explanation may be found for those cases in which microcline gives a higher age than biotite. During metamorphism, biotite could be recrystallized with the subsequent release of much of the argon. Conversely, microcline during metamorphism would lose all the argon in position I but the activation energy of position II is sufficiently high that some of this argon could be retained.

In a metamorphic event, biotite would be completely updated and as it appears to show complete retention of argon at normal temperatures, would give a date close to the time of metamorphism. The age given by microcline will depend on the fraction of the original argon retained during metamorphism and on the subsequent loss of argon by diffusion from position I during geological time. It is evident that either biotite or microcline can give the older age.

III Conclusions

1. In the Kinnekulle and Millcreek sanidines diffusion occurs from one position. In agreement with other authors (cf. Baadsgaard et al., 1961) it was found that clear, mono-crystalline bentonitic sanidines will show complete retention of radiogenic argon under normal geological conditions. The effective radius of diffusion was found to be equal to the grain size.
2. In the Crowsnest sanidine and in the two microclines, argon is held in two positions. These positions are related to the proximity of the argon atoms to planes of strain in the lattice.
3. In the Crowsnest sanidine the diffusion coefficient at 150°C. for position I is on the threshold value for loss of argon during geological time.
4. In the two microclines, the value of the diffusion coefficient at 150°C. for position I is such that a considerable loss of argon from this position can occur in geological time. The mica-feldspar age discordancy may therefore be explained as being due to volume diffusion from position I.
5. The activation energy of position II in the microclines is sufficiently high to explain the retention of most of the argon in this position during thermal metamorphism. In pre-Cambrian rocks that have been thermally metamorphosed in the Cretaceous-Tertiary orogeny, it should be quite common to find feldspars giving older ages than biotite.

BIBLIOGRAPHY

- Amirkhanov, Kh. I., Brandt, S.B. and Bartnitskii, E.N. (1959): The diffusion of radiogenic argon in feldspars. Dokl. Akad. Nauk. S.S.S.R., Vol. 125, pp. 1345-1347.
- Amirkhanov, Kh.I., Brandt, S.B., Bartnitskii, E.N. and Voronovskii, S.N. (1959): Diffusion of argon in sylvite. Geochemistry (English translation) no. 6, 1959, pp. 653-662.
- Amirkhanov, Kh.I., Brandt, S.B. and Bartnitskii, E.N. (1960): Discussion - Gerling's method of determination of activation energy of radiogenic gases in minerals. Geochemistry (English translation) no. 7, 1960, pp. 778-782.
- Amirkhanov, Kh.I., Brandt, S.B. and Bartnitskii, E.N. (1961): Radiogenic argon in minerals and its migration. Annals of the New York Academy of Sciences, Vol. 91, Art. 2, pp. 235-275.
- Aldrich, L.T. and Nier, A.O. (1948): Argon 40 in potassium minerals. Phys. Rev., Vol. 74, pp. 876-878.
- Ahrens, L.T. and Evans, R.D. (1948): The radioactive decay constants of K^{40} as determined from the accumulation of Ca^{40} in ancient minerals. Phys. Rev., Vol. 74, pp. 279-286.
- Atom Movements. A seminar on atom movements sponsored by the American Society for Metals. 1950.
- Baadsgaard, H., Lipson, J. and Folinsbee, R.E. (1961): The leakage of radiogenic argon from sanidine. Geochim. et Cosmochim. Acta, Vol. 25, pp. 147-157.
- Bailey, S.W. and Taylor, W.H. (1955): The structure of a triclinic potassium feldspar. Acta Cryst., Vol. 8, pp. 621-632.
- Barth, T.F.W. (1934): Polymorphic phenomena and crystal structure. Am. J. Sci., Vol. 27, pp. 273-286.
- Barth, T.F.W. (1959): The interrelations of the structural variants of the potash feldspars. Zeit. Krist., Vol. 112, pp. 263-274.
- Baskin, Y. (1956): A study of authigenic feldspars. Jour. Geol., Vol. 64, pp. 132-155.
- Barrer, R.M. (1951): Diffusion in and through solids. Cambridge University Press.
- Bowen, N.L. and Tuttle, O.F. (1950): The system $NaAlSi_3O_8 - KAlSi_3O_8 - H_2O$. Jour. Geol., Vol. 58, pp. 489-511.
- Bragg, W.L. (1937): Atomic structure of minerals. Cornell University Press.

- Brandt, S.B. and Bartnitskii, E.N. (1962): Losses of radiogenic argon in alkali (soda-potash) feldspars under thermal activation. *Geochemistry* (English translation) no. 12, 1962. pp. 23-31.
- Buerger, M.J. (1945): The genesis of twin crystals. *Am. Min.*, Vol. 30, pp. 469-482.
- Buerger, M.J. (1948): The role of temperature in mineralogy. *Am. Min.*, Vol. 33, pp. 101-121.
- Byström, Ann. (1954): Mineralogy of the Ordovician Bentonite Beds at Kinnekulle, Sweden. *Sveriges Geologiska Undersökning. Årsbok 48. No. 5.*
- Byström-Asklund, A.M., Baadsgaard, H. and Folinsbee, R.E. (1961): K/Ar age of biotite, sanidine, and illite from Middle Ordovician bentonites at Kinnekulle, Sweden. *Geologiska Föreningens Förhandlingar. Bd 83. H.1. pp. 92-96.*
- Carslow, H.S. and Jaeger, J.C. (1947): *Conduction of heat in solids.* Oxford University Press.
- Chao, S.W., Hargreaves, A. and Taylor, W.H. (1940): The structure of orthoclase. *Miner. Mag.*, Vol. 25, pp. 498-512.
- Cole, W.F., Sörum, H. and Kennard, O. (1949): The crystal structure of orthoclase and sanidinized orthoclase. *Acta Cryst.*, Vol. 2, pp. 280-287.
- Cottrell (1948): *Theoretical Structural Metallurgy,* Arnold.
- Crank, J. (1956): *Mathematics of diffusion.* Oxford University Press.
- Donnay, G. and Donnay, J.D.H. (1952): The symmetry change in the high temperature alkali-feldspar series. *Am. J. Sci., Bowen Volume,* pp. 115-132.
- Eitel (1958): Structural conversions in crystalline systems and their importance for geological problems. Chapter: Structural conversions in the alkali-feldspars. *Geol. Soc. Amer. Special Paper 66. pp. 80-105.*
- Everden, J.F., Curtis, G.H., Kistler, R.W. and Obradovich, J. (1960): Argon diffusion in glauconite, microcline, sanidine, leucite and phlogopite. *Am. J. Sci.*, Vol. 258, pp. 583-604.
- Fechtig, H., Gentner, W. and Zahringer, J. (1960): Argonbestimmungen an Kalium-mineralien-VII. Diffusion-verluste von Argon in Mineralien und ihre Auswirkung auf die Kalium-Argon-Altersbestimmung. *Geochim. et Cosmochim. Acta,* Vol. 19, pp. 70-79.
- Fechtig, H., Gentner, W. und Kalbitzer, S. (1961): Argonbestimmungen an Kalium-mineralien-IX. Messungen zu den Verschiedenen Arten der Argondiffusion. *Geochim. et Cosmochim. Acta,* Vol. 23, pp. 297-311.
- Ferguson, R.B., Traill, R.J. and Taylor, W.H. (1958): The crystal structures of low-temperature and high-temperature albites. *Acta Cryst.*, Vol. 11, pp. 331-348.

- Ferguson, R.B., Traill, R.J. and Taylor, W.H. (1959): Charge balance and the stability of alkali feldspars: a discussion. *Acta Cryst.*, Vol. 12, pp. 716-718.
- Ferguson, R.B. (1960): The low temperature phases of the alkali feldspars and their origin. *Canadian Min.*, Vol. 6, pp. 415-436.
- Folinsbee, R.E., Lipson, J. and Reynolds, J.H. (1956): Potassium argon dating. *Geochim. et Cosmochim. Acta*, Vol. 10, pp. 60-68.
- Gentner, W., Präg, R. und Smits, F. (1953): Argonbestimmungen an Kalium-mineralien. II Das Alter eines Kalilagers im Unteren Oligozen. *Geochim. et Cosmochim. Acta*, Vol. 4, pp. 11-20.
- Gentner, W. und Kley, W. (1957): Argonbestimmungen an Kaliummineralien - IV. Die Frage der Argonverluste in Kalifeldspäten und Glimmermineralien. *Geochim. et Cosmochim. Acta*, Vol. 12, pp. 323-329.
- Gerling, E.K. and Morozova, I.M. (1957): Determination of activation energy of argon liberation from micas. *Geochemistry (English translation)*, no. 4, 1957. pp. 359-367.
- Gerling, E.K. and Morozova, I.M. (1958): The kinetics of argon liberation from microcline-perthite. *Geochemistry (English translation)*, no. 7, 1958. pp. 775-781.
- Gerling, E.K. (1960): Concerning the article by Kh. I. Amirkanov, S.B. Brandt and E.N. Bartnitskii: 'Gerling's method of determination of activation energy of radiogenic gases in minerals'. *Geochemistry (English translation)*, no. 7, 1960. pp. 785-786.
- Gerling, E.K., Morozova, I.M. and Kurbatov, V.V. (1961): Retention of radiogenic argon in powdered potassium-bearing minerals. *Geochemistry (English translation)*, no. 1, 1961. pp. 45-56.
- Gerling, E.K., Morozova, I.M. and Kurbatov, V.V. (1961): The retentivity of radiogenic argon in ground micas. *Annals of the New York Academy of Sciences*, Vol. 91, Art. 2., pp. 227-234.
- Goldsmith, J.R. and Laves, F. (1954): The microcline-sanidine stability relations. *Geochim. et Cosmochim. Acta*, Vol. 5, pp. 1-19.
- Goldsmith, J.R. and Laves, F. (1954): Potassium feldspars structurally intermediate between microcline and sanidine. *Geochim. et Cosmochim. Acta*, Vol. 6, pp. 100-118.
- Gray, T.J. (1957): The defect solid state. Interscience Publishers. New York.
- Hart, S.R. (1960): Extracts from the thesis investigation of S.R. Hart. Department of Geology and Geophysics. M.I.T. N.Y.O. 3941. Eighth Annual Report for 1960. U.S. Atomic Energy Commission. Contract AT(30-1) - 1381.
- Hart, S.R. (to be published): The petrology and isotopic mineral age relations of a contact zone in the front range, Colorado. *Jour. Geol.*, (to be published).

- Jensen, M.L. (1952): Solid diffusion of radioactive sodium in perthite. *Am. J. Sci.*, Vol. 250, pp. 808-821.
- Jost, B. (1952): *Diffusion in solids, liquids and gases*. Academic Press, New York.
- Kuz'min, A.M. (1961): Retention of argon in microcline. *Geochemistry* (English translation), no. 5, 1961, pp. 485-488.
- Laves, F. (1950): The lattice and twinning of microcline and other potash feldspars. *Jour. Geol.*, Vol. 58, pp. 548-571.
- Laves, F. (1951): Artificial preparation of microcline. *Jour. Geol.*, Vol. 59, pp. 511-562.
- Laves, F. (1952): Phase relations of the alkali feldspars. *Jour. Geol.*, Vol. 60, pp. 436-450; 549-574.
- Lund, E.H. (1956): Igneous and metamorphic rocks of the Minnesota River Valley. *Bull. G.S.A.*, Vol. 67, pp. 1475-1490.
- MacKenzie, W.S. and Smith, J.V. (1955 and 1956): The alkali feldspars. I. Orthoclase microperthites. *Amer. Min.*, Vol. 40, pp. 706-732. III. An optical and X-ray study of high temperature feldspars. *Amer. Min.*, Vol. 41, pp. 405-427.
- MacKenzie, W.S. and Smith, J.V. (1959): Charge balance and the stability of alkali feldspars. *Acta. Cryst.*, Vol. 12, pp. 73-74.
- MacKenzie, W.S. and Smith, J.V. (1961): Experimental and geological evidence for the stability of alkali feldspars. *Cursillos y Conferencias*. Fasc. VIII, pp. 53-69.
- Nicolaysen, L.C. (1957): Solid diffusion in radioactive minerals and the measurement of absolute age. *Geochim. et Cosmochim. Acta*, Vol. 11, pp. 41-59.
- Orville, P.M. (1958): Feldspar investigations. *An. Rept., Geophys. Lab., Carnegie Inst., Washington*. 1957-1958. pp. 206-209.
- Ovchinnikov, L.N., Kelarev, V.V., Panova, M.V., Dunaev, V.A., Shangareev, F.L. and Osadchaya, R.I. (1959): Retention of argon in micas. *Geochemistry* (English translation), No. 9, 1959. pp. 874-881.
- Pronko, P.P. (1962): Ionic conductivity of mica and feldspar. Unpublished M.Sc. thesis, University of Pittsburgh.
- Reichenberg, D. (1953): Properties of ion-exchange resins in relation to their structure, III. Kinetics of exchange. *Jour. Amer. Chem. Soc.*, Vol. 75, pp. 589-597.
- Reynolds, John H. (1957): Comparative study of argon content and argon diffusion in mica and feldspar. *Geochim. et Cosmochimica Acta*, Vol. 12, pp. 177-184.
- Rosenqvist, I. Th. (1949): Some investigations in the crystal chemistry of silicates, I. Diffusion of Pb and Ra in feldspars. *Acta Chem. Scand.*, Vol. 3, Pt. 1, pp. 569-583.

- Sahama, Th. G. (1962): Order-disorder in Natural Nepheline Solid Solutions. *Jour. Pet.*, Vol. 3, pp. 65-81.
- Sardarov, S.S. (1957): Retention of radiogenic argon in microcline. *Geochemistry* (English translation), no. 3, 1957, pp. 233-238.
- Sardarov, S.S. (1961): Bond energy and retention of radiogenic argon in micas. *Geochemistry* (English translation), no. 1, 1961, pp. 33-44.
- Smith, J.V. (1954): A review of the Al-O and Si-O distances. *Acta Cryst.*, Vol. 7, pp. 479-483.
- Smith, J.V. and MacKenzie, W.S. (1959): The alkali feldspars. V. Orthoclase and microcline perthites. *Amer. Min.*, Vol. 44, pp. 1169-1186.
- Smith, J.V. and MacKenzie, W.S. (1961): Atomic, chemical and physical factors that control the stability of alkali feldspars. *Cursillos y Conferencias. Fasc. VIII*, pp. 39-52.
- Taylor, W.H. (1933): The structure of sanidine and other feldspars. *Zeit. Krist.*, Vol. 85, pp. 425-442.
- Tuttle, O.F. (1952): Optical studies on alkali feldspars. *Amer. Jour. Sci.*, Bowen Volume, pp. 553-567.
- Wasserburg, G.S. and Hayden, R.J. (1955): $\text{Ar}^{40}\text{-K}^{40}$ dating. *Geochim. et Cosmochim. Acta*, Vol. 7, pp. 51-60.
- Wasserburg, G.S., Hayden, R.J. and Jensen, K.S. (1956): $\text{Ar}^{40}\text{-K}^{40}$ dating of igneous rocks and sediments. *Geochim. et Cosmochim. Acta*, Vol. 10, pp. 153-165.
- Wetherill, G.W., Wasserberg, G.J., Aldrick, L.T., Tilton, G.R. and Hayden, R.J., (1956): Decay constants of K^{40} as determined by radiogenic argon content of potassium minerals. *Phys. Rev.*, Vol. 103, pp. 987-989.
- Wetherill, G.W., Aldrick, L.T. and Davis, G.L. (1955): $\text{Ar}^{40}\text{-K}^{40}$ ratios of feldspars and micas from the same rock. *Geochim. et Cosmochim. Acta*, Vol. 8, pp. 171-172.
- Wrage, E. (1961): Argonbestimmungen an Kaliummineralien VIII. Ein Nährungsverfahren zur Lösung von Diffusionsproblem. *Geochim. et Cosmochim. Acta*, Vol. 26, pp. 61-66.

APPENDIX A

The following tables present particular solutions of the approximation (3)-4.

Values of the fraction of argon released are tabulated against values of $(Dt/a^2)^{1/2}$.

As the time of diffusion is known, values of D/a^2 may be easily calculated. For values of the fraction of argon released >0.85 , one term of the equation (3)-1 is used.

Fraction
X 10⁻³ $(Dt/a^2)^{1/2}$

1.00	=	0.000275
1.25	=	0.000350
1.50	=	0.000425
1.75	=	0.000500
2.00	=	0.000575
2.25	=	0.000650
2.50	=	0.0007233
2.75	=	0.0007933
3.00	=	0.0008633
3.25	=	0.0009333
3.50	=	0.00100833
3.75	=	0.0010833
4.00	=	0.00115833
4.25	=	0.001233
4.50	=	0.00130833
4.75	=	0.0013833
5.00	=	0.00145833
5.25	=	0.00154166

Fraction
X 10⁻³ $(Dt/a^2)^{1/2}$

5.50	=	0.001625
5.75	=	0.00170
6.00	=	0.001775
6.25	=	0.00185
6.50	=	0.001925
6.75	=	0.002
7.00	=	0.002066
7.25	=	0.0021366
7.50	=	0.00220833
7.75	=	0.0022833
8.00	=	0.00235833
8.25	=	0.002433
8.50	=	0.00250833
8.75	=	0.0025833
9.00	=	0.00265833
9.25	=	0.002733
9.50	=	0.00280833
9.75	=	0.0028833

Fraction
X 10⁻² $(Dt/a^2)^{1/2}$

1.00	=	0.00295833
1.25	=	0.00369166
1.50	=	0.00445833
1.75	=	0.00519166
2.00	=	0.005925
2.25	=	0.00669166
2.50	=	0.007425
2.75	=	0.0081733
3.00	=	0.00890833
3.25	=	0.00969166
3.50	=	0.01044166
3.75	=	0.011175
4.00	=	0.01189166
4.25	=	0.01265833
4.50	=	0.0134266
4.75	=	0.01416
5.00	=	0.01494166
5.25	=	0.01570833

Fraction
X 10⁻² $(Dt/a^2)^{1/2}$

5.50	=	0.0164766
5.75	=	0.01721
6.00	=	0.0179733
6.25	=	0.01876
6.50	=	0.0195083
6.75	=	0.020275
7.00	=	0.0210433
7.25	=	0.02181
7.50	=	0.02259166
7.75	=	0.02335833
8.00	=	0.0241266
8.25	=	0.02491
8.50	=	0.0256766
8.75	=	0.02645833
9.00	=	0.02724166
9.25	=	0.02800833
9.50	=	0.0287766
9.75	=	0.0295933

Fractions
X 10⁻¹ (Dt/a²)^{1/2}

1.00	=	0.030375
1.25	=	0.0382
1.50	=	0.0462
1.75	=	0.0542833
2.00	=	0.0625333
2.25	=	0.0709166
2.50	=	0.079433
2.75	=	0.0881
3.00	=	0.0969333
3.25	=	0.10595
3.50	=	0.1151166
3.75	=	0.1245
4.00	=	0.1340833
4.25	=	0.1438833
4.50	=	0.1539166
4.75	=	0.1642
5.00	=	0.174766
5.25	=	0.1856
5.50	=	0.1967833
5.75	=	0.2083
6.00	=	0.2202
6.25	=	0.232533
6.50	=	0.24535
6.75	=	0.2587
7.00	=	0.27266
7.25	=	0.28733
7.50	=	0.3028166
7.75	=	0.319266
8.00	=	0.336933
8.25	=	0.356066
8.50	=	0.377166

APPENDIX B

The following tables present values for each of the nine runs of the area under the curve of mass spectrometer response against time. As the response of the mass spectrometer is proportional to the amount of argon entering the tube, the area under the response curve must be proportional to the volume of argon released.

The significance of these tables will be briefly reviewed. Referring to Figure 6, page 44, and to the first table for the Kinnekulle sanidine, page 107, the area A corresponds to 780 and the time $t_1 - t_0$ to 400 seconds. Similarly the area B corresponds to 7410 and the time $t_2 - t_1$ to 2600 seconds; the area C to 4492 and the time $t_3 - t_2$ to 320 seconds; the area D to 15213 and the time $t_4 - t_3$ to 880 seconds, et cetera.

In Chapter three, section V, a description is given of the determination of the diffusion coefficients using equations (3)-4 and (3)-5. Determination of the diffusion coefficient by means of Wragge's mathematical treatment, is described in Chapter five, section I.

I KINNEKULLE SANIDINE 170-230 mesh

Sample weight 0.5019 gms.

Areas under the curve of mass spectrometer response against time.

Temperature = 528 \pm 4°C.

780 in 400 secs.	Period of gradient adjustment
7410 in 2600 secs.	

Temperature = 621 \pm 4°C.

4492 in 320 secs.	Period of gradient adjustment
15213 in 880 secs.	
17516 in 1920 secs.	

Temperature = 722 \pm 3°C.

14620 in 320 secs.	Period of gradient adjustment
104168 in 3200 secs.	

Temperature = 821 \pm 4°C.

28935 in 320 secs.	Period of gradient adjustment
204050 in 2360 secs.	
74487 in 1440 secs.	

Temperature = 930 \pm 4°C.

73260 in 400 secs.	Period of gradient adjustment
206610 in 880 secs.	
324040 in 2440 secs.	
99850 in 1120 secs.	

Temperature = 1018 \pm 4°C.

69230 in 320 secs.	Period of gradient adjustment
554240 in 3160 secs.	

Temperature = 1135 \pm 9°C.

344050 in 520 secs.	Period of gradient adjustment
456107 in 3760 secs.	

II MILLCREEK SANIDINE

a) Millcreek Sanidine 80-120 mesh
Sample weight 0.9737 gms.

Areas under the curve of mass spectrometer response against time.

Temperature = $523 \pm 3^{\circ}\text{C}.$

638 in 240 secs.	Period of gradient adjustment
1785 in 920 secs.	

Temperature = $637 \pm 3^{\circ}\text{C}.$

1054 in 200 secs.	Period of gradient adjustment
4690 in 960 secs.	
3416 in 1600 secs.	

Temperature = $742 \pm 3^{\circ}\text{C}.$

2637 in 240 secs.	Period of gradient adjustment
19453 in 2000 secs.	
11000 in 2040 secs.	

Temperature = $844 \pm 3^{\circ}\text{C}.$

6732 in 280 secs.	Period of gradient adjustment
50592 in 1920 secs.	
31055 in 1920 secs.	
15620 in 1240 secs.	

Temperature = $937 \pm 3^{\circ}\text{C}.$

15849 in 320 secs.	Period of gradient adjustment
98817 in 2160 secs.	
67448 in 2960 secs.	

Temperature = $1036 \pm 3^{\circ}\text{C}.$

32251 in 520 secs.	Period of gradient adjustment
110821 in 2080 secs.	
80010 in 3040 secs.	
46140 in 3120 secs.	

Temperature = $1144 \pm 3^{\circ}\text{C}.$

36529 in 560 secs.	Period of gradient adjustment
125425 in 2440 secs.	
30678 in 1440 secs.	

Temperature = $1227 \pm 5^{\circ}\text{C}.$

32894 in 400 secs.	Period of gradient adjustment
55244 in 1240 secs.	

b) Millcreek Sanidine 120-170 mesh
Sample weight 1.1226 gms.

Areas under the curve of mass spectrometer response against time.

Temperature = $514 \pm 4^{\circ}\text{C}$.

570 in 360 secs.	Period of gradient adjustment
1570 in 1160 secs.	

Temperature = $632 \pm 3^{\circ}\text{C}$.

1015 in 200 secs.	Period of gradient adjustment
4840 in 1320 secs.	
2600 in 1600 secs.	

Temperature = $748 \pm 4^{\circ}\text{C}$.

2776 in 280 secs.	Period of gradient adjustment
16001 in 1560 secs.	
16190 in 2880 secs.	

Temperature = $842 \pm 3^{\circ}\text{C}$.

5420 in 280 secs.	Period of gradient adjustment
42700 in 1840 secs.	
57300 in 4680 secs.	

Temperature = $947 \pm 3^{\circ}\text{C}$.

18627 in 360 secs.	Period of gradient adjustment
153780 in 6080 secs.	

Temperature = $1046 \pm 3^{\circ}\text{C}$.

12905 in 360 secs.	Period of gradient adjustment
89800 in 2880 secs.	
22378 in 1400 secs.	

Temperature = $1146 \pm 4^{\circ}\text{C}$.

27388 in 480 secs.	Period of gradient adjustment
82165 in 1680 secs.	
35300 in 2080 secs.	

Temperature = $1230 \pm 6^{\circ}\text{C}$.

23383 in 360 secs.	Period of gradient adjustment
41065 in 1520 secs.	

c) Millcreek Sanidine 170-230 mesh
Sample weight 1.1773 gms.

Areas under the curve of mass spectrometer response against time.

Temperature = $529 \pm 4^{\circ}\text{C}$.

950 in 240 secs.	Period of gradient adjustment
3400 in 1400 secs.	

Temperature = $639 \pm 3^{\circ}\text{C}$.

1680 in 240 secs.	Period of gradient adjustment
6696 in 1280 secs.	
5236 in 1800 secs.	

Temperature = $762 \pm 3^{\circ}\text{C}$.

5040 in 360 secs.	Period of gradient adjustment
30761 in 2000 secs.	
19442 in 2160 secs.	

Temperature = $862 \pm 3^{\circ}\text{C}$.

11838 in 320 secs.	Period of gradient adjustment
73620 in 1880 secs.	
55800 in 2440 secs.	

Temperature = $954 \pm 3^{\circ}\text{C}$.

15006 in 280 secs.	Period of gradient adjustment
97749 in 2120 secs.	
31368 in 1640 secs.	

Temperature = $1052 \pm 3^{\circ}\text{C}$.

16335 in 360 secs.	Period of gradient adjustment
86683 in 3000 secs.	

Temperature = $1149 \pm 4^{\circ}\text{C}$.

25425 in 440 secs.	Period of gradient adjustment
96761 in 3000 secs.	

Temperature = $1225 \pm 5^{\circ}\text{C}$.

13700 in 320 secs.	Period of gradient adjustment
24230 in 680 secs.	

III CROWSNEST SANIDINE

- a) Crowsnest Sanidine 60-80 mesh
Sample weight 0.9644 gms.

Areas under the curve of mass spectrometer response against time.

Temperature = $380 \pm 3^{\circ}\text{C}.$

267 in 280 secs.	Period of gradient adjustment
2588 in 1960 secs.	

Temperature = $459 \pm 4^{\circ}\text{C}.$

901 in 120 secs.	Period of gradient adjustment
11004 in 2840 secs.	

Temperature = $564 \pm 4^{\circ}\text{C}.$

4293 in 240 secs.	Period of gradient adjustment
23463 in 2200 secs.	
5576 in 1360 secs.	

Temperature = $674 \pm 3^{\circ}\text{C}.$

8265 in 240 secs.	Period of gradient adjustment
49441 in 2680 secs.	
11685 in 1480 secs.	

Temperature = $726 \pm 3^{\circ}\text{C}.$

5376 in 320 secs.	Period of gradient adjustment
35210 in 2160 secs.	
14098 in 1400 secs.	

Temperature = $791 \pm 3^{\circ}\text{C}.$

5235 in 240 secs.	Period of gradient adjustment
28628 in 1080 secs.	
30939 in 2200 secs.	

Temperature = $857 \pm 3^{\circ}\text{C}.$

5382 in 240 secs.	Period of gradient adjustment
45346 in 2920 secs.	

Temperature = $953 \pm 3^{\circ}\text{C}.$

4732 in 240 secs.	Period of gradient adjustment
39940 in 3000 secs.	

a) Crowsnest Sanidine 60-80 mesh [continued]

Temperature = $1052 \pm 3^{\circ}\text{C}.$

5092	in	240 secs.	Period of gradient adjustment
46392	in	3200 secs.	

Temperature = $1155 \pm 4^{\circ}\text{C}.$

9627	in	360 secs.	Period of gradient adjustment
68082	in	2640 secs.	

Temperature = $1239 \pm 10^{\circ}\text{C}.$

258783	in	1920 secs.	Period of gradient adjustment
240057	in	5000 secs.	

b) Crowsnest Sanidine 170-200 mesh
Sample weight 1.0256 gms.

Area under the curve of mass spectrometer response against time

Temperature = $543 \pm 3^{\circ}\text{C}$.

4581 in 400 secs.	Period of gradient adjustment
23125 in 1920 secs.	

Temperature = $659 \pm 3^{\circ}\text{C}$.

8822 in 240 secs.	Period of gradient adjustment
54285 in 1480 secs.	
28530 in 1960 secs.	

Temperature = $765 \pm 3^{\circ}\text{C}$.

13933 in 280 secs.	Period of gradient adjustment
114822 in 3120 secs.	

Temperature = $862 \pm 4^{\circ}\text{C}$.

15565 in 280 secs.	Period of gradient adjustment
113594 in 3160 secs.	

Temperature = $958 \pm 3^{\circ}\text{C}$.

9467 in 320 secs.	Period of gradient adjustment
59529 in 3240 secs.	
39115 in 1320 secs.	

Temperature = $1051 \pm 3^{\circ}\text{C}$.

5253 in 280 secs.	Period of gradient adjustment
56202 in 3880 secs.	
36962 in 2040 secs.	

Temperature = $1159 \pm 4^{\circ}\text{C}$.

10053 in 400 secs.	Period of gradient adjustment
85209 in 3400 secs.	

Temperature = $1225 \pm 3^{\circ}\text{C}$.

111310 in 720 secs.	Period of gradient adjustment
214715 in 1240 secs.	
49753 in 2880 secs.	

c) Crowsnest Sanidine 270-325 mesh
Sample weight 1.0843 gms.

Area under the curve of mass spectrometer response against time.

Temperature = $511 \pm 3^{\circ}\text{C}$.

1372 in 200 secs.	Period of gradient adjustment
19254 in 2320 secs.	

Temperature = $643 \pm 4^{\circ}\text{C}$.

13644 in 280 secs.	Period of gradient adjustment
60245 in 1600 secs.	
44169 in 3440 secs.	

Temperature = $756 \pm 3^{\circ}\text{C}$.

15232 in 280 secs.	Period of gradient adjustment
104760 in 1920 secs.	
44361 in 1840 secs.	

Temperature = $859 \pm 3^{\circ}\text{C}$.

13491 in 240 secs.	Period of gradient adjustment
139963 in 3720 secs.	

Temperature = $951 \pm 3^{\circ}\text{C}$.

6094 in 240 secs.	Period of gradient adjustment
22740 in 760 secs.	
20568 in 1840 secs.	

Temperature = $1046 \pm 3^{\circ}\text{C}$.

3991 in 240 secs.	Period of gradient adjustment
14475 in 560 secs.	
35430 in 2840 secs.	

Temperature = $1149 \pm 4^{\circ}\text{C}$.

12095 in 440 secs.	Period of gradient adjustment
53967 in 1880 secs.	
36215 in 2160 secs.	

Temperature = $1225 \pm 4^{\circ}\text{C}$.

76629 in 680 secs.	Period of gradient adjustment
163815 in 1160 secs.	
32526 in 800 secs.	
13010 in 1120 secs.	

IV YELLOWKNIFE MICROCLINE 60-80 mesh

Sample weight 1.1129 gms.

Area Under the curve of mass spectrometer response against time

Temperature = $301 \pm 3^{\circ}\text{C}.$

20201 in 440 secs.	Period of gradient adjustment
83867 in 3080 secs.	

Temperature = $424 \pm 4^{\circ}\text{C}.$

69430 in 120 secs.	Period of gradient adjustment
160650 in 320 secs.	
225314 in 3360 secs.	
32680 in 1240 secs.	

Temperature = $526 \pm 5^{\circ}\text{C}.$

175353 in 120 secs.	Period of gradient adjustment
607500 in 520 secs.	
148190 in 1000 secs.	
206425 in 3240 secs.	

Temperature = $650 \pm 3^{\circ}\text{C}.$

108640 in 120 secs.	Period of gradient adjustment
374790 in 320 secs.	
444040 in 880 secs.	
371025 in 1320 secs.	
283835 in 1680 secs.	

Temperature = $756 \pm 4^{\circ}\text{C}.$

229930 in 240 secs.	Period of gradient adjustment
931060 in 880 secs.	
1225490 in 2640 secs.	

Temperature = $852 \pm 3^{\circ}\text{C}.$

404880 in 280 secs.	Period of gradient adjustment
2560800 in 2000 secs.	
955315 in 1760 secs.	

Temperature = $945 \pm 3^{\circ}\text{C}.$

322370 in 240 secs.	Period of gradient adjustment
1974850 in 1200 secs.	
1349120 in 2280 secs.	

Yellowknife Microcline 60-80 mesh [continued]

Temperature = $1047 \pm 3^{\circ}\text{C}.$

511300	in	400 secs.	Period of gradient adjustment
1503850	in	1200 secs.	
1798050	in	2520 secs.	

Temperature = $1150 \pm 4^{\circ}\text{C}.$

503440	in	320 secs.	Period of gradient adjustment
2680720	in	1560 secs.	
1635080	in	1640 secs.	

Temperature = $1226 \pm 5^{\circ}\text{C}.$

1158720	in	560 secs.	Period of gradient adjustment
6403420	in	2600 secs.	

TOTAL 64.3 per cent of argon lost during run
35.7 per cent remains in the sample

MONTIVIDEO MICROCLINE 35-60 mesh

Sample weight 1.0112 gms.

Area under the curve of mass spectrometer response against time.

Temperature = $254 \pm 5^{\circ}\text{C}.$

26900 in 200 secs.	Period of gradient adjustment
50600 in 520 secs.	
15653 in 1440 secs.	

Temperature = $418 \pm 4^{\circ}\text{C}.$

99102 in 140 secs.	Period of gradient adjustment
258360 in 580 secs.	
31040 in 2880 secs.	

Temperature = $546 \pm 3^{\circ}\text{C}.$

97172 in 93 secs.	Period of gradient adjustment
295735 in 626 secs.	
73400 in 1320 secs.	
54100 in 1800 secs.	

Temperature = $651 \pm 3^{\circ}\text{C}.$

67300 in 120 secs.	Period of gradient adjustment
279300 in 480 secs.	
151500 in 1080 secs.	
163400 in 2360 secs.	

Temperature = $749 \pm 3^{\circ}\text{C}.$

79500 in 140 secs.	Period of gradient adjustment
369200 in 500 secs.	
366040 in 1800 secs.	
148000 in 1440 secs.	

Temperature = $855 \pm 3^{\circ}\text{C}.$

64420 in 200 secs.	Period of gradient adjustment
475600 in 760 secs.	
245500 in 1080 secs.	
252750 in 2280 secs.	

Temperature = $940 \pm 4^{\circ}\text{C}.$

82370 in 160 secs.	Period of gradient adjustment
476500 in 920 secs.	
683200 in 3360 secs.	

Montivideo Microcline 35-60 mesh [continued]

Temperature = $1048 \pm 5^{\circ}\text{C}.$

311700	in	280 secs.	Period of gradient adjustment
523500	in	200 secs.	
604500	in	480 secs.	
860500	in	1040 secs.	
1611000	in	2600 secs.	

Temperature = $1149 \pm 4^{\circ}\text{C}.$

496500	in	200 secs.	Period of gradient adjustment
3819800	in	2280 secs.	
1297500	in	2160 secs.	

Temperature = $1243 \pm 5^{\circ}\text{C}.$

549500	in	320 secs.	Period of gradient adjustment
2321500	in	1240 secs.	
1805400	in	2040 secs.	

78.65 per cent of argon lost during run

21.35 per cent remains in the sample

MEMORANDUM FOR THE RECORD

DATE: 10/10/54

SUBJECT: [Illegible]
[Illegible]
[Illegible]
[Illegible]
[Illegible]

TO: [Illegible]

FROM: [Illegible]
[Illegible]
[Illegible]

RE: [Illegible]

[Illegible]
[Illegible]
[Illegible]

Very truly yours,
[Illegible]

APPENDIX C

	Kinnekulle Sanidine (Byström)	Millcreek Sanidine (Newland)	Crowsnest Sanidine (Baadsgaard)	Yellowknife Microcline (Stelmach)	Montevideo Microcline (Rock Analysis Lab., U. of Minnesota)
SiO ₂	64.3	64.46	64.21		
Al ₂ O ₃	20.3	18.93	18.71		
Fe ₂ O ₃	0.1	0.07	0.37		
FeO		0.16	0.12		
Na ₂ O	2.67	3.26	2.34	1.09	
K ₂ O	11.75	11.23	12.74	15.28	12.89
Rb ₂ O			0.02	0.01	
CaO	0.3	0.01	0.01		
MgO	0.03	0.05	0.03		
BaO	0.8	0.11	0.67		
	<hr/> 100.25	<hr/> 98.28	<hr/> 99.22		

B29812